

OPTICAL NEAR FIELD INTERACTION OF  
SPHERICAL QUANTUM  
DOTS

A THESIS  
SUBMITTED TO THE DEPARTMENT OF PHYSICS  
AND THE GRADUATE SCHOOL OF ENGINEERING AND SCIENCE  
OF BILKENT UNIVERSITY  
IN PARTIAL FULLFILMENT OF THE REQUIREMENTS  
FOR THE DEGREE OF  
MASTER OF SCIENCE

By  
Togay Amirahmadov  
July, 2012

I certify that I have read this thesis and that in my opinion it is fully adequate, in scope and in quality, as a thesis for the degree of Master of Science.

---

Assoc. Prof. Hilmi Volkan Demir (Supervisor)

I certify that I have read this thesis and that in my opinion it is fully adequate, in scope and in quality, as a thesis for the degree of Master of Science.

---

Prof. Oğuz Gülseren

I certify that I have read this thesis and that in my opinion it is fully adequate, in scope and in quality, as a thesis for the degree of Master of Science.

---

Assoc. Prof. Azer Kerimov

Approved for the Graduate School of Engineering and Sciences:

---

Prof. Levent Onural

Director of Graduate School of Engineering and Sciences

## ABSTRACT

# OPTICAL NEAR FIELD INTERACTION OF SPHERICAL QUANTUM DOTS

Togay Amirahmadov

M.S. in Physics

Supervisor: Assoc. Prof. Hilmi Volkan Demir

July, 2012

Nanometer-sized materials can be used to make advanced photonic devices. However, as far as the conventional far-field light is concerned, the size of these photonic devices cannot be reduced beyond the diffraction limit of light, unless emerging optical near-fields (ONF) are utilized. ONF is the localized field on the surface of nanometric particles, manifesting itself in the form of dressed photons as a result of light-matter interaction, which are bound to the material and not massless. In this thesis, we theoretically study a system composed of different-sized quantum dots involving ONF interactions to enable optical excitation transfer. Here this is explained by resonance energy transfer via an optical near-field interaction between the lowest state of the small quantum dot and the first dipole-forbidden excited state of the large quantum dot via the dressed photon exchange for a specific ratio of quantum dot size. By using the projection operator method, we derived the formalism for the transferred energy from one state to another for strong confinement regime for the first time. We performed numerical analyses of the optical near-field energy transfer rate for spherical colloidal quantum dots made of CdSe, CdTe, CdSe/ZnS and PbSe. We estimated that the energy transfer time to the dipole forbidden states of quantum dot is sufficiently shorter than the radiative lifetime of excitons in each quantum dot. This model of ONF is essential to understanding and designing systems of such quantum dots for use in near-field photonic devices.

*Keywords: optical near field, dressed photon, resonance energy transfer, excitons.*

## ÖZET

### KÜRESEL KUANTUM NOKTALARININ OPTİK YAKIN ALAN ETKİLEŞİMİ

Togay Amirahmadov

Fizik Bölümü, Yüksek Lisans

Tez Yöneticisi: Doç. Dr. Hilmi Volkan Demir

Temmuz 2012

Nano ölçekli malzemeler ileri fotonik cihazlar yapmak için kullanılabilir. Yeni ortaya konulan optik yakın alanlardan (OYA) faydalanılmadıkça, bilinen uzak alan ışığı kullanılarak, fotonik cihazların boyutu kırınım sınırının altına indirilemez. OYA nanometrik parçacıkların yüzeyi üzerinde yerleşmiş, malzemeye bağlı, kütesiz olmayan ve ışık madde etkileşimi sonucunda kendisini döşenmiş fotonlar şeklinde gösteren bir alandır. Bu tez çalışmasında, optik uyarılma transferi sağlamak için, farklı boyutlu kuantum noktalardan oluşan OYA etkileşimli bir sistemi teorik olarak inceledik. Burada, enerji aktarımı kuantum nokta boyutlarının belirli bir oranı için giyinmiş foton alışverişi yoluyla küçük kuantum noktasının taban seviyesi ve büyük kuantum noktasının ilk uyarılmış dipol yasaklı seviyesi arasındaki optik yakın alan etkileşimi aracılığıyla rezonans enerji aktarımı ile açıklanabilir. İzdüşüm operatörü yöntemini kullanarak, ilk kez güçlü sınırlandırma bölgesinde bir seviyeden diğerine aktarılan enerji için gereken formalizmi türettik. CdSe, CdTe, CdSe/ ZnS ve PbSe malzemelerinden yapılan küresel kolloidal kuantum noktaları için optik yakın alan enerji aktarım hızının sayısal analizini yaptık. Kuantum noktalarının dipol yasaklı seviyelerine enerji aktarım süresinin, kuantum noktalarında bulunan eksitonların ışımsal ömür süresinden yeterince kısa olduğunu hesapladık. Bu OYA modeli, yakın alan fotonik cihazlarında kullanılacak kuantum nokta sistemlerinin tasarımı ve anlaşılması için çok önemlidir.

*Anahtar kelimeler: Optik yakın alan, döşenmiş foton, rezonans enerji aktarımı, eksitonlar.*

# Acknowledgements

First I would like to acknowledge my advisor Assoc. Prof. Hilmi Volkan Demir. I had the opportunity to share two years of my academic life and experience with him and with our group members. I will never forget his kind attitude and encouragement. I am thankful to him to provide me with an opportunity to work with him and understand the first step for being a good researcher and scientist. In our group meetings I learned a lot of things from him. He is not only a good academic advisor, for me he is also a good teacher.

My special thanks go to Dr. Pedro Ludwig Hernandez Martinez for his help in my research. I cannot forget his friendship, encouragement and his optimistic way of handling problems when we faced during my research period.

Also I would like to thank Prof. Oğuz Gülseren and Assoc. Prof. Azer Kerimov for being on my jury and for their support and help.

Now come my friends. I would like to acknowledge our group members Burak Güzeltürk, Yusuf Keleştemur, Shahab Akhavan, Sayım Gökkyar, Evren Mutlugün, Cüneyt Eroğlu, Kıvanç Güngör, Can Uran, Ahmet Fatih Cihan, Veli Tayfun Kılıç, Talha Erdem, Aydan Yeltik, Yasemin Coşkun, Akbar Alipour and Ozan Yerli for their friendship and collaboration.

Also very importantly, among the management and technical team and the post doctoral researchers of the group: Dr. Nihan Kosku Perkgöz, Ozgun Akyuz, and Emre Unal; and Dr. Vijay Kumar Sharma. I am very thankful to you all for great friendship and support.

I am thankful to the present and former members of the Devices and Sensors Demir Research Group.

I would like to acknowledge Physics Department and all faculty members, staff graduate students especially Sabuhi Badalov, Semih Kaya and Fatmanur Ünal for their support and friendship.

My special thanks is for my family, especially for my father. Although he is not here with us, he would have been very happy. I am thankful to their support and encouragement despite all the difficulties. I dedicate this thesis to my father.

# Table of Contents

<b>ACKNOWLEDGEMENTS</b> .....	<b>V</b>
<b>1. INTRODUCTION</b> .....	<b>1</b>
1.1 THE OPTICAL FAR FIELD AND DIFFRACTION LIMIT OF LIGHT.....	1
1.2 WHAT IS OPTICAL NEAR-FIELDS .....	2
<b>2. THEORETICAL BACKGROUND OF OPTICAL NEAR FIELDS</b> .....	<b>6</b>
2.1 DIPOLE-DIPOLE INTERACTION MODEL OF OPTICAL NEAR FIELDS .....	6
2.2 PROJECTION OPERATOR METHOD. EFFECTIVE OPERATOR AND EFFECTIVE INTERACTION.....	12
2.3 OPTICAL NEAR-FIELD INTERACTION POTENTIAL IN THE NANOMETRIC SUBSYSTEM .....	14
2.4 OPTICAL NEAR-FIELD INTERACTION AS A VIRTUAL CLOUD OF PHOTONS AND LOCALLY EXCITED STATES .....	18
<b>3. OPTICAL NEAR-FIELD INTERACTION BETWEEN SPHERICAL QUANTUM DOTS</b> .....	<b>25</b>
3.1 INTRODUCTION .....	25
3.2 ENERGY STATES OF SEMICONDUCTOR QUANTUM DOTS .....	26
3.3 QUANTUM CONFINEMENT REGIMES. STRONG, INTERMEDIATE AND WEAK CONFINEMENTS. ....	32
3.4 OPTICAL NEAR-FIELD INTERACTION ENERGY BETWEEN SPHERICAL QUANTUM DOTS FOR STRONG AND WEAK CONFINEMENT REGIMES .....	36
3.4.1 STRONG CONFINEMENT .....	36
3.4.2 WEAK CONFINEMENT.....	39
3.5 NUMERICAL RESULTS FOR CdTe , CdSe, CdSe/ZNS AND PbSe QUANTUM DOTS.....	41
<b>CONCLUSIONS</b> .....	<b>53</b>

APPENDIX A	PROJECTION OPERATOR METHOD EFFECTIVE OPERATOR AND EFFECTIVE INTERACTION .....	61
APPENDIX B	DERIVATION OF THE INTERACTION POTENTIAL .....	66
APPENDIX C	OPTICAL NEAR FIELD INTERACTION BETWEEN QUANTUM DOTS FOR STRONG CONFINEMENT REGIME.....	75
APPENDIX D	DERIVATION OF THE PROPE SAMPLE INTERACTION POTENTIAL .....	83



# List of Figures

Figure 1.1.1 The schematic representation of residual defocusing.....1

Figure 1.2.1 The schematic representation of generation of an optical near fields (a) Generation of optical near fields on the surface of the sphere S. (b) Generation of optical near fields by a small subwavelength aperture. ....3

Figure 1.2.2 Generation of optical near field and electric field lines. (Taken from M. Ohtsu Principles of Nanophotonics 2008.) ..... 3

Figure 1.2.3 Nanometric subsystem composed of two nanometric particles and optical near fields generated between them.....5

Figure 2.1.1 Two point light sources with separation distance  $b$  .....8

Figure 2.1.2 Two positions  $\vec{r}_0$  and  $\vec{r}_1$  where  $|\vec{E}(\vec{r},t)|$  reaches its maximum value.....8

Figure 2.1.3 Electric dipole moment induced in the spheres S and P located very close to each other..... 10

Figure 2.2.1 The schematic representation of  $P$  space spanned by the eigenstates  $|\phi_1\rangle$  and  $|\phi_2\rangle$  and its complementary space  $Q$  ..... 13

Figure 2.4.1 Schematic representation of near-field optical system.  $\vec{r}_s$  and  $\vec{r}_p$  show the arbitrary positions in sample and probe.....19

Figure 2.4.2 Exchange of real and virtual exciton-polariton.....20

Figure 2.4.3 The system composed of QD S and P with two resonant coupled energy levels.  $|S\rangle$  and  $|A\rangle$  are correspond to symmetric and antisymmetric states..... 22

Figure 3.2.1 Band structure and energy band gap $E_g$ of bulk semiconductor. The diagram shows the creation of one electron-hole pair as a result of photon absorption.....	30
Figure 3.5.1 Optical near-field interactions between two spherical quantum dots with the size ratio of $R_2/R_1 \approx 1.43$ . There is a resonance between $(n,l,m) = (1,0,0)$ level of QDS and $(n',l',m') = (1,1,0)$ level of QDL.....	41
Figure 3.5.2 Optical near-field energy and distance relation for CdSe spherical quantum dots from $(n,l,m) = (1,0,0)$ state of QDS to $(n',l',m') = (1,1,0)$ state of QDL.....	43
Figure 3.5.3 Optical near-field transfer rate and distance relation for CdSe spherical quantum dots from $(n,l,m) = (1,0,0)$ state of QDS to $(n',l',m') = (1,1,0)$ state of QDL.....	44
Figure 3.5.4 Optical near-field energy and distance relation for CdTe spherical quantum dots from $(n,l,m) = (1,0,0)$ state of QDS to $(n',l',m') = (1,1,0)$ state of QDL.....	44
Figure 3.5.5 Optical near-field transfer rate and distance relation for CdTe spherical quantum dots from $(n,l,m) = (1,0,0)$ state of QDS to $(n',l',m') = (1,1,0)$ state of QDL.....	45
Figure 3.5.6 Optical near-field energy and distance relation for CdSe/ZnS spherical quantum dots from $(n,l,m) = (1,0,0)$ state of QDS to $(n',l',m') = (1,1,0)$ state of QDL.....	46
Figure 3.5.7 Optical near-field transfer rate and distance relation for CdSe/ZnS spherical quantum dots from $(n,l,m) = (1,0,0)$ state of QDS to $(n',l',m') = (1,1,0)$ state of QDL.....	47

Figure 3.5.8 Optical near-field energy and distance relation for PbSe spherical quantum dots from  $(n,l,m) = (1,0,0)$  state of QDS to  $(n',l',m') = (1,1,0)$  state of QDL.....47

Figure 3.5.9 Optical near-field transfer rate and distance relation for PbSe spherical quantum dots from  $(n,l,m) = (1,0,0)$  state of QDS to  $(n',l',m') = (1,1,0)$  state of QDL..... 48

Figure 3.5.10 Comparison of optical near-field energy transfer for PbSe, CdSe/ZnS, CdTe and CdSe spherical quantum dots from  $(n,l,m) = (1,0,0)$  state of QDS to  $(n',l',m') = (1,1,0)$  state of QDL. ....48

Figure 3.5.11 Optical near-field interactions between two cubic CuCl quantum dots with the size ratio of  $R_2/R_1 \approx 1.41$ . There is a resonance between  $(1,1,1)$  level of QD-S and  $(2,1,1)$  levels of QD-L.....50

Figure 3.5.12.a Optical near-field energy transfer for cubic CuCl quantum dots from  $(n_x,n_y,n_z) = (1,1,1)$  state of QDS to  $(n'_x,n'_y,n'_z) = (2,1,1)$  state of QDL.....51

Figure 3.5.12.b Optical near-field energy transfer rate for cubic CuCl quantum dots from  $(n_x,n_y,n_z) = (1,1,1)$  state of QDS to  $(n'_x,n'_y,n'_z) = (2,1,1)$  state of QDL.....52

*To my father...*

# Chapter 1

## Introduction

### 1.1 The optical far field and diffraction limit of light

One of the intrinsic characteristics of waves is diffraction. This phenomenon is explained as follows. Imagine that we have a plate with a very small aperture on the surface and plane light propagates on it. After the light passes through an aperture, it is converted into a diverging spherical wave. This divergence is called diffraction. The divergence angle is  $\lambda/a$  for a circular aperture where,  $\lambda$  is the wavelength of an incident light and  $a$  is the aperture radius. When the distance between the aperture and the plane in which the pattern is observed is large enough than the wavelength of light, then this region is often called a far field and expressed with a distance greater than  $D^2/4\lambda$ , where,  $D$  is the largest dimension in the aperture and  $\lambda$  is the wavelength of the incident light.

As shown in Figure 1.1.1, the plane wave incident on a positive lens is focused at a point by a convex lens. Even if we focus the light to the convex lens due to the diffraction limit, the spot size of the light cannot be zero. This phenomenon is called defocusing.

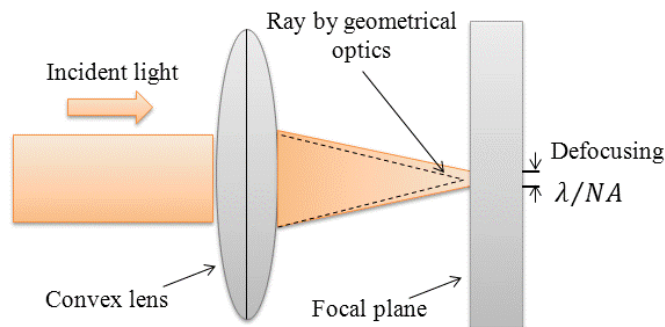


Figure 1.1.1 The schematic representation of residual defocusing.

The spot size of the light is about  $\lambda/NA$  where,  $NA$  is called the numerical aperture and usually is given as  $n\sin\theta$ . Here,  $n$  is the refractive index of the medium and the angle  $\theta$  is obtained from  $\sin\theta = (a/2)\sqrt{f^2 + (a/2)^2}$  where,  $f$  is focal length and  $a$  is the diameter of the lens.[2]

The semiconductor lasers, optical waveguides and related integrated photonic devices must confine the light within them for effective operation. However, as long as conventional light is used, the diffraction limit restrict the miniaturization of the optical science and technology. Therefore, to go beyond the diffraction limit we need nonpropagating localized light that is free of diffraction. Since optical near fields is free of diffraction it has been proposed to transcend the diffraction limit of light. [1]-[4]

## 1.2 What is optical near fields?

The optical near fields are spatially localized fields on the surface of nanometric particles. It is generated when we excite the nanometric material by incident light. Figure 1.2.1a represents the generation mechanism of optical near fields. Here the radius  $a$  of the sphere  $S$  is assumed to be much smaller than the wavelength of incident light. In the Figure 1.2.1.a the scattered light represents the light scattered from the surface of the sphere  $S$  and corresponds to the far field light. However, as a result of light-matter interaction an optical localized field with thickness about  $a$  is also generated on the surface of the sphere  $S$ . This localized field is called optical near-field. Since it is localized on the sphere  $S$  it cannot be separated from the sphere. The volume of this optical near field is smaller than the diffraction limited value because the size of a particle is much smaller than the wavelength of incident light  $a \ll \lambda$ . Figure 1.2.1b represents generation of an optical near field by a small aperture. The scattered light in the figure corresponds to the far field light and propagates to the far field. However, again the localized field around the aperture corresponds to the near fields. The decay length of near

field is much smaller than the wavelength of incident light and it does not depend on the wavelength. It only depends on the size of the nanometric material.

In figure 1.2.1a the thickness of the optical near field is about  $a$ . This can be explained as follows. By directing the light on the nanometric object  $S$  we excite electrons in  $S$ . As a result, due to the Coulomb forces generated from the electric field of incident light, the nuclei and electrons in atoms of  $S$  are displaced from their equilibrium position.

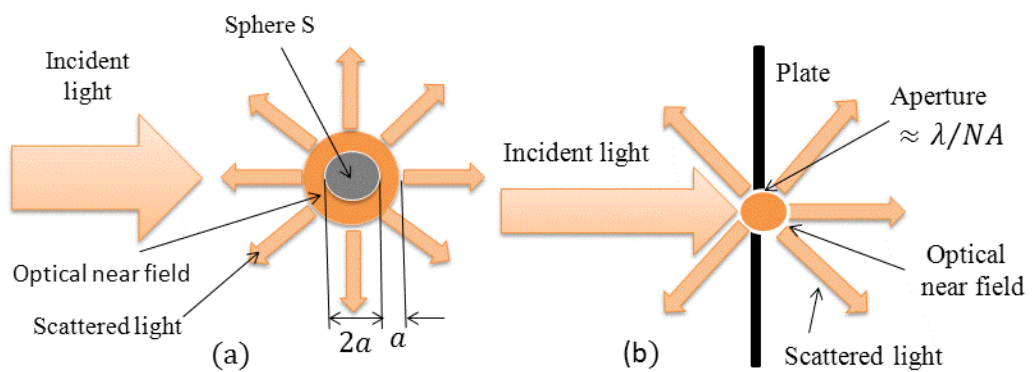


**Figure 1.2.1** The schematic representation of generation of an optical near field (a) Generation of optical near fields on the surface of the sphere  $S$ . (b) Generation of optical near fields by a small subwavelength aperture

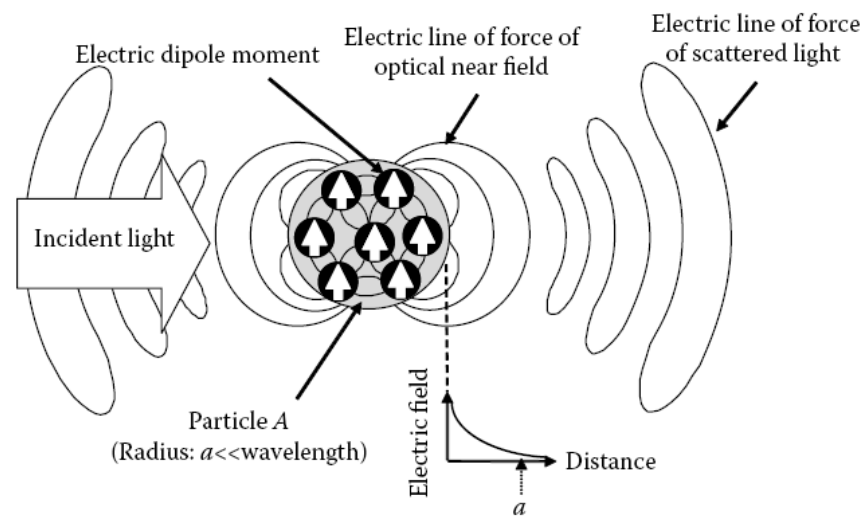


**Figure 1.2.2** Generation of optical near field and electric field lines. (Taken from M. Ohtsu Principles of Nanophotonics 2008.)

Since the nuclei and electrons are oppositely charged, their displacement direction are opposite. Therefore, electric dipoles are generated on the surface of the sphere  $S$ . The product of the charge and the displacement vector of electric dipole is called the electric dipole moment. These electric dipoles are oscillated with the oscillating electric field of incident light and attract or repel each other. As a result the spatially localized electric field with thickness  $a$  is generated on the surface of the sphere. Figure 1.2.2 shows the electric field lines of the dipoles on the sphere  $A$ . Represented electric field lines on the surface of the particle  $A$  corresponds to the optical near field. As shown in this figure the electric dipole moments are connected by these electric field lines. They represent the magnitude and orientations of the Coulomb forces. These electric lines tend to take possible shortest trajectory. They emanate from one electric dipole moment and terminate at another. This is the reason why optical near fields is very thin. As shown in the Figure 1.2.2 as we move away from the surface of the particle the optical near field potential decreases rapidly and at distance  $a$  it becomes negligible small. This arises from the fact that the most of the electric field lines are located on a close distances to the surface of a particle. The two kinds of electric field lines is shown in Figure 1.2.2. One is the electric lines of the optical near field which are at close proximity to the surface of particle  $A$ . The other force lines which form a closed loop correspond to the far field.

Figure 1.2.3 represents the nanometric and macroscopic subsystems. Nanometric subsystem consists optical near field and two particles. The macroscopic subsystem consists of the electromagnetic fields of scattered light incident light and substrate material. Since the optical near fields localized on the surface of the particle it does not carry energy to the far field, therefore it can not be detected. In order to detect the optical near fields the second particle  $P$  is placed near the particle  $S$ . By placing the particle  $P$  close to the near field of the particle  $S$  some of the force lines of the near field of the sphere  $S$  is directed to the surface of  $P$  and induces electric dipole moments on  $P$ . By this way, the near field of the particle  $S$  is disturbed by the particle  $P$  and disturbed near field is converted to the propogating light and its transferred energy can be detected by the photodetector.



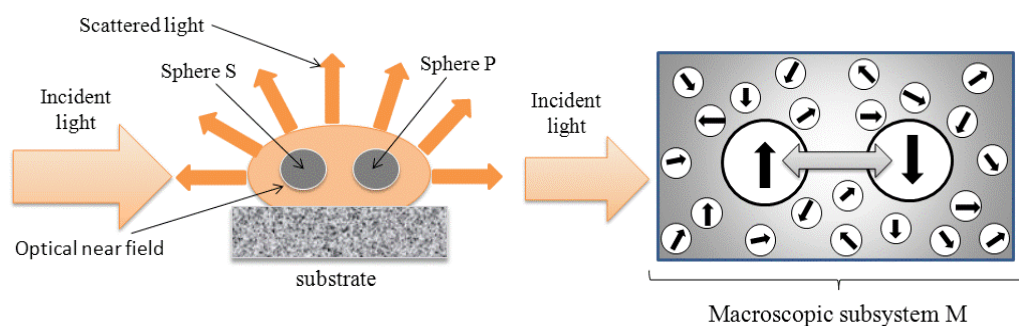


**Figure 1.2.3** Nanometric subsystem composed of two nanometric particles and optical near fields generated between them.

Here the two particles are considered interacting with each other by exchanging the exciton-polariton energies. Since the local electromagnetic interaction happens in a very short amount of time, the exchange of virtual exciton-polariton energies is allowed due to uncertainty principle. Optical near fields mediates this interaction, that is represented by Yukawa type function. [1]-[6] In the following chapters the theoretical background of the optical near fields and the numerical analysis for the energy transfer rate for different quantum dots is discussed. The organization of the rest of this thesis is given as following:

In Chapter 2 the theoretical background of optical near fields is presented. The near field conditions is shown and the dipole-dipole interaction model is described. By using the projection operator method the effective near field interaction potential is derived and the nature of the optical near field is described as a virtual cloud of photons.

In Chapter 3 the optical near field energy transfer is explained. The equation for the transferred energy from one state to another is derived for strong and weak confinement regime. The numerical analysis of the optical near-field energy transfer rate for spherical CdSe, CdTe, CdSe/ZnS and PbSe quantum dots was made. Finally, in Chapter 4 summarizing the thesis the application of the theory is briefly discussed.

## Chapter 2

# Theoretical Background of Optical Near Fields

### 2.1 Optical near field as a dipole-dipole interaction model

Let us investigate the optical near-field interaction in a viewpoint of dipole-dipole interaction model. For simplicity let us assume two separate nanometric particles with separation distance  $R$  and charge densities  $\rho_1$  and  $\rho_2$ . In this case the Coulomb interaction energy between these two nanometric object is given by

$$V_{12} = \frac{1}{4\pi\epsilon_0} \iint \frac{\rho_1(\vec{r}_1)\rho_2(\vec{r}_2)}{|\vec{r}_1 - \vec{r}_2|} d^3r_1 d^3r_2 \quad (2.1)$$

If we assume that the extent of the charge distributions  $\rho_1$  and  $\rho_2$  is much smaller than their separation  $R$ , we can expand the interaction potential  $V_{12}$  in a multiple series as

$$V_{12}(\vec{R}) = \frac{1}{4\pi\epsilon_0} \left[ \frac{q_1 q_2}{R} + \frac{q_1(\vec{p}_2 \cdot \vec{R})}{R^3} - \frac{q_2(\vec{p}_1 \cdot \vec{R})}{R^3} + \frac{R^2(\vec{p}_1 \cdot \vec{p}_2) - 3(\vec{p}_1 \cdot \vec{R})(\vec{p}_2 \cdot \vec{R})}{R^5} + \dots \right] \quad (2.2)$$

where  $\vec{R} = \vec{r}_2 - \vec{r}_1$ , and the multipole and dipole moments of the charge is defined as  $q = \int \rho(\vec{r}') d^3r'$  and  $\vec{p} = \int \rho(\vec{r}') \vec{r}' d^3r'$ , respectively. Here the first term of expansion is the charge-charge interaction and it spans over along distances since the distance dependence is  $R^{-1}$ . The next two terms correspond to the charge dipole interaction and has a distance dependence of  $R^{-2}$ . Therefore, it has a shorter range than the first term. The fourth term shows the dipole-dipole interaction and decays with  $R^{-3}$ . It is the most important interaction among neutral particles and strongly depends on the dipole orientations. This term gives

rise to Van der Waals forces and Förster-type energy transfer. In a similar way, the electric field vector can be given by [12],[33]

$$\vec{E} = \frac{1}{4\pi\epsilon_0} \left[ k^2 (\vec{n} \times \vec{p}) \times \vec{n} \left( \frac{1}{r} \right) + [3\vec{n}(\vec{n} \cdot \vec{p}) - \vec{p}] \left( -\frac{ik}{r^2} + \frac{1}{r^3} \right) \right] e^{ik\vec{r}} \quad (2.3)$$

Since the magnitude of the first term is larger for  $kr \gg 1$ , it represents the component dominating in the far field region. In contrast, the third term represents the electric field component that dominates in the close proximity of  $\vec{p}$  because it is the largest when  $kr \ll 1$ .

Now let us assume two point light sources. The separation distance between these two sources is  $b$  and it is assumed to be the size of material object as shown in Figure 2.1.1. The vector  $\vec{r}$  represents the separation distance between the object and the detection point S. Since we can treat the two particles as a point light source, the electric field  $\vec{E}(\vec{r}, t)$  at time  $t$  and the position  $\vec{r}$  can be defined as a superposition of the electric field vectors of the two point light sources

$$\vec{E}(\vec{r}, t) = \vec{E}_0 \frac{e^{-i\omega t + ik|\vec{r} + \vec{b}/2|}}{|\vec{r} + \vec{b}/2|^m} + \vec{E}_0 \frac{e^{-i\omega t + ik|\vec{r} - \vec{b}/2|}}{|\vec{r} - \vec{b}/2|^m} \quad (2.4)$$

where  $\vec{E}_0$  is the electric field vector of incident light,  $\omega = 2\pi\nu$  is the angular frequency and  $k = 2\pi/\lambda$  is the wave number. The quantity  $k|\vec{r} + \vec{b}/2|$  represents the phase delay  $\omega\Delta t$ . Here depending on the values of  $b$  and  $r$ , we can consider three possible cases.

### Case 1. $1 \ll kb \ll kr$

In this case, since  $1 \ll kb$ , the term proportional to  $r^{-1}$  in (2.3) is larger than the other terms and, hence, the value of  $m$  should be one. Therefore, (2.4) approximates to

$$\vec{E}(\vec{r}, t) = \vec{E}_0 \frac{e^{-i\omega t + ik\vec{r}}}{|\vec{r} + \vec{b}/2|} \left( \cos \frac{\vec{k}\vec{b}}{2} + i \sin \frac{\vec{k}\vec{b}}{2} \right) + \vec{E}_0 \frac{e^{-i\omega t + ik\vec{r}}}{|\vec{r} - \vec{b}/2|} \left( \cos \frac{\vec{k}\vec{b}}{2} - i \sin \frac{\vec{k}\vec{b}}{2} \right) \quad (2.5)$$

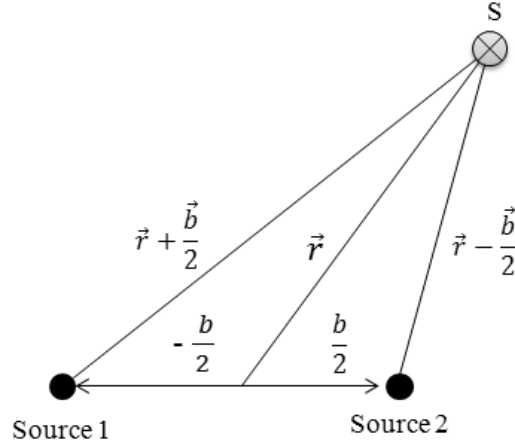


**Figure 2.1.1** Two point light sources with separation distance  $b$ .

where we used  $\exp\left(\pm i \frac{\vec{k}\vec{b}}{2}\right) = \cos \frac{\vec{k}\vec{b}}{2} \pm i \sin \frac{\vec{k}\vec{b}}{2}$ . Noticing that,  $\vec{n} = \frac{\vec{r}}{|\vec{r}|}$ ,  $\vec{n}_b = \frac{\vec{b}}{|\vec{b}|}$

and  $b \ll r$ , thus (2.5) becomes

$$\vec{E}(\vec{r}, t) \approx 2\vec{E}_0 \frac{e^{-i\omega t + i\vec{k}\vec{r}}}{r} \cos \frac{kb(\vec{n} \cdot \vec{n}_b)}{2} \quad (2.6)$$

To estimate the value  $b$  let us assume that  $|\vec{E}(\vec{r}, t)|$  is maximum at the position  $\vec{r}_0$  at which  $\vec{n}_0 = |\vec{r}_0|/r_0$  and  $(\vec{n}_0 \cdot \vec{n}_b) = 0$ . If at any other position  $\vec{r}_1$  the value of  $|\vec{E}(\vec{r}, t)|$  is maximum again, the relation  $kb(\vec{n}_1 \cdot \vec{n}_b)/2 = \pi$ . From this relation we can find  $b$  as  $b = 2\pi/k(\vec{n}_1 \cdot \vec{n}_b)$

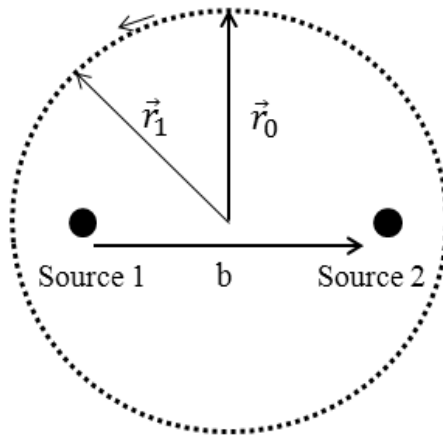


**Figure 2.1.2** Two positions  $\vec{r}_0$  and  $\vec{r}_1$  where  $|\vec{E}(\vec{r}, t)|$  reaches its maximum value.

### Case 2. $kb \ll 1 \ll kr$

In this case, since  $kb \ll kr$  again, the value of  $m$  in (2.4) takes unity. To estimate  $b$  from (2.6), the inequality  $kb |\vec{n} \cdot \vec{n}_b| \geq 2\pi$  should be satisfied. In other words the phase difference between the light waves of the two light sources has to be larger than  $\pi$  at the detection point. Since we have  $|\vec{n} \cdot \vec{n}_b| \leq 1$ , the requirement above changes to  $kb \geq 2\pi$ . This condition represents the diffraction limit of light. However, since  $kb \ll 1$  this requirement cannot be met and, therefore, the value of  $b$  cannot be obtained. In other words, since the phase difference between the two light waves is sufficiently small, we cannot measure the sub-wavelength-sized object at the detection point  $\vec{r}$  in the far field.

### Case 3. $kb < kr \ll 1$

In this case, since  $kr \ll 1$ , the terms in (2.3) proportional to  $r^{-1}$  and  $r^{-2}$  are very small and, thus, the term proportional to  $r^{-3}$  dominates. Therefore, we choose  $m=3$ . Also, since the phase delay  $k|\vec{r} + \vec{b}/2|$  is sufficiently small, (2.4) approximates to

$$\vec{E}(\vec{r}, t) = \vec{E}_0 e^{-i\omega t} \left( \frac{1}{|\vec{r} + \vec{b}/2|^3} + \frac{1}{|\vec{r} - \vec{b}/2|^3} \right) \quad (2.7)$$

If we assume that the electric field amplitude at point  $\vec{r}_0$  is  $|\vec{E}_1|$  and  $\vec{r}_0$  is normal to the vector  $\vec{b}$ , then the value  $b$  is derived from relation  $(\vec{n}_0 \cdot \vec{n}_b) = 0$  as

$$b = 2 \left[ \left( \frac{2|\vec{E}_0|}{|\vec{E}_1|} \right)^{2/3} - r_0^2 \right]^{1/2} \quad (2.8)$$

From this relation, we find  $\vec{E}_1$  to be  $|\vec{E}_1| = 2|\vec{E}_0| / \left[ \vec{r}_0^2 + (b/2)^2 \right]^{3/2}$ . It means that we can determine the value of  $b$  by the near field measurement. To conclude, the relation  $kb < kr \ll 1$  is called the near field condition and the range of  $r$  satisfying this condition  $kr \ll 1$  is called the near field.

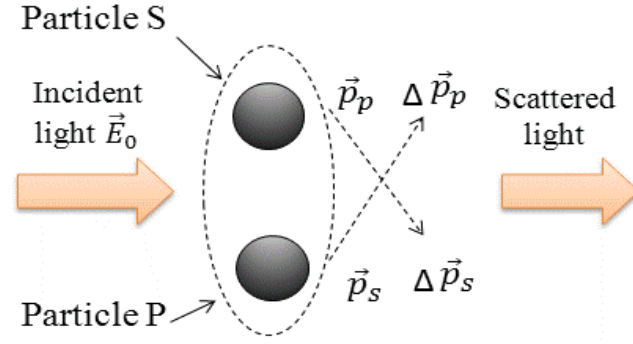


**Figure 2.1.3** Electric dipole moment induced in the spheres S and P located very close to each other.

Now let us assume that we have two spheres (sphere S and sphere P) and incident light with electric field  $\vec{E}_0$  as shown in Figure 2.1.3. Here the sphere P can be used as probe and the sphere S as a sample. The electric dipole moments induced in the spheres S and P by the electric field  $\vec{E}_0$  of the incident light are  $\vec{p}_p$  and  $\vec{p}_s$  respectively. The electric dipole moment  $\vec{p}_s$  of the sphere S generates an electric field in the sphere P. This field induces the change  $\Delta\vec{p}_p$  in the electric dipole moment of the sphere P. In a similar way, the electric field generated by the electric dipole moment  $\vec{p}_p$  induces the change  $\Delta\vec{p}_s$  in the electric dipole moment of the sphere S. We can repeat this process infinitely. This process, which mutually induces electric dipole moments in the spheres S and P, is called dipole-dipole interaction. In this case, the main contribution to the electric field comes from the terms proportional to  $r^{-3}$ , which is

$$\vec{E} = \frac{3\vec{n}(\vec{n} \cdot \vec{p}) - \vec{p}}{4\pi\epsilon_0 r^3} \quad (2.9)$$

Here since we have  $kr \ll 1$  we approximate the exponential part  $e^{-ik\vec{r}}$  to 1. When we take  $\vec{r} \parallel \vec{p}$ , the expression becomes

$$\vec{E} = \frac{2\vec{p}}{4\pi\epsilon_0 r^3} \quad (2.10)$$

Similarly, when  $\vec{r}$  is perpendicular to  $\vec{p}$  ( $\vec{r} \perp \vec{p}$ ), the equation turns into [2],[32]

$$\vec{E} = -\frac{\vec{p}}{4\pi\epsilon_0 r^3} \quad (2.11)$$

Equations (2.10) and (2.11) represent the optical near field generated around the spheres S and P. If we assume that the spheres S and P are dielectric, the electric dipole moment  $\vec{p}_s$  induced by the incident electric field  $\vec{E}_0$  is

$$\vec{p}_s = \alpha_s \vec{E}_0 \quad (2.12)$$

Here  $\alpha_s$  is the polarizability of the dielectric.

In the near field case, if the conditions  $kR \ll 1$  and  $\vec{R} \parallel \vec{p}$  are satisfied, the electric field generated in the sphere P by the electric dipole moment  $\vec{p}_s$  can be written as

$$\vec{E}_s = \frac{2\vec{p}_s}{4\pi\epsilon_0 R^3} \quad (2.13)$$

Therefore, we can write the change in the electric dipole moment of the sphere P as

$$\Delta\vec{p}_p = \alpha_p \vec{E}_s = \frac{2\alpha_p \alpha_s}{4\pi\epsilon_0 R^3} \vec{E}_0 \quad (2.14)$$

Since we can represent the change in the dipole moment as  $\Delta\vec{p}_p = \Delta\alpha_p \vec{E}_0$ , the change in the polarizability of the sphere P can be given as

$$\Delta\alpha_p = \frac{\alpha_p \alpha_s}{2\pi\epsilon_0 R^3} \quad (2.15)$$

where  $\alpha_s$  and  $\alpha_p$  are  $\alpha_i = g_i a_i^3$  and  $g_i = 4\pi\epsilon_0 \frac{\epsilon_i - \epsilon_0}{\epsilon_i + 2\epsilon_0}$  for (i=S,P),  $a_s$  and  $a_p$  are

the respective radii, and  $\epsilon_s$  and  $\epsilon_p$  are the electric constants of the spheres S and P, respectively. If we replace the role of the spheres S and P, the discussion above will be still valid. The electric dipole moment  $\vec{p}_p = \alpha_p \vec{E}_0$  will generate the electric field  $\vec{E}_p = 2\vec{p}_p / 4\pi\epsilon_0 \vec{R}^3$  in the sphere S and induce the change  $\Delta\vec{p}_s = \Delta\alpha_s \vec{E}_0$  in the electric dipole moment. Therefore,  $\Delta\alpha_s$  and  $\Delta\alpha_p$  takes the same value as

$$\Delta\alpha_s = \Delta\alpha_p = \Delta\alpha = \frac{\alpha_p \alpha_s}{2\pi\epsilon_0 R^3} \quad (2.16)$$

Since in the near field condition ( $kR \ll 1$ ) we assume that the two spheres are very close to each other, they can be recognized as a single object for the far-field detection. Therefore, the intensity  $I_s$  of the scattered light generated from the total electric dipole moment  $\vec{p}_p + \Delta\vec{p}_p + \vec{p}_s + \Delta\vec{p}_s$  is

$$I_S \propto |(\vec{p}_P + \Delta\vec{p}_P) + (\vec{p}_S + \Delta\vec{p}_S)|^2 \quad (2.17)$$

Taking into account that  $\vec{p}_S = \alpha_S \vec{E}_0$  and  $\Delta\vec{p}_S = \Delta\alpha_S \vec{E}_0$ , we have

$$I_S \propto (\alpha_S + \alpha_P)^2 |\vec{E}_0|^2 + 4\Delta\alpha(\alpha_S + \alpha_P) |\vec{E}_0|^2 \quad (2.18)$$

Here the first term  $(\alpha_S + \alpha_P)^2 |\vec{E}_0|^2$  corresponds to the intensity of the light scattered directly by the spheres S and P, whereas the second term  $4\Delta\alpha(\alpha_S + \alpha_P) |\vec{E}_0|^2$  represents the intensity of scattered light as a result of dipole-dipole interaction. From the equation above, we obtain [2]

$$\Delta\alpha = \frac{g_P g_S}{2\pi\epsilon_0} \frac{\alpha_P^3 \alpha_S^3}{R^3} \quad (2.19)$$

Relation 2.19 shows that the optical near field intensity strongly depends on the size of the spheres.

## 2.2 Projection operator method, relevant nanometric irrelevant macroscopic subsystems, P and Q spaces

We can use the projection operator method to derive effective interaction in the nanometric material system illuminated by an incident light. This type of interaction is called optical near-field interaction. It is estimated that optical near-field interaction potential between the nanometric objects with a separation distance  $R$  is given as a sum of Yukawa potentials

$$\Upsilon = \frac{\exp(-\alpha R)}{R} \quad (2.20)$$

Here  $\alpha^{-1}$  represents the range of the interaction and corresponds to the characteristic size of nanometric material system. It depends on the size of the nanomaterial and does not depend on the wavelength of the incident light.

$\alpha^{-1}$  represents the localization of photons around the nanomaterial. [1], [7]



On the basis of projection operator method, we can investigate the formulation of the optical near-field system. In order to describe optical near-field interaction in a nanometric system, we think of the relevant nanometric subsystem N and irrelevant macroscopic subsystem M. The macroscopic subsystem M is mainly composed of the incident light and the substrate. The subsystem N is composed of the sample, the probe tip, and the optical near-field. To describe the quantum mechanical state of matter in the subsystems N and M, the energy states of the sample and probe in the subsystem N are expressed as  $|s\rangle$  and  $|p\rangle$ . The relevant excited states for the sample and probe tip are  $|s^*\rangle$  and  $|p^*\rangle$ . It is most reasonable to express the subsystem M as an exciton-polariton. The macroscopic subsystem M is composed of the mixed state of electromagnetic field and material excitation. Since the sample or the probe tip is excited by the electromagnetic interaction, the state of the subsystem N can be expressed as the mixed states of the excited and ground states. Therefore, we define the  $P$  space, which is spanned by the eigenstates  $|\phi_1\rangle$  and  $|\phi_2\rangle$ ,  $P_{Space} \in \{|\phi_1\rangle, |\phi_2\rangle\}$ . [3],[7] Since it is expressed as a mixture of the excited and ground states, we can define  $|\phi_1\rangle$  and  $|\phi_2\rangle$  as

$$|\phi_1\rangle = |s^*\rangle |p\rangle \otimes |0_{(M)}\rangle \quad |\phi_2\rangle = |s\rangle |p^*\rangle \otimes |0_{(M)}\rangle \quad (2.21)$$

where  $|s\rangle$  and  $|s^*\rangle$  are the ground and excited eigenstates of the sample and  $|p\rangle$  and  $|p^*\rangle$  are the ground and excited eigenstates of the probe tip. Here  $|0_{(M)}\rangle$  represents the vacuum state for exciton-polaritons to describe the macroscopic subsystem M. The complementary space to  $P$  space is called  $Q$  space.

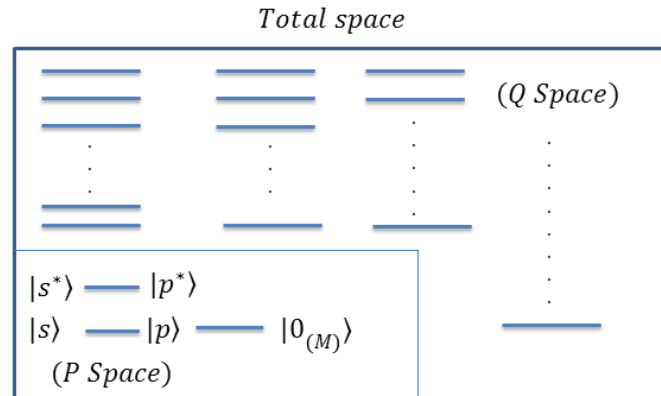


**Figure 2.2.1** The schematic representation of  $P$  space spanned by the eigenstates  $|\phi_1\rangle$  and  $|\phi_2\rangle$  and its complementary space  $Q$ .

In Figure 2.2.1 we have the schematic representation of  $P$  and its complementary space  $Q$ . The complementary  $Q$  space is spanned by a huge number of basis that is not included in  $P$  space. This method of description is called projection operator method.

The projection operator method is used to describe the quantum mechanical approach of the optical near-field interaction system that is nanometric materials surrounded by the incident light. The reason why  $|\phi_1\rangle$  and  $|\phi_2\rangle$  contain the vacuum state  $|0\rangle$  is to introduce the effect of the subsystem (M) by eliminating its degree of freedom. This treatment is useful to derive consistent expression for the magnitude of effective near-field interaction potential between the elements of the subsystem (N). As a result of this approach, the subsystem (N) can be treated as an independent system that is regarded to be isolated from the subsystem (M). [1],[3].

## 2.3 Optical near-field interaction potential in the nanometric subsystem

By using projection operator method, we can evaluate effective interaction in  $P$  space, which is derived in Appendix B, as

$$\hat{V}_{eff} = (P\hat{J}^+ \hat{J}P)^{-1/2} (P\hat{J}^+ \hat{V} \hat{J}P) (P\hat{J}^+ \hat{J}P)^{-1/2} \quad (2.22)$$

This result gives us an effective interaction potential of the nanometric subsystem N, which can be found in Appendix A. The Hamiltonian for the interaction between a sample or a probe and electromagnetic fields as a dipole approximation can be expressed as

$$\hat{V} = -\left\{ \hat{\mu}_s \cdot \hat{D}^\perp(\vec{r}_s) + \hat{\mu}_p \cdot \hat{D}^\perp(\vec{r}_p) \right\} \quad (2.23)$$

The electric dipole operator is denoted by  $\hat{\mu}_\alpha$  ( $\alpha = s, p$ ), where the subscript  $s$  and  $p$  represent the physical quantities related to the sample and the probe tip,

respectively.  $\vec{r}_s$  and  $\vec{r}_p$  are the vectors representing the position of the sample and the tip, respectively;  $\hat{D}^\perp(\vec{r})$  is the transverse component of the quantum mechanical electric displacement operator.  $\hat{D}^\perp(\vec{r})$  can be expressed in terms of the photons creation  $\hat{a}_\lambda^*(\vec{k})$  and annihilation  $\hat{a}_\lambda(\vec{k})$  operators as follows

$$\hat{D}^\perp(\vec{r}) = i \sum_{\vec{k}} \sum_{\lambda=1}^2 \left( \frac{2\pi\hbar\omega_{\vec{k}}}{V} \right)^{1/2} \vec{e}_\lambda(\vec{k}) \{ \hat{a}_\lambda(\vec{k}) e^{i\vec{k}\vec{r}} - \hat{a}_\lambda^*(\vec{k}) e^{-i\vec{k}\vec{r}} \} \quad (2.24)$$

where  $\vec{k}$  is the wavevector,  $\omega_{\vec{k}}$  is the angular frequency of photon,  $V$  is the quantization volume in which electromagnetic fields exist and  $\vec{e}_\lambda(\vec{k})$  is the unit vector related to the polarization direction of the photon. [34] Since exciton-polariton states as bases are employed as the bases to describe the macroscopic subsystem M, the creation and annihilation operators for photon can be replaced with the creation and annihilation operators of exciton-polariton. Therefore, after replacing photons creation and annihilation operators with exciton-polaritons and substituting  $\hat{\mu}_s = \vec{\mu}_s (\hat{B}(\vec{r}_\alpha) + \hat{B}^+(\vec{r}_\alpha))$  into (2.24), we can change the notation from photon base to exciton-polariton base as

$$\hat{V} = -i \sum_{\alpha=s}^p \sum_{\vec{k}} \left( \frac{2\pi\hbar}{V} \right)^{1/2} (\hat{B}(\vec{r}_\alpha) + \hat{B}^+(\vec{r}_\alpha)) \{ K_\alpha(\vec{k}) \hat{\xi}(\vec{k}) - K_\alpha^*(\vec{k}) \hat{\xi}^+(\vec{k}) \} \quad (2.25)$$

Here  $\hat{B}(\vec{r}_\alpha)$  and  $\hat{B}^+(\vec{r}_\alpha)$  denote the annihilation and creation operators for the electronic excitation in the sample or probe ( $\alpha = s, p$ ) and  $K_\alpha(\vec{k})$  is the coefficient of the coupling strength between the exciton-polariton and the nanometric subsystem N and it is given by

$$K_\alpha(\vec{k}) = \sum_{\lambda=1}^2 (\vec{\mu}_\alpha \cdot \vec{e}_\lambda(\vec{k})) f(k) e^{i\vec{k}\vec{r}_\alpha} \quad (2.26)$$

we define  $f(k)$  as

$$f(k) = \frac{ck}{\sqrt{\Omega(k)}} \sqrt{\frac{\Omega^2(k) - \Omega^2}{2\Omega^2(k) - \Omega^2 - (ck)^2}} \quad (2.27)$$

$\Omega(k)$  and  $\Omega$  are the eigenfrequencies of both exciton-polariton and electronic excitation of the macroscopic subsystem M. [10],[31]

The amplitude of effective probe-tip interaction exerted in the nanometric subsystem can be defined as

$$V_{eff}(2,1) \equiv \langle \phi_2 | \hat{V}_{eff} | \phi_1 \rangle \quad (2.28)$$

In order to derive the explicit form of effective interaction  $V_{eff}(2,1)$ , the initial and final states ( $|\phi_1\rangle = |s^*\rangle |p\rangle \otimes |0_{(M)}\rangle$  and  $|\phi_2\rangle = |s\rangle |p^*\rangle \otimes |0_{(M)}\rangle$ ) are employed in  $P$  space before and after interaction. The approximation of  $\hat{J}$  to the first order is (see Appendix B for derivations) given by

$$\begin{aligned} V_{eff}(2,1) &= \langle \phi_2 | P \hat{V} Q \hat{V} (E_P^0 - E_Q^0)^{-1} P | \phi_1 \rangle + \langle \phi_2 | P (E_P^0 - E_Q^0)^{-1} \hat{V} Q \hat{V} P | \phi_1 \rangle = \\ &= \sum_m \langle \phi_2 | P \hat{V} Q | m \rangle \langle m | Q \hat{V} P | \phi_1 \rangle \left( \frac{1}{E_{P1}^0 - E_{Qm}^0} + \frac{1}{E_{P2}^0 - E_{Qm}^0} \right) \end{aligned} \quad (2.29)$$

where  $E_P^0$  and  $E_Q^0$  are eigenvalues of the unperturbed Hamiltonian  $\hat{H}_0$  in  $P$  and  $Q$  spaces. The equation shows that the matrix element  $\langle m | Q (E_P^0 - E_Q^0)^{-1} \hat{V} P | \phi_1 \rangle$  represents a virtual transition from the initial state  $|\phi_1\rangle$  in  $P$  space to the intermediate state  $|m\rangle$  in  $Q$  space and  $\langle \phi_2 | P \hat{V} Q | m \rangle$  represents the virtual transition from the intermediate state  $|m\rangle$  in  $Q$  space to the final state  $|\phi_2\rangle$  in  $P$  space. So, we can transform (2.10) to the following equation (please refer to Appendix B)

$$V_{eff}(2,1) = -\frac{1}{(2\pi)^2} \int d^3k \left[ \frac{K_p(\vec{k}) K_s^*(\vec{k})}{\Omega(k) - \Omega_0(s)} + \frac{K_s(\vec{k}) K_p^*(\vec{k})}{\Omega(k) + \Omega_0(p)} \right] \quad (2.30)$$

where the summation over  $\vec{k}$  is replaced by  $\vec{k}$ -integration, which is  $\sum_{\vec{k}} \rightarrow \frac{V}{(2\pi)^3} \int d^3k$  and  $E_s = \hbar\Omega_0(s)$  and  $E_p = \hbar\Omega_0(p)$  are the excitation energies of the sample (between  $|s^*\rangle$  and  $|s\rangle$ ) and the probe tip (between  $|p^*\rangle$  and  $|p\rangle$ ), respectively. Similarly, the probe-sample interaction  $V_{eff}(1,2)$  can be written as follows

$$V_{eff}(1,2) = -\frac{1}{(2\pi)^2} \int d^3k \left[ \frac{K_s(\vec{k})K_p^*(\vec{k})}{\Omega(k) - \Omega_0(p)} + \frac{K_p(\vec{k})K_s^*(\vec{k})}{\Omega(k) + \Omega_0(s)} \right] \quad (2.31)$$

The total amplitude of the effective sample-probe tip interaction can be defined as the sum of  $V_{eff}(1,2)$  and  $V_{eff}(2,1)$

$$V_{eff}(\vec{r}) = -\frac{1}{4\pi^2} \sum_{\alpha=s,p} \sum_{\lambda=1}^2 \int d^3k \left[ \vec{\mu}_s(\vec{r}) \cdot \vec{e}_\lambda(\vec{k}) \right] \left[ \vec{\mu}_p(\vec{r}) \cdot \vec{e}_\lambda(\vec{k}) \right] \hbar f^2(k) \times \left( \frac{e^{i\vec{k}\vec{r}}}{E(k) + E(\alpha)} + \frac{e^{-i\vec{k}\vec{r}}}{E(k) - E(\alpha)} \right) d^3k \equiv \sum_{\alpha=s,p} \left[ V_{eff,\alpha+}(\vec{r}) + V_{eff,\alpha-}(\vec{r}) \right] \quad (2.32)$$

where  $E(k) = E_m + \frac{(\hbar k)^2}{2m_{pol}}$  is the eigenenergy of exciton-polariton and  $m_{pol}$  is effective mass of polariton. The integration gives us the following result

$$V_{eff,\alpha\pm f}(\vec{r}) = \mp \frac{1}{2} \left[ (\vec{\mu}_s \cdot \vec{\mu}_p) W_{\alpha\pm} e^{-\Delta_{\alpha\pm} r} \left\{ \frac{(\Delta_{\alpha\pm})^2}{r} + \frac{\Delta_{\alpha\pm}}{r^2} + \frac{1}{r^3} \right\} \mp \right. \\ \left. \mp \frac{1}{2} \left[ -(\vec{\mu}_s \cdot \hat{r})(\vec{\mu}_p \cdot \hat{r}) W_{\alpha\pm} e^{-\Delta_{\alpha\pm} r} \left\{ \frac{(\Delta_{\alpha\pm})^2}{r} + \frac{3\Delta_{\alpha\pm}}{r^2} + \frac{3}{r^3} \right\} \right] \right] \quad (2.33)$$

where  $\Delta_{\alpha\pm} \equiv \frac{1}{\hbar c} \sqrt{2E_{pol}(E_m \pm E_\alpha)}$  and  $W_{\alpha\pm}$  is defined as

$$W_{\alpha\pm} = \frac{E_{pol}}{E_\alpha} \frac{E_m^2 - E_\alpha^2}{(E_m \pm E_\alpha)(E_m - E_{pol} \mp E_\alpha) - E_m^2/2} \quad (2.34)$$

After summing up and taking the angular average of  $(\vec{\mu}_s \cdot \hat{r})(\vec{\mu}_p \cdot \hat{r}) = (\vec{\mu}_s \vec{\mu}_p)/3$ , we have

$$V_{eff}(\vec{r}) = -\frac{(\vec{\mu}_A \cdot \vec{\mu}_B)}{3} \sum_{\alpha=s,p} \left\{ W_{\alpha+} (\Delta_{\alpha+})^2 \frac{e^{-\Delta_{\alpha+} r}}{r} - W_{\alpha-} (\Delta_{\alpha-})^2 \frac{e^{-\Delta_{\alpha-} r}}{r} \right\} \quad (2.35)$$

Equation(2.35) shows effective near-field interaction potential in the nanometric subsystem. The effective near-field interaction is expressed as a sum of Yukawa functions  $\Upsilon(\Delta_{\alpha\pm} r) = e^{-\Delta_{\alpha\pm} r}/r$  with a heavier effective mass  $\Delta_{\alpha+}$  (shorter interaction range) and a lighter effective mass  $\Delta_{\alpha-}$  (longer interaction range). This

part of the interaction comes from the mediation of massive virtual photons or polaritons and this formulation indicates a “dressed photon” picture in which as result of light-matter interaction, photons are not massless but massive[1],[2],[3],[7]-[10]

## 2.4 Optical near-fields as a virtual cloud of photons and locally excited states

To investigate the behavior of optical near field in a viewpoint of virtual photons let us first calculate probe sample interaction potential  $V_{eff}(p, s)$

$$V_{eff}(p, s) = -\frac{1}{(2\pi)^2} \int d^3k \left( \frac{K_p(\vec{k})K_s^*(\vec{k})}{\Omega(k) - \Omega_0(s)} + \frac{K_s(\vec{k})K_p^*(\vec{k})}{\Omega(k) + \Omega_0(p)} \right) \quad (2.36)$$

If we consider two infinitely deep potential wells with the widths  $a_p$  and  $a_s$ , the eigenenergies of sample and probe are given as

$$\hbar\Omega_0(s) = \frac{3\hbar^2}{2m_{eS}} \left( \frac{\pi}{a_s} \right)^2 \quad (2.37, a)$$

$$\hbar\Omega_0(p) = \frac{3\hbar^2}{2m_{eP}} \left( \frac{\pi}{a_p} \right)^2 \quad (2.37, b)$$

Where  $m_{eS}$  and  $m_{eP}$  are the effective masses of electron in the sample and probe.

Since the coefficient  $K_\alpha(\vec{k})$  is expressed as  $K_\alpha(\vec{k}) = \sum_{\lambda=1}^2 (\vec{\mu}_\alpha \cdot \vec{e}_\lambda(\vec{k})) f(k) e^{i\vec{k}\vec{r}_\alpha}$ , the effective sample probe interaction is then

$$V_{eff}(p, s) = -\frac{1}{(2\pi)^2} \int d^3k \left( \frac{\sum_{\lambda=1}^2 (\vec{\mu}_s \cdot \vec{e}_\lambda(\vec{k})) (\vec{\mu}_p \cdot \vec{e}_\lambda(\vec{k})) f^2 \cdot e^{i\vec{k}(\vec{r}_p - \vec{r}_s)}}{\left( \frac{\hbar k^2}{2m_p} + \Omega \right) - \frac{3\hbar}{2m_{eS}} \left( \frac{\pi}{a_s} \right)^2} \right) - \frac{1}{(2\pi)^2} \int d^3k \left( \frac{\sum_{\lambda=1}^2 (\vec{\mu}_s \cdot \vec{e}_\lambda(\vec{k})) (\vec{\mu}_p \cdot \vec{e}_\lambda(\vec{k})) f^2 \cdot e^{i\vec{k}(\vec{r}_s - \vec{r}_p)}}{\left( \frac{\hbar k^2}{2m_p} + \Omega \right) + \frac{3\hbar}{2m_{eS}} \left( \frac{\pi}{a_p} \right)^2} \right) \quad (2.38)$$

Defining heavy and light effective masses as  $\Delta_+$  and  $\Delta_-$  where we have

$$\Delta_+ = \left( \frac{3\pi^2 m_p}{m_{eS} a_p^2} + \frac{2m_p \Omega}{\hbar} \right)^{1/2} \quad \Delta_- = \left( \frac{3\pi^2 m_p}{m_{eS} a_s^2} - \frac{2m_p \Omega}{\hbar} \right)^{1/2} \quad (2.39)$$

Therefore (2.38) changes to

$$V_{eff}^{p,s} = -\frac{1}{(2\pi)^2} \int d^3k \sum_{\lambda=1}^2 (\vec{\mu}_s \cdot \vec{e}_\lambda(\vec{k})) (\vec{\mu}_p \cdot \vec{e}_\lambda(\vec{k})) f^2 \left( \frac{e^{i\vec{k}(\vec{r}_p - \vec{r}_s)}}{\frac{\hbar}{2m_p}(k^2 - \Delta_-^2)} + \frac{e^{i\vec{k}(\vec{r}_s - \vec{r}_p)}}{\frac{\hbar}{2m_p}(k^2 + \Delta_+^2)} \right) \quad (2.40)$$

where we approximate some of the terms as a constant and take  $f(k)$  as  $f$ .

In Figure 2.4.1 the positions given by  $\vec{r}_s$  and  $\vec{r}_p$  represent the arbitrary positions in the sample and probe, respectively, and the position vector is defined as  $\vec{r} = |\vec{r}_p - \vec{r}_s|$ . The integration of complex integral with respect to  $k$  gives us the following result for  $V_{eff}(p, s)$  (refer to Appendix D for derivations)

$$V_{eff}(p, s) = -\frac{1}{2} \sum_{i,j=1}^3 (\vec{\mu}_{si} \cdot \vec{\mu}_{pj}) \delta_{ij} \left[ \frac{\exp(-\Delta_+ r)}{r} + \frac{\exp(i\Delta_- r)}{r} \right] \propto \frac{\exp(-\Delta_+ r)}{r} + \frac{\exp(i\Delta_- r)}{r} \quad (2.41)$$

and 
$$V_{eff}(p, s) \propto \frac{\exp(-\pi\mu_p r/a_p)}{r} + \frac{\exp(i\pi\mu_s r/a_s)}{r} \quad (2.42)$$

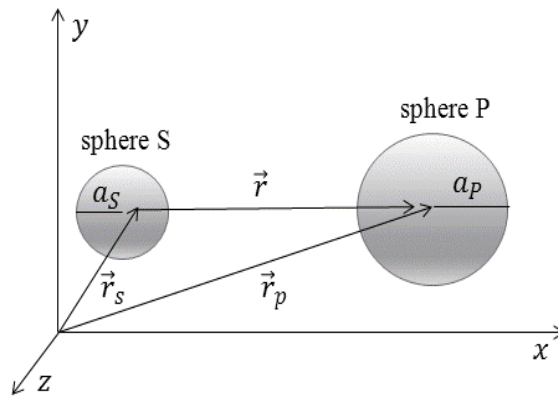


**Figure 2.4.1.** Schematic representation of near-field optical system.  $\vec{r}_s$  and  $\vec{r}_p$  show the arbitrary positions in sample and probe.

where

$$\mu_p = \frac{\sqrt{3}m_p}{m_{eP}}, \quad \mu_s = \frac{\sqrt{3}m_s}{m_{eS}} \quad (2.43)$$

The first term in Equation (2.42) represents Yukawa function behavior. Its decay length is  $a_p/\pi\mu_p$  and proportional to the probe size  $a_p$ . The first term  $\exp(-\pi\mu_p r/a_p)/r$  shows that there is optical electromagnetic field around the probe and the extent of spatial distribution of this field is equivalent to the probe size. This field localizes around the probe like an electron cloud localized around an atomic nucleus. However, since the real photon does not have a localized nature, it is considered that optical near fields contain massive virtual photons. As a result of light-matter interaction, the two particles are considered to be interacting by exchanging real and virtual exciton-polariton energies.

Figure 2.4.2 represents the real and virtual transitions. In this energy transfer process, the virtual transition is mediated by the virtual exciton-polariton and does not follow the conventional energy conservation law. This can be explained by the fact that this virtual transition occurs in a sufficiently short period of time  $\Delta t$  and satisfies the uncertainty principle  $\Delta E\Delta t \geq \hbar/2$ . In other words, since the required time for this local near-field interaction is sufficiently small, due to the uncertainty principle the exchange of virtual exciton-polariton energy between these two nanometric particles is allowed. [1],[2],[4]

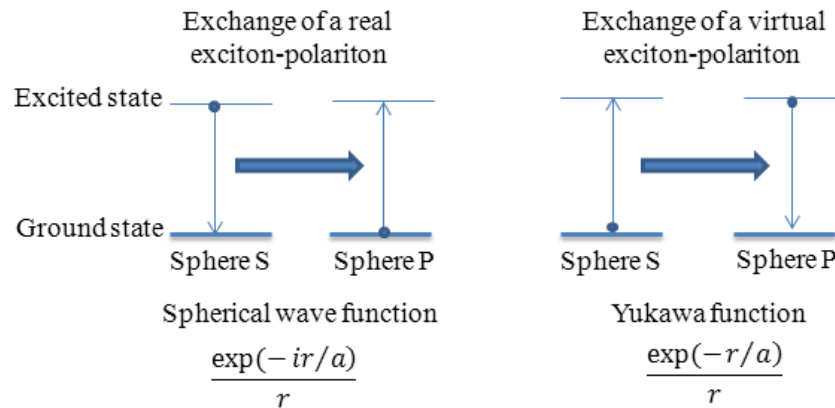


**Figure 2.4.2** Exchange of real and virtual exciton-polariton.



When the quantum dot is excited by propagating light, the conventional classical electrodynamics explains that an electric dipole at the center of QD is induced and the electric field generated from this electric dipole is detected in the far-field region. However, in a quantum theoretical view, the electron in the quantum dot is excited from the ground state to an excited state due to the interaction between the electric dipole and electric field of the propagating light, which is called electric dipole transition. It is assumed that two anti parallel electric dipoles are induced in a quantum dot and the electric field generated by one electric dipole is cancelled by the other in the far field region and thus the transition from the excited state cannot take place. Then the transition and excited state are said to be dipole forbidden [2].

Figure 2.4.3 illustrates the system composed of two coupled quantum dots with two arbitrary resonantly coupled energy levels. These two resonant energy levels are coupled as a result of the near field interaction and as a result of this coupling, the quantized energy levels of exciton are split in two parts. One half of them corresponds to the symmetric state of the exciton, and the other half corresponds to the antisymmetric state of the exciton in the quantum dot. These two symmetric and antisymmetric states correspond to the parallel and antiparallel electric dipole moments that is induced in these relevant quantum dots.[1],[2],[11].

The ground and excited states of exciton in quantum dot S are expressed as  $|s_e\rangle$  and  $|s_g\rangle$ . Similarly, the ground and excited states in quantum dot P are expressed as  $|p_e\rangle$  and  $|p_g\rangle$ . The energy eigenvalues of the excited states  $|s_e\rangle$  and  $|p_e\rangle$  are expressed as  $E_e$  while the energy eigenvalues of the ground states  $|s_g\rangle$  and  $|p_g\rangle$  is  $E_g$ . Since they have the equal energy eigenvalues, the states  $|s_e\rangle$  and  $|p_e\rangle$  also  $|s_g\rangle$  and  $|p_g\rangle$  are said to be in resonance with each other.

The Hamiltonian of this two level system is expressed as following

$$\hat{H} = \hat{H}_0 + \hat{H}_{\text{int}} \quad (2.44)$$

where,  $\hat{H}_0$  and  $\hat{H}_{\text{int}}$  represent the unperturbed and interaction Hamiltonian.

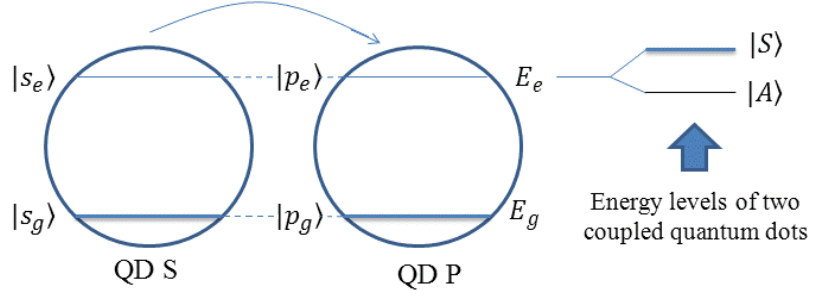


**Figure 2.4.3** The system composed of QD S and P with two resonant coupled energy levels.  $|S\rangle$  and  $|A\rangle$  are correspond to symmetric and antisymmetric states.

When two isolated quantum dots placed close enough in order to induce the effective near-field interaction  $V_{eff}(r)$ , the energy eigenstate and eigenvalue for symmetric state  $|S\rangle$  are expressed as

$$|S\rangle = \frac{1}{\sqrt{2}}(|p_e\rangle|s_g\rangle + |p_g\rangle|s_e\rangle) \quad (2.45.a)$$

$$E_S = E_g + E_e + V_{eff}(r) \quad (2.45.b)$$

while for antisymmetric state  $|A\rangle$  are

$$|A\rangle = \frac{1}{\sqrt{2}}(|p_e\rangle|s_g\rangle - |p_g\rangle|s_e\rangle) \quad (2.46.a)$$

$$E_A = E_g + E_e - V_{eff}(r) \quad (2.46.b)$$

Equation (2.45.a) means that since exciton exists in both quantum dot S and quantum dot P with equal probabilities, an exciton in this system cannot be distinguished.

Now, let us evaluate the scalar product of the transition dipoles  $\vec{\mu}_s \cdot \vec{\mu}_p$  in terms of the states  $|S\rangle$  and  $|A\rangle$ . For simplicity we take transition dipole moments parallel with magnitudes as  $\mu_i = |\vec{\mu}_i| > 0$  ( $i = s, p$ ). We can express the dipole moment by creation and annihilation operators as

$$\hat{\vec{\mu}}_i = \vec{\mu}_i(\hat{b}_i + \hat{b}_i^\dagger), \quad (i = s, p) \quad (2.47)$$

where

$$\hat{b}_i^\dagger |i_g\rangle = |i_e\rangle \quad \text{and} \quad \hat{b}_i |i_g\rangle = |0\rangle \quad (2.48)$$

therefore we have

$$\begin{aligned}\langle S | \vec{\mu}_s \cdot \vec{\mu}_p | S \rangle &= \frac{\vec{\mu}_s \vec{\mu}_p}{2} \left( \langle s_e | \langle p_g | + \langle s_g | \langle p_e | \right) (\hat{b}_s + \hat{b}_s^+) (\hat{b}_p + \hat{b}_p^+) \left( | p_e \rangle | s_g \rangle + | p_g \rangle | s_e \rangle \right) = \\ &= \frac{\vec{\mu}_s \vec{\mu}_p}{2} \left( \langle s_e | \langle p_g | \hat{b}_s \hat{b}_p^+ | p_e \rangle | s_g \rangle + \langle s_g | \langle p_e | \hat{b}_s^+ \hat{b}_p | p_g \rangle | s_e \rangle \right) = \mu_s \mu_p > 0 \\ \langle S | \vec{\mu}_s \cdot \vec{\mu}_p | S \rangle &= \mu_s \mu_p > 0\end{aligned}\quad (2.49)$$

It indicates that the transition dipole moments  $\vec{\mu}_s$  and  $\vec{\mu}_p$  are parallel in symmetric state  $|S\rangle$ . Similarly for antisymmetric state  $|A\rangle$  we have

$$\langle A | \vec{\mu}_s \cdot \vec{\mu}_p | A \rangle = -\mu_s \mu_p < 0 \quad (2.50)$$

and shows that they are antiparallel in antisymmetric state. It follows from equations (2.49) and (2.50) that excitation of quantum dots with far field light leads to the symmetric state with parallel dipoles produced in QDs S and P. In contrast the near-field excitation of QDs can produce either one or both of the symmetric and antisymmetric states. Therefore, the symmetric state is called the bright state and antisymmetric state is called the dark state. This is one of the major differences between the near-field and far-field excitations. In particular locally excited states can be created in this two level system. These locally excited states can be expressed by a linear combination of symmetric and antisymmetric states as [1],[2],[5],[6],[7]

$$| p_e \rangle | s_g \rangle = \frac{1}{\sqrt{2}} (| S \rangle + | A \rangle) \quad (2.51.a)$$

$$| p_g \rangle | s_e \rangle = \frac{1}{\sqrt{2}} (| S \rangle - | A \rangle) \quad (2.51.b)$$

The right-hand terms of (2.51.a) and (2.51.b) describes the coupled states via an optical near-field. Here, the optical near-field excites both of the coupled states. However, in the far field excitation the only symmetric state is excited. The state vector  $|\psi(t)\rangle$  at time  $t$  is

$$|\psi(t)\rangle = \frac{1}{\sqrt{2}} \left[ \exp\left(-\frac{iE_S t}{\hbar}\right) | S \rangle + \exp\left(-\frac{iE_A t}{\hbar}\right) | A \rangle \right] \quad (2.52)$$

where the state vectors  $|\psi(t)\rangle$  are also normalized and at  $t = 0$   $|\psi(0)\rangle = |p_e\rangle |s_g\rangle$

and

$$|\psi(t)\rangle = \exp\left(-\frac{i\bar{E}t}{\hbar}\right) \left[ \cos\left(\frac{V_{eff}(r)t}{\hbar}\right) |p_e\rangle |s_g\rangle - i \sin\left(-\frac{V_{eff}(r)t}{\hbar}\right) |p_g\rangle |s_e\rangle \right] \quad (2.53)$$

$$\bar{E} = \frac{E_S + E_A}{2} = E_g + E_e \quad (2.54)$$

Then the occupation probability that the electrons in QD-P occupy the excited and the electrons in QD-S occupy the ground state is expressed as

$$\rho_{p_e s_g} = |\langle s_g | \langle p_e || \psi(t) \rangle|^2 = \cos^2\left(\frac{V_{eff}(r)t}{\hbar}\right) \quad (2.55)$$

Similarly, the occupation probability that the electrons in QD-P occupy the ground and the electrons in QD-S occupy the excited state is expressed as

$$\rho_{p_g s_e} = |\langle s_e | \langle p_g || \psi(t) \rangle|^2 = \sin^2\left(\frac{V_{eff}(r)t}{\hbar}\right) \quad (2.54)$$

The equations (2.55) and (2.54) shows that the probability varies periodically with period of  $T = \pi\hbar/V_{eff}(r)$ . It means that the excitation energy of the system is periodically transferred between the coupled resonant energy levels of QD-S and QD-P. This process is called nutation.

## Chapter 3

# Optical Near Field Interaction between Spherical Quantum Dots

### 3.1 Introduction

There are three regimes of confinement introduced depending on the ratio of the crystallite radius  $R$  to the Bohr radius of electrons, holes, and electron-hole pairs, respectively. Very small quantum dots belong to strong confinement regime. In this confinement regime the Bohr radius of the exciton is several times larger than the size of quantum dot. In these quantum dots we can neglect the Coulomb interaction between the electron and the hole. Therefore, the individual motions of the electron and the hole are quantized separately. The Bohr radius of PbSe nanocrystal is 46 nm and it is a good example for strong confinement.

If effective mass of the holes is much bigger than that of the electrons one can speak of intermediate confinement regime. In this confinement regime the radius of the quantum dot has to be smaller than the Bohr radius of electron and larger than the Bohr radius of the hole because the mass of the electron is smaller than that of the hole [14]

In weak confinement regime the radius of quantum dot is at least a few times larger than the Bohr radius of an exciton. In this case the Coulomb interaction potential between the electron and the hole is so strong that we can assume the electron-hole pair as a single particle called an exciton. Since the Bohr radius of CuCl nanocrystal is 0.7 nm, this can be a typical example of weak confinement regime.

## 3.2 Energy states of semiconductor quantum dots

Quantum dots are nanostructures in which electrons and holes are confined to a small region in all the three dimensions. An electron-hole pair created in these nanostructures by irradiating light has discrete eigenenergies. This assumption arises from the fact that the wave functions of electron-hole pairs are confined in these nanomaterials. This is called quantum confinement effect.

Since the property of nanostructures is determined by a lot of electron-hole pairs, it is useful to employ the envelope function and effective mass approximation. Therefore, the one-particle wavefunction in a semiconductor nanostructure can be given by the product of the envelope function satisfying the boundary conditions of the quantum dot and one-particle wavefunction in bulk form of the same semiconductor material. Thus, the eigenstate vector for single electron is given by

$$|\psi_e\rangle = \int d^3r \xi_e(\vec{r}) \hat{\psi}_e^+(\vec{r}) |\Phi_g\rangle \quad (3.1)$$

where  $\xi_e(\vec{r})$  is the envelope function of the electron,  $\hat{\psi}_e^+(\vec{r})$  is the field operator for electron creation, and  $|\Phi_g\rangle$  is the crystal ground state. Here the field operators for the electron creation  $\hat{\psi}_e^+(\vec{r})$  and annihilation  $\hat{\psi}_e(\vec{r})$  satisfy the following Fermi anti-commutation relation

$$\left[ \hat{\psi}_e(\vec{r}'), \hat{\psi}_e^+(\vec{r}) \right]_+ = \hat{\psi}_e(\vec{r}') \hat{\psi}_e^+(\vec{r}) - \hat{\psi}_e^+(\vec{r}) \hat{\psi}_e(\vec{r}') = \delta(\vec{r} - \vec{r}') \quad (3.2)$$

where  $\delta(\vec{r} - \vec{r}')$  is the Dirac delta function. Since neither an electron in the conduction band nor a hole in the valence band exists, we can consider the ground state of a crystal as a vacuum state [13]. Therefore applying electron annihilation operator to the crystal ground state gives us zero

$$\hat{\psi}_e(\vec{r}) |\Phi_g\rangle = 0 \quad (3.3)$$

We can find the equation for envelope function  $\xi_e(\vec{r})$  by using the Schrödinger equation

$$\hat{H}_e |\psi_e\rangle = E_e |\psi_e\rangle \quad (3.4)$$

Here,  $E_e$  is the energy eigenvalue. From quantum mechanics we know that the Hamiltonian of non-interacting electron-hole system is

$$\hat{H}_{e,h} = \sum_{\alpha=e,h} \int d^3r \cdot \hat{\psi}_\alpha^+(\vec{r}) \left( -\frac{\hbar^2 \nabla^2}{2m_\alpha} + E_g \right) \hat{\psi}_\alpha(\vec{r}) \quad (3.5)$$

Since we are looking for a single electron in the QD, the Hamiltonian will change to

$$\hat{H}_e = \int d^3r \cdot \hat{\psi}_e^+(\vec{r}) \left[ -\frac{\hbar^2}{2m_e} \nabla^2 \right] \hat{\psi}_e(\vec{r}) + E_g \int d^3r \cdot \hat{\psi}_e^+(\vec{r}) \hat{\psi}_e(\vec{r}) \quad (3.6)$$

where  $m_e$  is the effective mass of electron and  $E_g$  is the energy band gap of the bulk semiconductor material. Substituting the Hamiltonian for a single electron into the Schrödinger equation, we obtain

$$\begin{aligned} \hat{H}_e |\psi_e\rangle &= \int d^3r' \hat{\psi}_e^+(\vec{r}') \left[ -\frac{\hbar^2}{2m_e} \nabla^2 \right] \hat{\psi}_e(\vec{r}') \int d^3r \xi_e(\vec{r}) \hat{\psi}_e^+(\vec{r}) |\Phi_g\rangle + \\ &+ E_g \int d^3r' \hat{\psi}_e^+(\vec{r}') \hat{\psi}_e(\vec{r}') \int d^3r \xi_e(\vec{r}) \hat{\psi}_e^+(\vec{r}) |\Phi_g\rangle = \int d^3r' \hat{\psi}_e^+(\vec{r}') \left[ -\frac{\hbar^2}{2m_e} \nabla^2 \right] \times \\ &\times \int d^3r (\delta(\vec{r} - \vec{r}') - \hat{\psi}_e^+(\vec{r}) \hat{\psi}_e(\vec{r}')) \xi_e(\vec{r}) |\Phi_g\rangle + E_g \int d^3r' \hat{\psi}_e^+(\vec{r}') \times \\ &\times \int d^3r (\delta(\vec{r} - \vec{r}') - \hat{\psi}_e^+(\vec{r}) \hat{\psi}_e(\vec{r}')) \xi_e(\vec{r}) |\Phi_g\rangle = -\frac{\hbar^2}{2m_e} \int d^3r' \int d^3r \delta(\vec{r} - \vec{r}') \times \\ &\times \nabla^2 \xi_e(\vec{r}) \hat{\psi}_e^+(\vec{r}') |\Phi_g\rangle + E_g \int d^3r' \int d^3r \delta(\vec{r} - \vec{r}') \xi_e(\vec{r}) \hat{\psi}_e^+(\vec{r}') |\Phi_g\rangle = \\ &= \int d^3r \left[ -\frac{\hbar^2}{2m_e} \nabla^2 \xi_e(\vec{r}) \right] \hat{\psi}_e^+(\vec{r}) |\Phi_g\rangle + E_g \int d^3r \xi_e(\vec{r}) \hat{\psi}_e^+(\vec{r}) |\Phi_g\rangle \end{aligned} \quad (3.7)$$

Here we used the Fermi anticommutation relation. So, the Schrödinger equation simplified to the following expression

$$\hat{H}_e |\psi_e\rangle = \int d^3r \left[ -\frac{\hbar^2}{2m_e} \nabla^2 \xi_e(\vec{r}) \right] \hat{\psi}_e^+(\vec{r}) |\Phi_g\rangle + E_g \int d^3r \xi_e(\vec{r}) \hat{\psi}_e^+(\vec{r}) |\Phi_g\rangle \quad (3.8)$$

where we have

$$E_e |\psi_e\rangle = E_e \int d^3r \xi_e(\vec{r}) \hat{\psi}_e^+(\vec{r}) |\Phi_g\rangle \quad (3.9)$$

From Equations (3.7) and (3.8) it follows that the envelope function satisfy the following eigenvalue equation for a single electron

$$-\frac{\hbar^2}{2m_e} \nabla^2 \xi_e(\vec{r}) = (E_e - E_g) \xi_e(\vec{r}) \quad (3.10)$$

Similarly, we can obtain envelope function for one hole state as follows

$$-\frac{\hbar^2}{2m_h} \nabla^2 \xi_h(\vec{r}) = E_h \xi_h(\vec{r}) \quad (3.11)$$

where  $E_g = 0$  is used for hole.

Since we study spherical quantum dots, we assume that the envelope function satisfies the following spherical boundary condition.

$$\xi_e(\vec{r}) = \xi_h(\vec{r}) = 0 \text{ for } |\vec{r}| > R \quad (3.12)$$

The Laplace operator in spherical coordinates is then

$$\begin{aligned} \nabla^2 &= \frac{1}{r} \frac{\partial}{\partial r^2} r - \frac{\vec{L}^2}{r^2} \\ \vec{L}^2 &= - \left( \frac{1}{\sin \theta} \frac{\partial}{\partial \theta} \sin \theta \frac{\partial}{\partial \theta} + \frac{1}{\sin^2 \theta} \frac{\partial^2}{\partial \phi^2} \right) \end{aligned} \quad (3.13)$$

We can separate the envelope function  $\xi(\vec{r})$  into radial and angular parts as follows

$$\xi(\vec{r}) = f_l(r) Y_{lm}(\theta, \phi)$$

Here  $\vec{L}$  is the orbital angular momentum operator and satisfies the following eigenvalue equation

$$\vec{L}^2 Y_{lm}(\theta, \phi) = l(l+1) Y_{lm}(\theta, \phi) \quad (3.14)$$

where  $|m| \leq l$  ( $m = 0, \pm 1, \pm 2, \dots$ ) and functions  $Y_{lm}(\theta, \phi)$  are the spherical harmonics with  $l = 0, 1, 2, \dots$ . To find the envelope function we have to solve the eigenvalue equation (3.10). Writing the Laplacian in the spherical coordinates the eigenvalue equation changes to

$$-\frac{\hbar^2}{2m_e} \left( \frac{1}{r} \frac{\partial^2}{\partial r^2} r - \frac{\vec{L}^2}{r^2} \right) f_l(r) Y_{lm}(\theta, \phi) = (E_e - E_g) f_l(r) Y_{lm}(\theta, \phi) \quad (3.15)$$

and

$$Y_{lm}(\theta, \phi) \frac{1}{r} \frac{\partial^2}{\partial r^2} (r f_l(r)) - \frac{f_l(r)}{r^2} \vec{L}^2 Y_{lm}(\theta, \phi) = -\frac{2m_e}{\hbar^2} (E_e - E_g) f_l(r) Y_{lm}(\theta, \phi) \quad (3.16)$$

taking the derivatives we have

$$\frac{2}{r} \frac{df_l(r)}{dr} + \frac{d^2 f_l(r)}{dr^2} - \frac{f_l(r)}{r^2} l(l+1) = -\alpha^2 f_l(r)$$



and finally we have

$$\frac{d^2 f_l}{dr^2} + \frac{2}{r} \frac{df_l}{dr} + [\alpha^2 - l(l+1)] f_l = 0 \quad (3.17)$$

with  $\alpha^2 \equiv \frac{2m_e}{\hbar^2} (E_e - E_g)$  for electron, or  $\alpha^2 \equiv \frac{2m_h}{\hbar^2} E_h$  for hole. [35]

The solution for (3.17) has the form of spherical Bessel function of order  $l$  as

$$f_{nl}(r) = \sqrt{\frac{2}{R^3}} \frac{j_l(\alpha_{nl} r/R)}{j_{l+1}(\alpha_{nl})} \quad (3.18)$$

where  $j_l$  is the spherical Bessel function of order  $l$  and  $\alpha_{nl}$  can be determined from the boundary conditions as  $j_l(\alpha_{nl}) = 0$  for  $(n=0,1,2,\dots)$  and  $\alpha_{n0} = n\pi$ ,  $\alpha_{11} = 4.4934$ . The energy eigenvalues are discrete and given by [15], [25], [26], [27].

$$E_{e,nlm} = E_g + \frac{\hbar^2}{2m_e} \left( \frac{\alpha_{nl}}{R} \right)^2 \quad \text{and} \quad E_{h,nlm} = \frac{\hbar^2}{2m_h} \left( \frac{\alpha_{nl}}{R} \right)^2 \quad (3.19)$$

These are the energy levels of one particle states in a semiconductor quantum dots.

Next, let us concentrate on the electron-hole pair states in a quantum dot. The hole is a quasiparticle relevant to an electron in the valence band from which an electron is removed. The hole is characterized by the positive charge  $+e$ , effective mass  $m_h^*$ , spin  $1/2$  and kinetic energy with a sign opposite to that of electron's kinetic energy. When an electron acquires enough energy to move from valence band to conduction band, a free hole is created in the valence band and electron-hole pairs are generated. [13]

Here, we consider crystal ground state as a vacuum state. In this state neither electron nor hole exists in the conduction and valence band, respectively. However, in the first excited state there exists one electron in the conduction band and also there is one hole in the valence band. Therefore one electron-hole pair is generated. The minimum energy which is sufficient for the creation of one

electron-hole pair is called band gap energy and defined by  $E_g$ . When electrons are excited across the gap, the bottom of the conduction band and the top of valence band are populated by the electrons and holes, respectively.

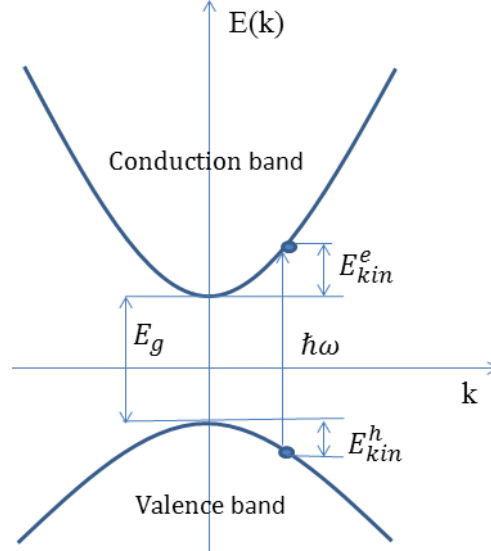


**Figure 3.2.1** Band structure and energy band gap  $E_g$  of bulk semiconductor. The diagram shows the creation of one electron-hole pair as a result of photon absorption.

Because of the photon absorption there occurs a transition from the ground state to the first excited state. The conservation of energy and momentum can be written as following

$$\begin{aligned}\hbar\omega &= E_g + E_{kin}^e + E_{kin}^h \\ \hbar\vec{k}_p &= \hbar\vec{k}_e + \hbar\vec{k}_h\end{aligned}\tag{3.20}$$

where  $E_{kin}^e$  and  $E_{kin}^h$  are the kinetic energy of the electron and hole. Similarly,  $\hbar\vec{k}_e$  and  $\hbar\vec{k}_h$  are the momentum of electron and hole, respectively. This is the process of electron-hole pair creation. The reverse process which is equivalent to the annihilation of the electron-hole pair and creation of photon is also possible.

Sometimes to make calculations easier we ignore the interaction between electrons and holes. However, in reality, since electrons and holes are charged particles they interact with each other via the Coulomb interaction potential and form an extra quasiparticle called an exciton. Interacting electrons and holes can be described by the following Hamiltonian [13],[16]

$$\hat{H} = -\frac{\hbar^2}{2m_e^*} \nabla_e^2 - \frac{\hbar^2}{2m_h^*} \nabla_h^2 + \frac{e^2}{\varepsilon |\vec{r}_e - \vec{r}_h|} + U(r) \quad (3.21)$$

where  $m_e^*$  and  $m_h^*$  are the effective mass of the electron and the hole, respectively, and  $\varepsilon$  is the dielectric constant of the crystal.

Now, to compute the energies and wavefunctions of electron-hole systems in spherical quantum dots, let us consider the following eigenstate vectors for an electron-hole pair

$$|\psi_{eh}\rangle = \iint d^3r_e d^3r_h \psi(\vec{r}_e, \vec{r}_h) \hat{\psi}_e^+(\vec{r}_e) \hat{\psi}_h^+(\vec{r}_h) |\Phi_g\rangle \quad (3.22)$$

where  $|\Phi_g\rangle$  is the crystal ground state,  $\hat{\psi}_e^+(\vec{r}_e)$  and  $\hat{\psi}_h^+(\vec{r}_h)$  are the field operators for the electron creation in the conduction and hole creation in the valence band.  $\psi(\vec{r}_e, \vec{r}_h)$  is the envelope function for an electron-hole pair and satisfies the following equation

$$\left[ -\frac{\hbar^2}{2m_e} \nabla_e^2 - \frac{\hbar^2}{2m_h} \nabla_h^2 + V_C + V_{Conf} \right] \psi_{eh}(\vec{r}_e, \vec{r}_h) = (E - E_g) \psi_{eh}(\vec{r}_e, \vec{r}_h) \quad (3.23)$$

where  $V_C$  is the Coulomb interaction potential and  $V_{Conf}$  is the confinement potential. If the confinement region is a sphere with radius  $R$ ,  $V_{Conf}(\vec{r}) = 0$  for  $|\vec{r}| \leq R$  [25].

It might be useful if we examine electron-hole pair states by comparing the confinement radius  $R$  with the Bohr radius of exciton. Depending on the radius of the quantum dots and the exciton Bohr radius, we can introduce three types of confinement regimes. First is the strong confinement where the radius of quantum dot is smaller than the Bohr radius of exciton  $R \ll a_B$ . As an example intermediate confinement we consider the case where the radius of quantum dot is smaller than Bohr radius of electron and bigger than the Bohr radius of the hole  $a_h < R < a_e$ . The third is weak confinement regime in which the quantum dot size is a few times larger than the exciton Bohr radius  $R \gg a_B$ .

## 3.3 Quantum confinement regimes

### 3.3.1 Strong confinement

In strong confinement regime, the size of the quantum dot is smaller than the Bohr radius of exciton  $R \ll a_B$ . In this case the Coulomb interaction between an electron and hole pair is weak and each electron and hole can independently move in the corresponding electron or hole confinement potential [1]. For this quantum dots it might be a good approximation if we take Coulomb interaction potential to be zero. This is the basic assumption behind the strong confinement approximation. Since individual motions of the electron and the hole quantized separately and the size quantization effect of the electron and the hole is much larger than the exciton effect, we can neglect the quantization effect of exciton. The envelope function in this case is then

$$\Psi(\vec{r}_e, \vec{r}_h) = \psi_{nlm}(\vec{r}_e) \psi_{n'l'm'}(\vec{r}_h) \quad (3.24)$$

where  $\psi_{nlm}(\vec{r}_e)$  and  $\psi_{n'l'm'}(\vec{r}_h)$  are the envelope functions of an electron in the conduction band and the envelope function of the hole in the valence band, respectively. The explicit form of these functions for spherical quantum dots is [27]

$$\psi_{nlm} = \sqrt{\frac{2}{R^3}} \frac{j_l(\alpha_{nl} \cdot r/R)}{j_{l+1}(\alpha_{nl})} Y_{lm}(\Omega) \quad (3.25)$$

The optical transitions is allowed between the conduction and valence band states only with the same quantum numbers ( $nlm \rightarrow n'l'm'$ ) and the energy levels are given as

$$E_{nlm} = E_g + \frac{\hbar^2}{2m_r} \left( \frac{\alpha_{nl}}{R} \right)^2 \quad (3.26)$$

where  $m_r$  is the reduced mass and defined as  $\frac{1}{m_r} = \frac{1}{m_e} + \frac{1}{m_h}$

By using variational approach the energy of the ground state (1s) of an electron-hole pair can be expressed in the following form

$$E_{1s} = E_g + \frac{\hbar^2}{2m_r} \left( \frac{\pi}{R} \right)^2 - 1.786 \frac{e^2}{\varepsilon R} \quad (3.27)$$

where the term  $e^2/\varepsilon R$  describes effective Coulomb interaction between electron-hole pairs and  $\varepsilon$  is the dielectric permittivity of the medium. PbSe, PbS, HgSe, GaAs, and InSb nanocrystals can be good example for strong confinement regime.

### 3.3.2 Intermediate confinement

The second confinement regime is known as intermediate confinement. For example, in the case when the effective mass of the holes is much bigger than that of the electrons ( $m_e/m_h \ll 1$ ) we can speak of intermediate confinement regime. In this particular situation the radius of quantum dot is smaller than the Bohr radius of the electron but still bigger than the Bohr radius of the hole  $a_h < R < a_e$  where

$$a_e = \frac{\varepsilon_1 \hbar^2}{m_e e^2} \quad a_h = \frac{\varepsilon_1 \hbar^2}{m_h e^2} \quad (3.28)$$

Then one may assume that a hole can move in an average potential generated by a free-electron confined within a QD, and approximate the envelope function of the exciton in the quantum dot as

$$\Psi(\vec{r}_e, \vec{r}_h) = \psi_{nlm}(\vec{r}_e) \chi_{nlm}^{n'l'm'}(\vec{r}_h) \quad (3.29)$$

Using the orthonormalization of  $\psi_{nlm}(\vec{r}_e)$  we can write the equation for the envelope function of the holes as

$$\left[ -\frac{\hbar^2}{2m_h} \nabla_h^2 - \int d\vec{r}_e |\psi_{nlm}(\vec{r}_e)|^2 V_c \right] \chi_{nlm}^{n'l'm'}(\vec{r}_h) = \left( E - E_g - \frac{\hbar^2}{2m_e} \frac{\alpha_{nl}^2}{R^2} \right) \chi_{nlm}^{n'l'm'}(\vec{r}_h) \quad (3.30)$$

Here  $V_{conf} = 0$  and spherical confinement is assumed. For spherical confinement

the discrete energy levels are  $\frac{\hbar^2}{2m_e} \frac{\alpha_{nl}^2}{R^2}$  and the envelope function of the electron is

$\psi(\vec{r}_e) = \psi_{nlm}(\vec{r}_e)$ . When the electron is in the state  $(n, l=0, m=0)$  the hole experiences the following spherically symmetric potential

$$V_{n00} = -\frac{e^2}{\varepsilon_0} \int \frac{|\Psi_{n00}(\vec{r}')|}{|\vec{r} - \vec{r}'|} d\vec{r}' = -\frac{e^2}{\varepsilon_0 R_0} \beta_n + \frac{1}{2} m_h \omega_n^2 r^2 \quad (3.31)$$

where  $\beta_n = 2 \int_0^{n\pi} \frac{\sin^2 x}{x} dx$  and  $\omega_n^2 = \frac{2}{3} \frac{\pi^2 n^2}{m_h R_0^2} \frac{e^2}{\varepsilon_0 R_0}$ .

Here  $R_0$  is the radius of a quantum dot. The explicit form of eigenfunction  $\chi_{n00}^{n'00}(\vec{r})$  solved with the potential (3.31) is [15]

$$\chi_{n00}^{n'00}(\vec{r}) = \left[ \frac{m_h \omega_n}{\pi \hbar} \right]^{1/4} \frac{1}{\sqrt{2^{n'} n'!}} \exp\left(-\frac{m_h \omega_n}{2\hbar} r^2\right) \frac{H_{n'}\left[r \sqrt{\frac{m_h \omega_n}{\hbar}}\right]}{r} \quad (3.32)$$

where  $H_{n'}$  is the  $n'$ th order Hermite polynomial and the energy states is defined as

$$E_{n00}^{n'00} = E_g - \frac{e^2}{\varepsilon_0 a} \beta_n + \hbar \omega_n \left(n' + \frac{1}{2}\right) \quad (3.33)$$

### 3.3.3 Weak confinement

In larger quantum dots when the dot radius  $R$  is small but still a few times larger than the exciton Bohr radius,  $R \gg a_B$  quantization of the exciton center-of-mass motion occurs [8]. The confinement effects in this size regime are relatively small. Because the Coulomb interaction between an electron and a hole becomes strong, it is good approximation to treat an electron-hole pair as a single particle, which is called an exciton. Defining the mass of exciton as  $M = m_e + m_h$ , the center of mass coordinates as  $\vec{r}_{CM} = (m_e \vec{r}_e + m_h \vec{r}_h)/M$ , and the relative coordinates as  $\vec{\beta} = \vec{r}_e - \vec{r}_h$ , the approximate electron-hole-pair wavefunction is [1]

$$\Psi_{nlm}(\vec{r}_e, \vec{r}_h) = \phi(\vec{\beta}) \psi_{nlm}(\vec{r}_{CM}) \quad (3.34)$$

where the function  $\phi(\vec{\beta}) = \frac{1}{\sqrt{\pi a_0^3}} e^{\left(\frac{-\vec{\beta}}{a_0}\right)}$  describes the relative motion in the lowest (1s) bound state of the bulk material and  $\psi_{nlm}(\vec{r}_{CM})$  is the wavefunction for the confined motion of the mass center  $\vec{r}_{CM} = (m_e \vec{r}_e + m_h \vec{r}_h)/M$ . For spherical boundary conditions the wavefunction  $\psi_{nlm}$  is

$$\psi_{nlm} = \sqrt{\frac{2}{R^3}} \frac{j_l(\alpha_{nl} \cdot r/R)}{j_{l+1}(\alpha_{nl})} Y_{lm}(\Omega) \quad (3.35)$$

The wavefunction(3.6) is an exact solution of the one electron-hole pair stationary Schrödinger equation (Wannier equation). Corresponding exciton eigenenergies for spherical quantum dots are

$$E_{nlm} = E_g - E_R + \frac{\hbar^2 \alpha_{nl}^2}{2MR^2} \quad (3.36)$$

where  $E_R$  is the binding energy of the exciton in the bulk semiconductor nanocrystal. This is sometimes called Rydberg energy. Since for the lowest state quantum numbers satisfy  $(n=1, l=0)$  condition and  $(\alpha_{10} = \pi)$ , the exciton energy for this lowest (1s) state is expressed as

$$E_{1s} = E_g - E_{Ry} + \frac{\hbar^2}{2M} \left(\frac{\pi}{R}\right)^2 \quad (3.37)$$

A weak confinement is realizable in wide-band semiconductors of I-VII compounds having a small exciton Bohr radius and large exciton Rydberg energy. Copper chloride (CuCl) nanocrystals is the typical example for weak confinement regime. Its exciton Rydberg energy is  $E_{Ry} = 200meV$  and the Bohr radius is  $a_B = 0.7nm$ .

### 3.4 Optical near field interaction energy between spherical quantum dots for strong and weak confinement regimes

There has been introduced various theories to investigate the excitation energy transfer between nanometric objects. Förster resonance energy transfer (FRET) is one of the typical modeling of excitation energy transfer from smaller quantum dot to larger quantum dot. But since it is the point dipole modelings of excitation energy transfer between nanometric materials, the transitions to forbidden energy levels which is the case in the experimental conditions when the two quantum dots are placed very close to each other, doesn't allowed, [17] The novel theory based on dressed photon model can explain the allowance of this forbidden transitions.

#### 3.4.1 Strong confinement

To calculate the optical near-field energy transfer driven by the exciton dynamics between two quantum dots we can begin with the interaction Hamiltonian. The interaction Hamiltonian between photons and nanomaterial is given by [19]

$$\hat{H}_{\text{int}} = -\int \psi^+(\vec{r}) \vec{\mu}(\vec{r}) \psi(\vec{r}) \cdot \hat{D}(\vec{r}) d\vec{r} \quad (3.38)$$

where  $\psi^+(\vec{r})$  and  $\psi(\vec{r})$  are the field operators for the electron creation in the conduction band and annihilation in the valence band.  $\vec{\mu}(\vec{r})$  and  $\hat{D}(\vec{r})$  are the dipole moment and the electric displacement operators. The explicit form of displacement operator in exciton-polariton base (in terms of exciton-polariton creation and annihilation operators  $\hat{\zeta}_k^+$  and  $\hat{\zeta}_k^-$ ) is [19]

$$\hat{D} = i \sqrt{\frac{2\pi}{V}} \sum_k \sum_{\lambda=1}^2 \vec{e}_{\lambda}(\vec{k}) f(k) \left( \hat{\zeta}_k^- e^{i\vec{k}\vec{r}} - \hat{\zeta}_k^+ e^{-i\vec{k}\vec{r}} \right) \quad (3.39)$$

In the case of strong confinement regime the Coulomb interaction is weak and the electron and the hole can move independently. Therefore, the wave function of electron-hole pair can be written as



$$\Psi(\vec{r}_e, \vec{r}_h) = F_\mu(\vec{r}_e)F_{\mu'}(\vec{r}_h) \quad (3.40)$$

where  $F_\mu(\vec{r}_e)$  is the envelope function of conduction-band electron and  $F_{\mu'}(\vec{r}_h)$  is the envelope function of valence-band hole.  $\mu = (m, n, l)$  and  $\mu' = (m', n', l')$  are the set of quantum numbers corresponding to electron and hole, respectively. Therefore, the exciton state  $|\Phi_\nu\rangle$  is [15]

$$|\Phi_\nu\rangle = \sum_{\vec{R}, \vec{R}'} F_\mu(\vec{r}_e)F_{\mu'}(\vec{r}_h)\hat{a}_{c\vec{R}}^+\hat{a}_{v\vec{R}'}|\Phi_g\rangle \quad (3.41)$$

Here,  $\nu = (\mu, \mu')$  and  $\hat{a}_{c\vec{R}}^+$ ,  $\hat{a}_{v\vec{R}'}$  are the electron creation operator at  $\vec{R}$  in the conduction band and hole annihilation operator at  $\vec{R}'$  in the valence band, and  $|\Phi_g\rangle$  is the crystal ground state. Thus, to estimate the effective interaction between two quantum dots, we must first calculate transition matrix elements from the exciton state  $|\Phi_\nu\rangle$  to the ground state  $|\Phi_g\rangle$ . The expansion of exciton-polariton field in terms of plane wave is then given by

$$\langle\Phi_g|\hat{H}_{\text{int}}|\Phi_{\mu\nu}\rangle = -i\sqrt{\frac{2\pi\hbar}{V}}\sum_{\vec{R}}\sum_{\vec{k}}\sum_{\lambda=1}^2f(k)\left[\vec{\mu}(\vec{r})\cdot\vec{e}_\lambda(\vec{k})\right]F_\mu(\vec{r}_e)F_{\mu'}(\vec{r}_h)\left(\hat{\zeta}_{\vec{k}}\cdot e^{i\vec{k}\vec{R}} - \hat{\zeta}_{\vec{k}}^+\cdot e^{-i\vec{k}\vec{R}}\right) \quad (3.42)$$

Since we are looking at the near field here, we do not use long wave approximation  $e^{\pm i\vec{k}\vec{r}} \approx 1$ , which is usually used for the far field [19]. Optical near-field interaction energy between two quantum dots in the lowest order is given by

$$V_{\text{eff}} = \hbar U = \sum_m \langle\psi_f^P|P\hat{V}Q|m^Q\rangle\langle m^Q|Q\hat{V}P|\psi_i^P\rangle\left(\frac{1}{E_{0i}^P - E_{0m}^Q} + \frac{1}{E_{0f}^P - E_{0m}^Q}\right) \quad (3.43)$$

where  $E_{0i}^P$  and  $E_{0f}^P$  are the eigenenergies of the unperturbed Hamiltonian in  $P$  space for initial and final states and  $E_{0m}^Q$  is the eigenenergy in  $Q$  space for intermediate state [1]. We set the explicit form of initial and final states in  $P$  space as  $|\psi_i^P\rangle = |\Phi_{\mu_A\mu'_A}^A\rangle|\Phi_g^B\rangle|0\rangle$  and  $|\psi_f^P\rangle = |\Phi_g^A\rangle|\Phi_{\mu_B\mu'_B}^B\rangle|0\rangle$  whereas the intermediate states in  $Q$  space that involve exciton-polariton wave vector  $\vec{k}$  can be defined as the combination of the ground and excited states as

$|m^Q\rangle = |\Phi_g^A\rangle |\Phi_g^B\rangle |\vec{k}\rangle$  and  $|m^Q\rangle = |\Phi_{\mu_A\mu'_A}^A\rangle |\Phi_{\mu_B\mu'_B}^B\rangle |\vec{k}\rangle$ , respectively. Using the explicit form of transition matrix elements (3.42), we obtain the effective interaction energy between two quantum dots as follows (for derivation, see Appendix C)

$$\hbar U = \iint F_{\mu_A}^A(\vec{r}_e) F_{\mu'_A}^A(\vec{r}_h) F_{\mu_B}^{B*}(\vec{r}_e) F_{\mu'_B}^{B*}(\vec{r}_h) \{Y_A(\vec{r}_{AB}) + Y_B(\vec{r}_{AB})\} d^3r_A d^3r_B \quad (3.44)$$

here ( $\alpha = A, B$ ),  $\vec{r}_{AB} = \vec{r}_A - \vec{r}_B$  and  $Y_\alpha(\vec{r}_{AB})$  is defined as

$$Y_\alpha(\vec{r}_{AB}) = -\frac{1}{4\pi^2} \sum_{\lambda=1}^2 \int d^3k [\vec{\mu}_A \cdot \vec{e}_\lambda(\vec{k})] [\vec{\mu}_B \cdot \vec{e}_\lambda(\vec{k})] \hbar f^2(k) \left( \frac{e^{i\vec{k}\vec{r}_{AB}}}{E(k) + E(s)} + \frac{e^{-i\vec{k}\vec{r}_{AB}}}{E(k) - E(s)} \right) d^3k \quad (3.45)$$

where  $\mu_\alpha$  is transition dipole moment and  $E_\alpha$  is the exciton energy in QD  $\alpha$ , and  $E(k)$  is the eigenenergy of the exciton-polariton defined by

$$E(k) = \hbar\Omega + \frac{(\hbar k)^2}{2m_{pol}} \quad (3.46)$$

$E_m$  is electronic excitation energy of the macroscopic subsystem and  $m_{pol}$  is the effective mass of the exciton-polariton. After integration, the Equation (3.45) can be converted to

$$Y_\alpha(\vec{r}_{AB}) = -\frac{(\mu_A \cdot \mu_B)}{3} \left\{ W_{\alpha+} (\Delta_{\alpha+})^2 \frac{e^{-\Delta_{\alpha+} r_{AB}}}{r_{AB}} - W_{\alpha-} (\Delta_{\alpha-})^2 \frac{e^{-\Delta_{\alpha-} r_{AB}}}{r_{AB}} \right\} \quad (3.47)$$

where  $W_{\alpha\pm}$  and  $\Delta_{\alpha\pm}$  are e constants defined as (refer to Appendix B)

$$W_{\alpha\pm} = \frac{E_{pol}}{E_\alpha} \frac{E_m^2 - E_\alpha^2}{(E_m \pm E_\alpha)(E_m - E_{pol} \mp E_\alpha) - E_m^2/2} \quad (3.48)$$

$$\text{and} \quad \Delta_{\alpha\pm} \equiv \frac{1}{\hbar c} \sqrt{2E_{pol}(E_m \pm E_\alpha)}, \quad (E_m \succ E_\alpha) \quad (3.49)$$

Here  $Y_\alpha(\vec{r}_{AB})$  is the optical near-field interaction potential between two quantum dots located in close proximity. Depending on the magnitudes of  $E_m$  and  $E_\alpha$ ,  $\Delta_{\alpha\pm}$  can be real or imaginary, which corresponds to the localized or propagation modes of the light.

The spatial integral  $\int F_\mu(\vec{r})d^3r$  in Equation (3.44) provide the criterion whether the electric dipole transition is allowed or forbidden between the crystal ground state  $|\Phi_g\rangle$  and the exciton state  $|\Phi_v\rangle$ . It follows that it is forbidden if the spatial integral is zero  $\int F_\mu(\vec{r})d^3r=0$  and allowed if the integral is not zero  $\int F_\mu(\vec{r})d^3r \neq 0$

The integration of spatial integral for spherical quantum dots gives us the delta function

$$\int F_\mu(\vec{r})d^3r = \sqrt{\frac{2}{R^3}} \int_0^R \frac{j_l\left(\frac{\alpha_{nl}r}{R}\right)}{j_{l+1}(\alpha_{nl})} r^2 dr \iint \Upsilon_{lm}(\theta\varphi) \sin\theta d\theta d\varphi = \frac{1}{n} \sqrt{\frac{2R^3}{\pi^2}} \delta_{l0} \delta_{m0} \quad (3.50)$$

The delta function shows that only the transition to the state specified by the quantum numbers  $l = m = 0$  is allowed [1].

### 3.4.2 Weak confinement

In a similar way, since in weak confinement regime the Coulomb interaction between electron and hole is strong, we can treat an electron-hole pair as a single particle i.e., exciton. Therefore, the mass of exciton can be defined as  $M = m_e + m_h$  and the center of mass coordinates as  $\vec{r}_{CM} = (m_e\vec{r}_e + m_h\vec{r}_h)/M$  and relative motion as  $\vec{\beta} = \vec{r}_e - \vec{r}_h$  and the envelope function of the exciton is then

$$\Psi_{nlm}(\vec{r}_e, \vec{r}_h) = \phi(\vec{\beta}) F_m(\vec{r}_{CM}) \quad (3.51)$$

where the function  $\phi_\mu(\vec{\beta}) = \frac{1}{\sqrt{\pi a_0^3}} e^{\left(\frac{-\vec{\beta}}{a_0}\right)}$  represents the relative motions of excitons and  $F_m(\vec{r}_{CM})$  is the envelope function for center of mass motion defined as

$$F_m(\vec{r}_{CM}) = \sqrt{\frac{2}{R^3}} \frac{j_l(\alpha_{nl} \cdot r/R)}{j_{l+1}(\alpha_{nl})} \Upsilon_{lm}(\Omega) \quad (3.52)$$

Therefore, the excitonic states in a quantum dot can be defined by the quantum numbers  $m$  and  $\mu$  and in a Wannier representation it can be expressed as a superposition of excitons as

$$|\Phi_{m\mu}\rangle = \sum_{\vec{R}, \vec{R}'} F_m(\vec{r}_{CM}) \phi_\mu(\vec{\beta}) \hat{c}_{c\vec{R}}^+ \hat{c}_{v\vec{R}'} |\Phi_g\rangle \quad (3.53)$$

where  $\hat{c}_{c\vec{R}}^+$  is the creation operator of an electron at  $\vec{R}$  in the conduction band and  $\hat{c}_{v\vec{R}'}$  is the annihilation operator of an electron at  $\vec{R}'$  in the valence band.  $|\Phi_g\rangle$  is the crystal ground state. Then the transition matrix elements from the exciton state  $|\Phi_{m\mu}\rangle$  to ground state is defined by

$$\langle \Phi_g | \hat{H}_{\text{int}} | \Phi_{m\mu} \rangle = -i \sqrt{\frac{2\pi\hbar}{V}} \sum_{\vec{R}} \sum_{\vec{k}} \sum_{\lambda=1}^2 f(k) [\vec{\mu}_{uc}(\vec{r}) \cdot \vec{e}_\lambda(\vec{k})] F_m(\vec{R}) \phi_\mu(0) (\hat{\zeta}_{\vec{k}}^- \cdot e^{i\vec{k}\vec{R}} - \hat{\zeta}_{\vec{k}}^+ \cdot e^{-i\vec{k}\vec{R}}) \quad (3.54)$$

where  $\vec{\mu}_{uc}(\vec{r}) = \int_{uc} \omega_{v\vec{R}}^*(\vec{r}) \vec{\mu}(\vec{r}) \omega_{c\vec{R}}(\vec{r}) d^3r$  is the transition dipole moment for each unit cell and  $\hat{\zeta}_{\vec{k}}^-$  and  $\hat{\zeta}_{\vec{k}}^+$  are the exciton-polariton creation and annihilation operators, respectively. The optical near-field interaction energy between two quantum dots in the lowest order is defined by Equation (3.43). Here, we define the initial and final states in the  $P$  space as  $|\psi_i^P\rangle = |\Phi_{m\mu}^A\rangle |\Phi_g^B\rangle |0\rangle$  and  $|\psi_f^P\rangle = |\Phi_g^A\rangle |\Phi_{m'\mu'}^B\rangle |0\rangle$  and intermediate states in the  $Q$  space as  $|m^Q\rangle = |\Phi_g^A\rangle |\Phi_g^B\rangle |\vec{k}\rangle$  and  $|m^Q\rangle = |\Phi_{m\mu}^A\rangle |\Phi_{m\mu}^B\rangle |\vec{k}\rangle$  [15],[19],[20].

Using the transition matrix elements in Equation (3.43), we find the optical near-field interaction energy between two coupled quantum dots as

$$\hbar U = \varphi_\mu^A(0) \varphi_{\mu'}^{B*}(0) \iint F_m^A(\vec{r}_A) F_{m'}^{B*}(\vec{r}_B) \{ \Upsilon_A(\vec{r}_{AB}) + \Upsilon_B(\vec{r}_{AB}) \} d^3r_A d^3r_B \quad (3.55)$$

where  $\Upsilon_\alpha(\vec{r}_{AB})$  is given by Equation (3.45)

### 3.5 Numerical results for CdSe, CdTe, CdSe/ZnS and PbSe quantum dots

Here we investigate optical near-field interaction between spherical quantum dots for strong confinement regime. Based on the previous theory of optical near fields (which was proposed by M. Ohtsu Group from the University of Tokyo), we theoretically estimated the magnitude of the optical near-field interaction potential between  $(1,0,0)$  and  $(1,1,0)$  energy levels of the first and second quantum dots, respectively. In conventional electrodynamics for the case where we consider spherical quantum dots, only transitions to the states defined by  $(l=m=0)$  are allowed. Here,  $l$  and  $m$  are the orbital angular momentum and magnetic quantum numbers. Note that the propagating far field generates a symmetric states from the interaction of two resonant energy levels of excitons. Therefore, for conventional far-field light the state  $(1,1,0)$  is dipole-forbidden energy level for exciton and according to the selection rules, optical transition from  $(1,0,0)$  state of small quantum dot (QDS) to the  $(1,1,0)$  state of large quantum dot (QDL) is prohibited. However, since the quantum dots are very close to each other, due to the localized nature and large spatial inhomogeneity of optical near-fields localized on the surface of nanoparticles, transitions to the dipole forbidden energy levels is allowed.

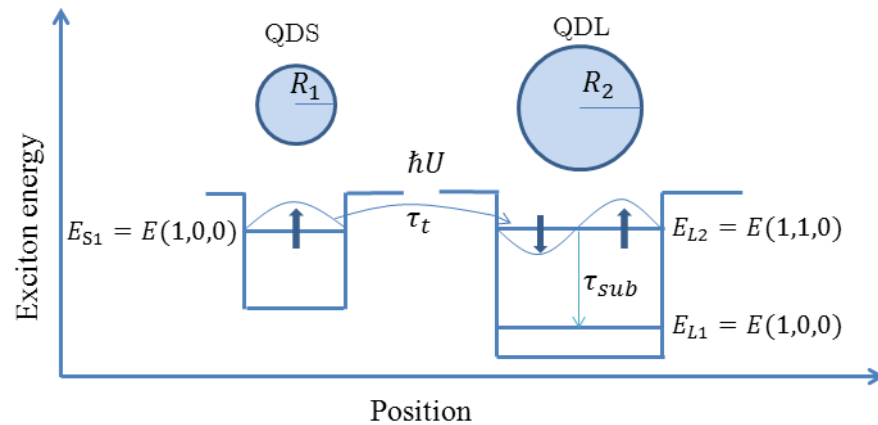


**Figure 3.5.1** Optical near-field interactions between two spherical quantum dots with the size ratio of  $R_2/R_1 \approx 1.43$ . There is a resonance between  $(1,0,0)$  level of QDS and  $(1,1,0)$  level of QDL.

There exists a resonance between (1,0,0) energy level of (QDS) and (1,1,0) energy level of (QDL) when the ratio of the radius of QDL and QDS satisfies the condition of  $R_2/R_1 \approx 1.43$  [17],[18], [47],[48]

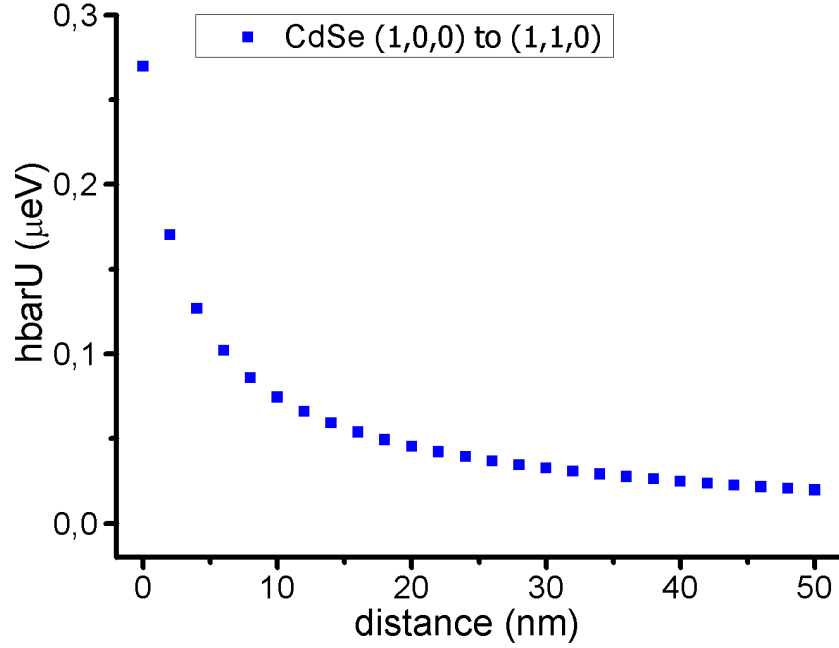
Figure 3.5.1 is the schematic representation of dipole-forbidden transition where the local dipoles at the near side of the quantum dot is excited by optical near field. In the figure we introduce the optical near-field energy transfer mechanism between (1,0,0) and (1,1,0) levels of the first and second spherical quantum dots based on dressed photon model.

The energy transfer is explained via the optical near-field interaction between the excitons lowest excited state  $E_{S1}$  in QDS and the second-lowest excited state  $E_{L2}$  in QDL. These two levels are electric dipole allowed and forbidden energy levels. However, in the case of the resonance condition  $E_{S1} = E_{L2}$ , due to the localized nature of optical near-fields, the energy transfer to the forbidden state is allowed. Thus, we observe optical near-field excitation transfer from one state to other. Since the sublevel transition to the lowest state is much shorter than the energy transfer time, the transferred energy dissipated from  $E_{L2}$  to  $E_{L1}$  very fast. [21], [32], [42]. The energy eigenvalues in the QD with size  $R$  are expressed as

$$E_{nlm} = E_g + \frac{\hbar}{2m_r} \left( \frac{\alpha_{nl}}{R} \right)^2 \quad (3.56)$$

and represent discrete energy levels, where  $m_r$  is the reduced mass of the exciton,  $E_g$  is the bandgap of the bulk semiconductor and  $R$  is the size of quantum dot.

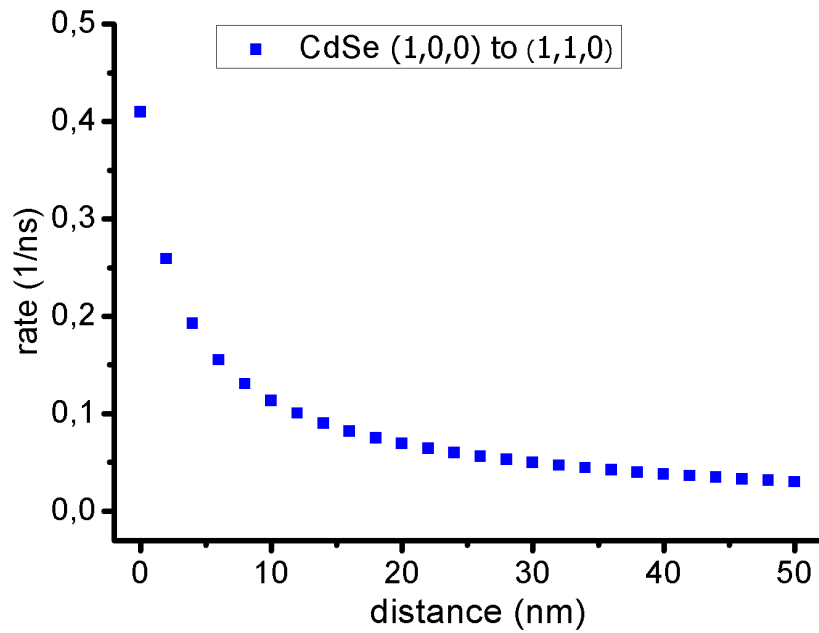
We numerically estimate the optical near field energy transfer from ground state to the first dipole forbidden energy state. We used different quantum dots such as CdSe, CdTe, CdSe/ZnS, and PbSe with different sizes, Bohr radius and excitation energies. We examine strong dependence of optical near-field energy transfer on size, and structure of the quantum dots. Also, near field potential strongly depends on the distance between the two quantum dots and by changing the composition it changes drastically. We analysed the strong confinement regime in different quantum dots. [43], [44]



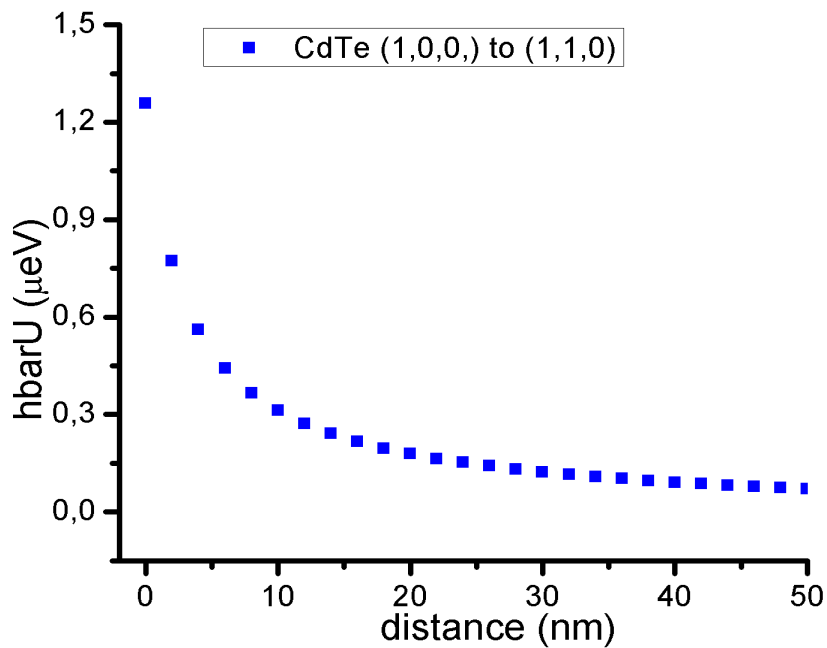
**Figure 3.5.2** Optical near-field energy and distance relation for CdSe spherical quantum dots from  $(n, l, m) = (1, 0, 0)$  state of QDS to  $(n', l', m') = (1, 1, 0)$  state of QDL.

Figure 3.5.2 represents optical near field interaction energy between two spherical CdSe quantum dots. The parameters for this coupling are set to  $L_D = 2.6 \text{ nm}$ ,  $L_A = 3.72 \text{ nm}$ ,  $E_m = 3.3 \text{ eV}$ ,  $E_g = 1.74 \text{ eV}$ ,  $E_A = E_B = 2.17 \text{ eV}$ ,  $\mu_D = 0.08\sqrt{\text{eV} \cdot (\text{nm})^3}$ ,  $\mu_A = 0.12\sqrt{\text{eV} \cdot (\text{nm})^3}$ ,  $Ry_{CdSe}^* = 16 \cdot 10^{-3} \text{ eV}$ ,  $R_B = 5.6 \text{ nm}$ ,  $m_r = 0.1 m_e$ .

The coupling corresponds to the resonant transition from the state  $(1,0,0)$  to the state  $(1,1,0)$ . The Bohr radius for CdSe quantum dots is estimated as  $R_B = 5.6 \text{ nm}$ . Since the Bohr radius is larger than the size of the particle, we can assume it as an example of the strong confinement regime. For the distance  $d = 1.5 \text{ nm}$  the coupling strength between the quantum dots is estimated as  $\hbar U = 0.245 \mu\text{eV}$ . This distance is in a range of the particle's radius and corresponds to the near field of the particle. The energy transfer time for this local electromagnetic interaction is estimated as  $\tau = 2.69 \text{ ns}$ . Figure 3.5.3 represent the energy transfer rate. The transfer rate for the distance of  $d = 1.5 \text{ nm}$  is estimated as  $\gamma = 0.37 \text{ 1/ns}$ . The graph shows that the energy transfer rate for CdSe quantum dots is very small and after the distance  $d = 1.5 \text{ nm}$  it become even smaller. [45]



**Figure 3.5.3** Optical near-field transfer rate and distance relation for CdSe spherical quantum dots from  $(n, l, m) = (1, 0, 0)$  state of QDS to  $(n', l', m') = (1, 1, 0)$  state of QDL.



**Figure 3.5.4** Optical near-field energy and distance relation for CdTe spherical quantum dots from  $(n, l, m) = (1, 0, 0)$  state of QDS to  $(n', l', m') = (1, 1, 0)$  state of QDL.

The Figure 3.5.4 shows the coupling strength and distance relation between  $(1,0,0)$  and  $(1,1,0)$  states of spherical CdTe quantum dots.



Here, the parameters are set to  $L_D = 2.6 \text{ nm}$ ,  $L_A = 3.7 \text{ nm}$ ,  $E_m = 3.3 \text{ eV}$ ,  $E_g = 1.5 \text{ eV}$ ,  $E_A = E_B = 2.08 \text{ eV}$ ,  $\mu_D = 0.13\sqrt{\text{eV} \cdot (\text{nm})^3}$ ,  $\mu_A = 0.19\sqrt{\text{eV} \cdot (\text{nm})^3}$ ,  $Ry_{CdTe}^* = 10 \cdot 10^{-3} \text{ eV}$ ,  $R_B = 6.9 \text{ nm}$ , and  $m_r = 0.082 m_e$ .

Since the Bohr radius is larger than the quantum confinement it can be treated as an example of the strong confinement regime. For CdTe quantum dots the interaction energy and the energy transfer time for the distance  $d = 2 \text{ nm}$  is estimated as  $\hbar U = 0,773 \mu\text{eV}$  and  $\tau = 852 \text{ ps}$ . Figure 3.5.5 shows the energy transfer rate and distance relation. From the rate distance relation, for the distance  $d = 2 \text{ nm}$  the energy transfer rate is estimated as  $\gamma = 1,173 \text{ ns}^{-1}$ . The numerical results show that after the distance of  $d = 2 \text{ nm}$  the graph decays faster. As we know from the Chapter 1 this distance corresponds to the near-field of the quantum dot. After the distance of  $10 \text{ nm}$  the rate decreases even faster and after  $40 \text{ nm}$  it approximately goes to zero. The composition of the quantum dots also affect the transfer rate. Although the particle sizes is almost the same for both cases, the transfer rate for CdTe is five times larger than that of CdSe. [22],[23],[24]

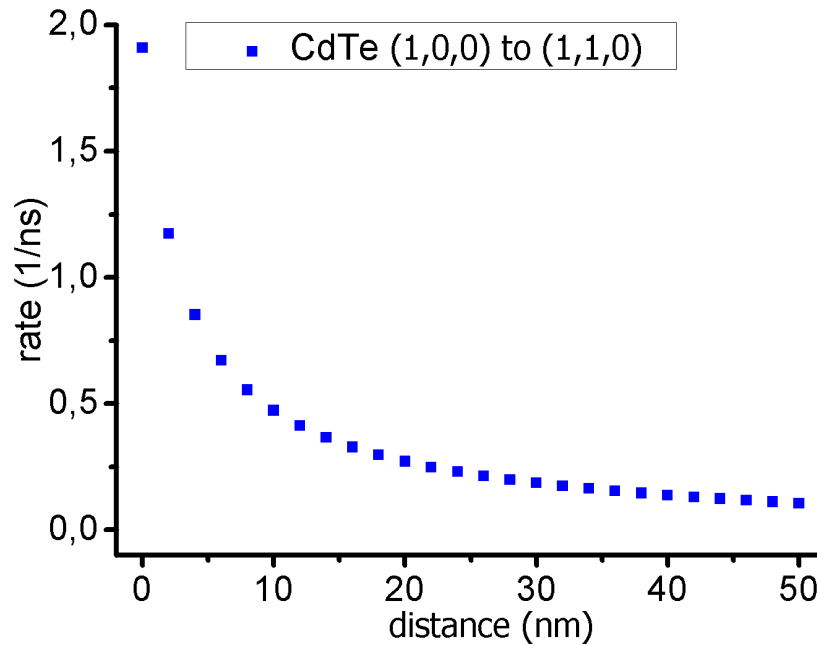


**Figure 3.5.5** Optical near-field transfer rate and distance relation for CdSe spherical quantum dots from  $(n, l, m) = (1, 0, 0)$  state of QDS to  $(n', l', m') = (1, 1, 0)$  state of QDL.

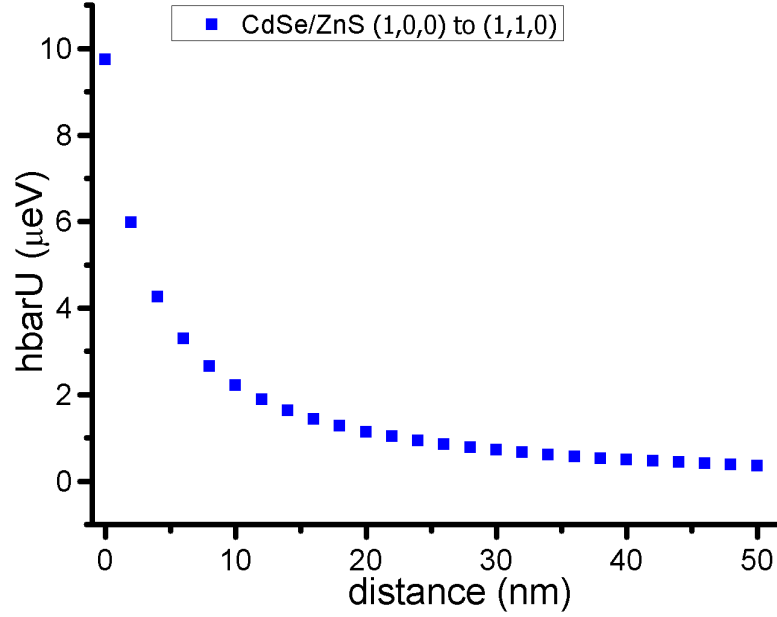


**Figure 3.5.6** Optical near-field energy and distance relation for CdSe/ZnS spherical quantum dots from  $(n, l, m) = (1, 0, 0)$  state of QDS to  $(n', l', m') = (1, 1, 0)$  state of QDL.

Here the parameters are set to  $L_D = 2.8 \text{ nm}$ ,  $L_A = 4 \text{ nm}$ ,  $E_m = 3.3 \text{ eV}$ ,  $E_g = 1.84 \text{ eV}$ ,  $E_A = E_B = 2.55 \text{ eV}$ ,  $\mu_D = 0.14\sqrt{eV \cdot (nm)^3}$ ,  $\mu_A = 0.2\sqrt{eV \cdot (nm)^3}$ ,  $Ry_{CdSe/ZnS}^* = 16 \cdot 10^{-3} \text{ eV}$ ,  $R_B = 4.9 \text{ nm}$ , and  $m_r = 0.088 m_e$

The figure 3.5.6 shows the distance dependence of coupling strength between  $(1,0,0)$  and  $(1,1,0)$  states of spherical CdSe/ZnS core-shell quantum dot structures. Since the expression we derived is not for core/shell structures it can give us unreliable result for CdSe/ZnS quantum dots. However, since the electron and the hole is assumed to be in the core, we can treat it as strong confinement. Therefore, the results gives sense. For these quantum dots the coupling strength and energy transfer time for the distance  $d = 3 \text{ nm}$  is estimated as  $\hbar U = 5 \mu\text{eV}$  and  $\tau = 132 \text{ ps}$ . Figure 3.5.7 represents the energy transfer rate for CdSe/ZnS quantum dots. In a distance  $d = 3 \text{ nm}$ , the transfer rate is estimated as  $\gamma = 7.57 \text{ ns}^{-1}$ . The graph shows that, after the distance of  $d = 3 \text{ nm}$  the fast decay is observed for the transfer rate and after the distance of  $d = 40 \text{ nm}$  it approximately goes to zero. From the comparison of the transfer rates for CdSe and CdSe/ZnS we realize the huge difference. The results show that, as we change the structure of a particle, the rate changes drastically. [46]

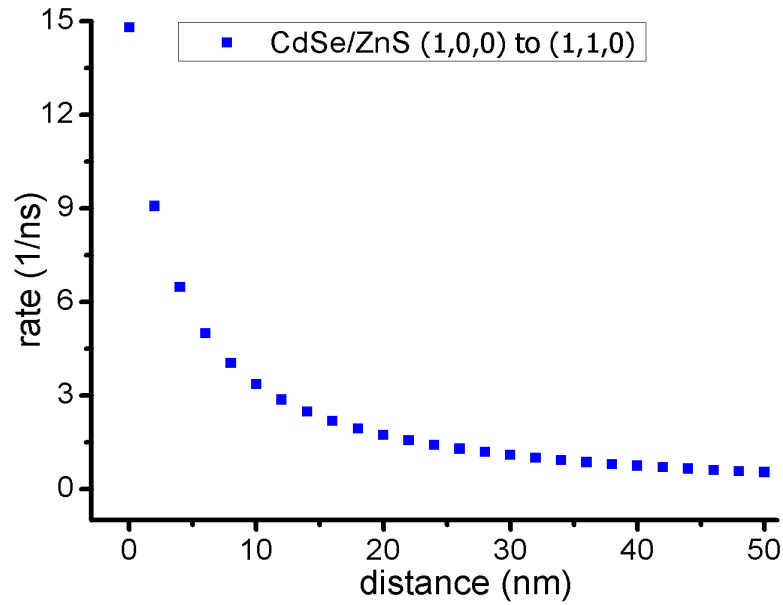


**Figure 3.5.7** Optical near-field transfer rate and distance relation for CdSe/ZnS spherical quantum dots from  $(n,l,m) = (1,0,0)$  state of QDS to  $(n',l',m') = (1,1,0)$  state of QDL.

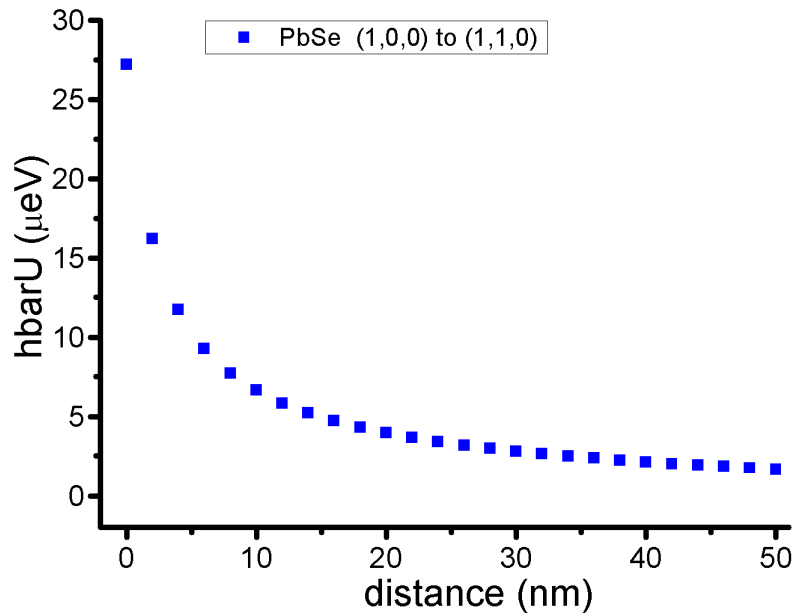


**Figure 3.5.8** Optical near-field energy and distance relation for PbSe spherical quantum dots from  $(n,l,m) = (1,0,0)$  state of QDS to  $(n',l',m') = (1,1,0)$  state of QDL.

The figure 3.5.8 shows the coupling between  $(1,0,0)$  and  $(1,1,0)$  states of spherical PbSe quantum dots. Here, to estimate the energy transfer rate the experimental values for the dipole moment of PbSe quantum dots is used. [28],[29].

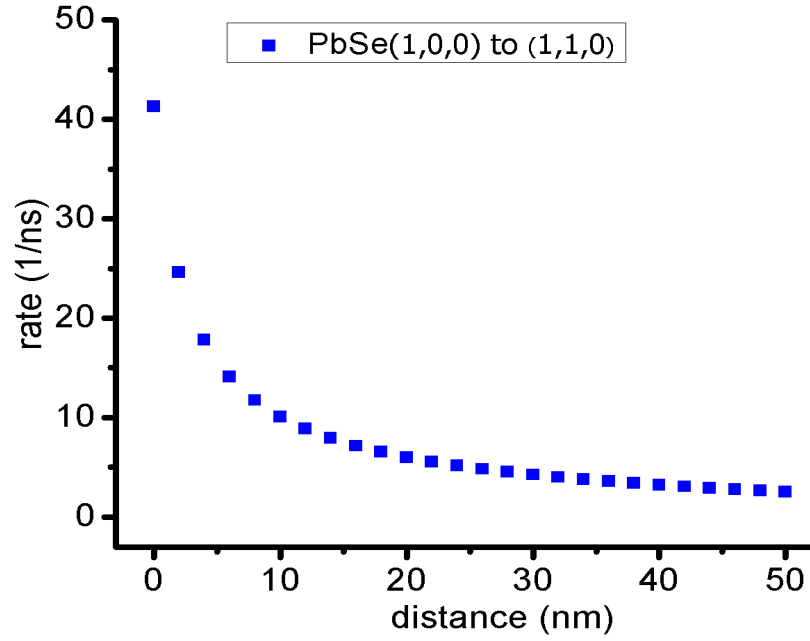


**Figure 3.5.9** Optical near-field transfer rate and distance relation for PbSe spherical quantum dots from  $(n, l, m) = (1, 0, 0)$  state of QDS to  $(n', l', m') = (1, 1, 0)$  state of QDL. The parameters for PbSe QDs are set to  $L_D = 2.3 \text{ nm}$ ,  $L_A = 3.39 \text{ nm}$ ,  $E_m = 3.3 \text{ eV}$ ,  $E_g = 0.28 \text{ eV}$ ,  $E_A = E_B = 2.15 \text{ eV}$ ,  $\mu_D = 0.75\sqrt{\text{eV} \cdot (\text{nm})^3}$ ,  $\mu_A = 1\sqrt{\text{eV} \cdot (\text{nm})^3}$ ,  $R_B = 46 \text{ nm}$ ,  $Ry_{PbSe}^* = 2.05 \cdot 10^{-3} \text{ eV}$ , and  $m_r = 0.035 m_e$ .

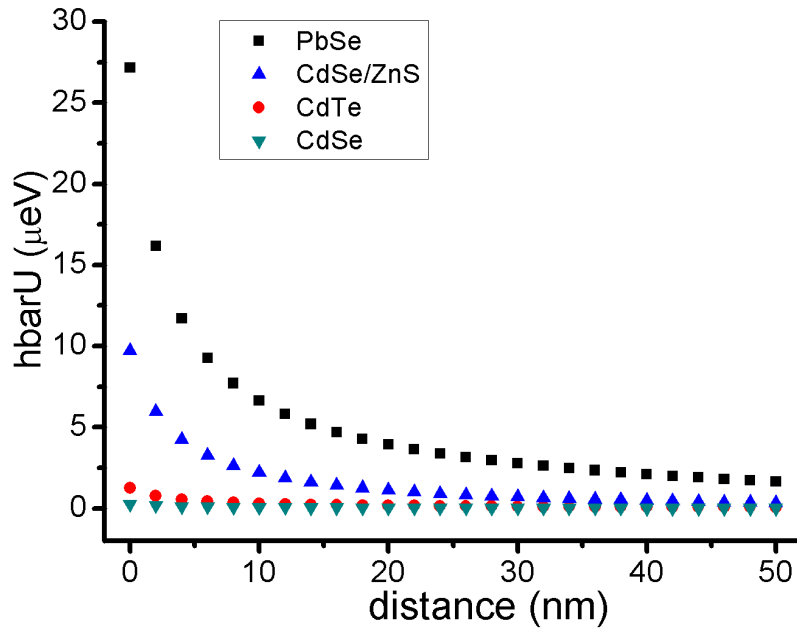


**Figure 3.5.10** Comparison of optical near-field energy transfer for PbSe, CdSe/ZnS, CdTe and CdSe spherical quantum dots from  $(1, 0, 0)$  state of QDS to  $(1, 1, 0)$  state of QDL.

Since the Bohr radius of PbSe quantum dots is  $R_B = 46 \text{ nm}$ , it is the typical example of strong confinement regime and we can treat the electron and the hole as an independent particles from each other. The Figure 3.5.8 and and Figure 3.5.9 represent the distance dependence of near field potential and the energy transfer rate respectively. For spherical PbSe QDs, the interaction energy and energy transfer time for the distance  $d = 1.5 \text{ nm}$  is estimated as  $\hbar U = 18 \mu\text{eV}$  and  $\tau = 37 \text{ ps}$ . The transfer rate for  $d = 1.5 \text{ nm}$  is  $\gamma = 37 \text{ ns}^{-1}$ . For the distance  $d = 3 \text{ nm}$  the interaction energy and energy transfer time is  $\hbar U = 13.6 \mu\text{eV}$  and  $\tau = 48.5 \text{ ps}$ . On the other hand the time for sublevel transition from the state (1,0,0) to (1,1,0) of large quantum dot is estimated as a few picoseconds. Calculations show that the stronger confinement we choose the better result we get. This is very fast energy transfer between two resonant energy levels and suitable for the operation of nanophotonic devices.

Here, the dipole moments for quantum dots is estimated by using the known formula for radiative lifetime [22],[30]

$$\gamma_{rad}^0 = \frac{8\pi\sqrt{\varepsilon_0}\omega_{exc}^3 e^2 d_{exc}^2}{3(\varepsilon_{eff}/\varepsilon_0)^2 \hbar \cdot c^3} \quad (3.57)$$

Therefore, we find the dipole moment of quantum dots as follows

$$ed_{exc} = \sqrt{\frac{3\gamma_{rad}^0 (\varepsilon_{eff}/\varepsilon_0)^2 \hbar^4 c^3}{4\sqrt{\varepsilon_0} E_{exc}^3}} \quad (3.58)$$

where,  $\varepsilon_{eff} = (2\varepsilon_0 + \varepsilon)/3$  is the effective dielectric constant,  $E_{exc}$  is the excitation energy of quantum dots, and the radiation lifetime is

$$\gamma_{rad}^0 = \Upsilon \frac{1}{\tau_D} \quad (3.59)$$

where  $\Upsilon$  is the quantum yield and  $\tau_D$  is the exciton lifetime in donor.

To estimate the transition dipole moment the Equation (3.58) is used. For example, the experimental results for CdTe quantum dots are  $\tau_A = 5.54 \text{ ns}$ ,  $\tau_D = 7.13 \text{ ns}$ . By using the radiative lifetime of excitons in quantum dots we

estimated the the transition dipole moments for both quantum dots. For the seperation distance of  $d = 2 \text{ nm}$  the energy transfer time to the dipole forbidden energy level is calculated as  $\tau = 852 \text{ ps}$ . The calculations show that the transfer time to the dipole-forbidden energy level is shorter enough than the radiative lifetime of the excitons in each quantum dot. Also, the time for sublevel transition to the first excited state of the QDL is estimated as a few picoseconds. Therefore, excitation transfer by an energy dissipation process occurs and the unidirectional energy transfer to the first dipole-forbidden energy level of the QDL is achieved.[36],[37],[38],[41]

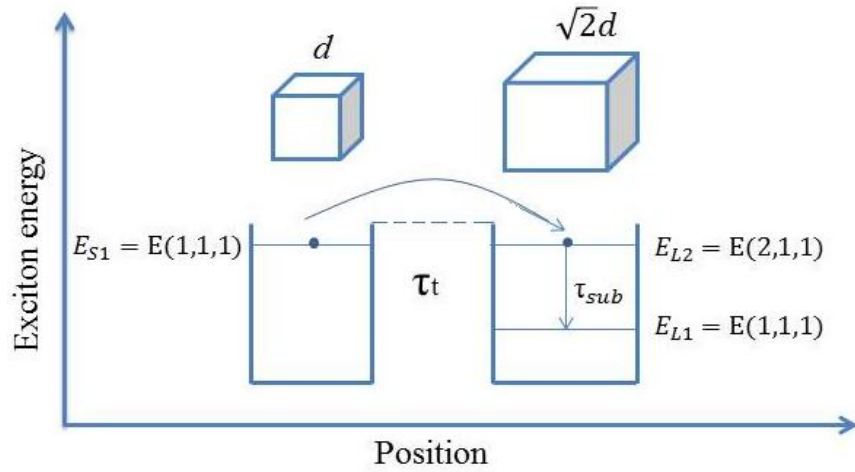


**Figure 3.5.11** Optical near-field interactions between two cubic CuCl quantum dots with the size ratio of  $R_2/R_1 \approx 1.41$ . There is a resonance between (1,1,1) level of QD-S and (2,1,1) levels of QD-L

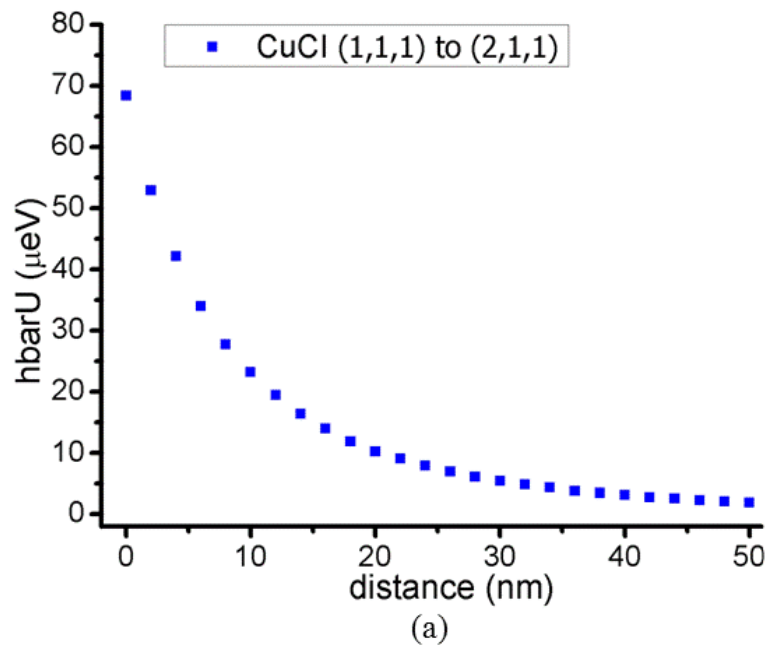
Figure 3.5.11 shows optical near-field interaction of CuCl quantum cubes. There occurs resonant coupling between (1,1,1) and (2,1,1) states of the quantum dots with side lengths  $d$  and  $\sqrt{2}d$ . The excitation energy levels of the exciton in a quantum cubes is represented by

$$E_{n_x, n_y, n_z} = E_B + \frac{\pi^2 \hbar^2}{2Md^2} (n_x^2 + n_y^2 + n_z^2) \quad n_x, n_y, n_z = 1, 2, \dots \quad (3.60)$$

Note that the propogating far field generates a symmetric states from the interaction of two resonant energy levels of excitons. Therefore, for conventional far field light, the state (2,1,1) is dipole forbidden energy level for exciton and it is

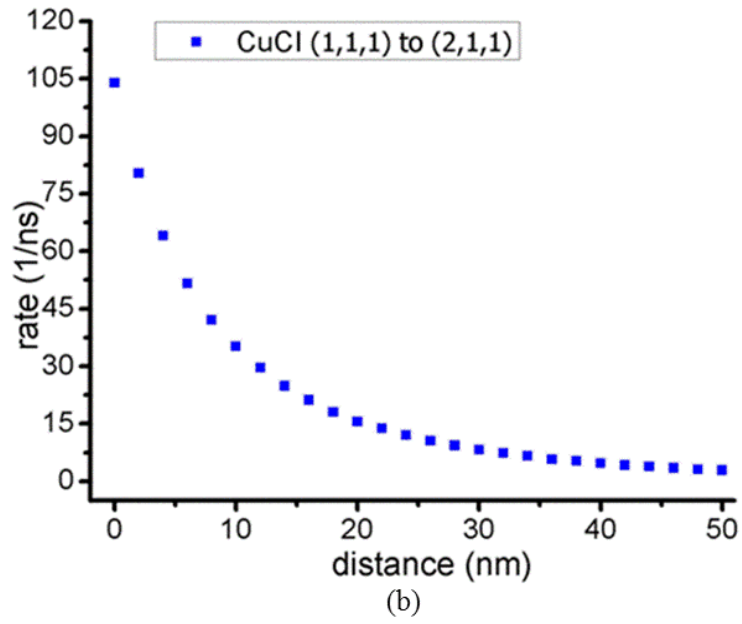
prohibited for the far-field excitation. However, due to a steep electric field of optical near-fields, in the close proximity of quantum dots, the dipole forbidden transition that violates conventional optical selection rules, is allowed. Therefore, the exciton can move to the (2,1,1) state of the large quantum dot [52]. In the second quantum dot due to exciton phonon coupling the intersublevel energy relaxation occurs. The sublevel transitions is generally a few picoseconds and much shorter than the energy transfer time from one state to other. Therefore, the unidirectional exciton transfer from one state to other is occurred for cubic CuCl quantum dots. [39], [40], [47]- [51]

Figure 3.5.12 (a) shows the distance dependence of the near field coupling between (1,1,1) and (2,1,1) states of CuCl quantum dots. The Figure 3.5.12 (b) represents the transition rate for the energy transfer from (1,1,1) state of the first quantum dot to (2,1,1) state of the second quantum dot. [21], [32] For cubic CuCl quantum dots for the distance  $d = 3 \text{ nm}$  the interaction energy and energy transfer time is estimated as  $\hbar U = 46.7 \mu\text{eV}$  and  $\tau = 14 \text{ ps}$ . This is a very high speed for the operation of the advanced photonic devices.



**Figure 3.5.12.a** Optical near-field energy transfer for cubic CuCl quantum dots from  $n \rightarrow (n_x, n_y, n_z) \rightarrow (1,1,1)$  state of QDS to  $n' \rightarrow (n'_x, n'_y, n'_z) \rightarrow (2,1,1)$  state of QDL

Both CuCl and PbSe are the typical examples of weak and strong confinement regimes respectively. In both cases we have good results for transfer rates. However, in the case of CuCl quantum dots the excitation energy is  $E_m = 6.9 \text{ eV}$ . It is high energy and it corresponds to the UV range excitation while, for PbSe spherical quantum dots we set the excitation energy as  $E_m = 3.3 \text{ eV}$  which is two times smaller. Having a lower excitation energy is suitable for the application.



**Figure 3.5.12.b** Optical near-field energy transfer rate for cubic CuCl quantum dots from  $n \rightarrow (n_x, n_y, n_z) \rightarrow (1,1,1)$  state of QDS to  $n' \rightarrow (n'_x, n'_y, n'_z) \rightarrow (2,1,1)$  state of QDL.

Here, the parameters are set to  $L_D = 10 \text{ nm}$ ,  $L_A = 14.1 \text{ nm}$ ,  $E_m = 6.9 \text{ eV}$ ,  $E_g = 3.2 \text{ eV}$ ,  
 $E_A = E_B = 2.207 \text{ eV}$ ,  $R_B = 0.7 \text{ nm}$ ,  $\mu_D = 0.0173\sqrt{\text{eV} \cdot (\text{nm})^3}$ ,  $\mu_A = 0.0241\sqrt{\text{eV} \cdot (\text{nm})^3}$ ,  
 $Ry_{CuCl}^* = 190 \cdot 10^{-3} \text{ eV}$ ,  $m_r = 2.3 m_e$



# Conclusions

In this thesis the excitation energy transfer between two different quantum dot is discussed. The energy can be transferred from one quantum dot to other by optical near field interaction. The optical near fields are localized fields on the surface of nanometric particles, that is, dressed photons, where the photons are not massless as a result of light-matter interaction. It can be expressed as a sum of Yukawa functions with different kind of effective masses and interaction ranges and allows transitions to dipole forbidden energy levels which is optically forbidden for conventional far field light.

Involving the optical near field interactions, we studied a system with different-sized quantum dots in order to induce effective optical excitation energy transfer. We derived the equations for the energy transfer for strong and weak confinement regimes and showed that dipole-forbidden energy levels can be accessed by using the optical near fields. However, since the energy levels are in resonance, there should be a nutation process and back energy transfer between two resonance energy levels. In order to guarantee irreversibility of the transferred energy between QDs, the sublevel energy relaxation from (1,1,0) state to (1,0,0) state of the second quantum dot has to be in the order of 10s or less of ps.

We numerically analysed the optical near-field energy transfer rate for spherical CdSe, CdTe, CdSe/ZnS and PbSe quantum dots. We estimated that the energy transfer time to the dipole forbidden states of quantum dot is shorter enough than the radiative lifetime of the excitons in each quantum dot. Therefore, the unidirectional energy transfer between two resonant energy levels of quantum dots is achieved. Transfer rate for different quantum dots gives us different values. The numerical analyses show that the energy transfer rate to the dipole forbidden energy levels is quite fast in order to enable optical excitation transfer, and it is strongly depends on the shape, size, and structure of the quantum dots.

The use of optical near-fields is proposed for design and operation of nanophotonic devices for their low power consumption, high efficiency and small

size. Ohtsu group from the University of Tokyo, use the optical near fields under the nonresonant condition to fabricate the nanophotonic devices with the photochemical vapor deposition. By using this approach the technology of optical excitation transfer including efficient long-range signal transfer and fabrication technology of geometry-controlled quantum nanostructures is under development.

# Bibliography

- [1] M. Ohtsu, K. Kobayashi, T. Kawazoe, T. Yatsui, M. Naruse “Principles of Nanophotonics” (Taylor and Francis, Boca Raton, 2008)
- [2] M. Ohtsu and K. Kobayashi, “Optical Near Fields” *Springer-Verlag*, Berlin (2004)
- [3] M. Ohtsu “Progress in Nano-Electro-Optics III”, *Springer-Verlag*, Berlin (2005)
- [4] M. Ohtsu “Progress in Nano-Electro-Optics V”, *Springer-Verlag*, Berlin (2006)
- [5] M. Ohtsu, "Progres in Nanophotonics 1" *Springer-Verlag*, Berlin (2011)
- [6] M. Ohtsu “Progress in Nano-Electro-Optics VII”, *Springer-Verlag*, Berlin (2010)
- [7] M. Ohtsu “Progress in nano-electro optics VI”, K. Kobayashi, Y. Tanaka, T. Kawazoe and M. Ohtsu “Localized Photon Model Including Phonons” Degrees of Freedom” *Springer series in optical sciences* (2008)
- [8] M. Ohtsu, K. Kobayashi, T. Kawazoe, S. Sangu and T. Yatsui, “Nanophotonics: Design, fabrication and operation of nanometric devices using optical near fields” *IEEE J. Sel. Top. Quantum Electron.* **8**(4), 839–863 (2002)
- [9] M. Ohtsu, T. Kawazoe, T. Yatsui, and M. Naruse “Nanophotonics: application of dressed photons to novel photonic devices and systems” *IEEE J. Sel. Top. Quantum Electron.* **14**(6), 1404–1417 (2008)
- [10] K. Kobayashi, S. Sangu, H. Ito, and M. Ohtsu, “Near-field optical potential for a neutral atom” *Phys. Rev. A* **63**(1), 013806 (2001)
- [11] M. Ohtsu, “Nanophotonics in Japan” *J. Nanophot.* **1**, 011590 (2007)

- [12] Lukas Novotny, Bert Hecht “Principles of Nano Optics” Cambridge University Press (2006)
- [13] Sergey V. Gaponenko “Introduction to Nanophotonics” Cambridge University Press (2010)
- [14] L. Banyai and S.W.Koch, “Semiconductor quantum dots” World Scientific Series on Atomic Molecular and Optical Physics. Vol.2 (1993)
- [15] E. Hanamura, “Very large optical nonlinearity of semiconductor microcrystallites” *Physical Review B* **37**(3) (1988)
- [16] M.Ali.Omar, “Elementary Solid State Physics Principles and applications”, Addison- Wesley series in solid state sciences (1975)
- [17] M. Naruse, E. Runge, K Kobayashi and M. Ohtsu, “Efficient optical excitation transfer in layered quantum dot nanostructures networked via optical near-field interactions” *Phys. Rev. B* **82**, 125417 (2010)
- [18] M. Naruse, T. Kawazoe, R. Ohta, W. Nomura and M.Ohtsu, “Optimal mixture of randomly dispersed quantum dots for optical excitation transfer via optical near –field interactions” *Phys. Rev. B* **80**, 125325 (2009)
- [19] S. Sangu, K. Kobayashi, A.Shojiguchi and M. Ohtsu “Logic and functional operations using a near-field optically coupled quantum-dot system”, *Phys. Rev. B* **69**, 115334 (2004)
- [20] K. Kobayashi, S. Sangu, T. Kawazoe, M. Ohtsu “Exciton dynamics and logic operations in a near-field optically coupled quantum-dot system” *Journal of luminescence* **112** (2005)
- [21] Z. K. Tang, A. Yanase, T. Yasui and Y. Segawa “Optical selection rule and oscillator strength of confined exciton system in CuCl thin films” *Phys. Rev. Lett.* **71**(9), (1993).

- [22] A. O. Govorov, G. W. Bryant, W. Zhang, T. Skeini, J. Lee, N.A. Kotov, J.M. Slocik and R.R. Naik “Exciton-plasmon interaction and hybrid excitons in semiconductor-metal nanoparticle assemblies” *Nano Letters* Vol. **6**, No. **5** (2006)
- [23] W. William Yu, Lianhua Qu, Wenzhuo Guo, and Xiaogang Peng “Experimental Determination of the Extinction Coefficient of CdTe, CdSe, and CdS Nanocrystals” *Chem. Mater.* 2003, **15**, 2854-2860
- [24] Osamu Oda “Compound semiconductor bulk materials and characterizations” *World Scientific Publishing* (2007)
- [25] Hartmut Haug, Stephan W. Koch “Quantum theory of the optical and electronic properties of semiconductors” *Second edition, World Scientific* (1993)
- [26] Paul Harrison “Quantum wells, wires and dots”, “Theoretical and computational physics of semiconductor nanostructures”, *Second edition, Wiley Interscience* (2005)
- [27] E. Hanamura “Rapid radiative decay and enhanced optical nonlinearity of excitons in a quantum well” *Phys. Rev. B* **38**, 2 (1988)
- [28] Joonhee M. An, Marco Califano, Alberto Franceschetti and Alex Zunger “Excited-state relaxation in PbSe quantum dots” *J. Chem. Phys.* **128**, 164720 (2008)
- [29] Mark Klokkenburg, Arjan J. Houtepen, Rolf Koole, Julius W. J. de Folter, Ben H. Erne, Ernst van Faassen and D. Vanmaekelbergh “Dipolar Structures in Colloidal Dispersions of PbSe and CdSe Quantum Dots” *Nano Letters* Vol. **7**, No. **9** (2007)
- [30] A. Thranhardt, C. Ell, G. Khitrova, and H. M. Gibbs “Relation between dipole moment and radiative lifetime in interface fluctuation quantum dots” *Phys. Rev. B, Vol.* **65**, 035327 (2002)

- [31] K.Kobayashi and M. Ohtsu “Quantum theoretical approach to a near-field optical system” *Journal of microscopy*, Vol. **194**, pp. 249-254. (1999)
- [32] T. Kawazoe, K. Kobayashi, J. Lim, Y. Narita, and M. Ohtsu, “Direct observation of optically forbidden energy transfer between CuCl quantum cubes via near-field optical spectroscopy” *Phys. Rev. Lett.* **88**(6), 067404 (2002).
- [33] J.D.Jackson “Classical Electrodynamics” *third edition, John Wiley* (1999)
- [34] C. Cohen-Tannoudji, Photons and Atoms “Introduction to Quantum electrodynamics” *John Wiley* (1987)
- [35] George B. Arfken, Hans B. Weber “Mathematical Methods for Physicists” *Elsevier academis Press* (2005)
- [36] T. Kawazoe, K. Kobayashi, and M. Ohtsu “Optical nanofountain: a biomimetic device that concentrates optical energy in a nanometric region” *Appl. Phys. Lett.* **86**(10), 103102 (2005)
- [37] S. Sangu, K. Kobayashi, A. Shojiguchi, T. Kawazoe, and M. Ohtsu “Excitation energy transfer and population dynamics in a quantum dot system induced by optical near-field interaction”, *J. Appl. Phys.* **93**, 2937 (2003)
- [38] M.Naruse, T. Kawazoe, S. Sangu, K. Kobayashi and M. Ohtsu “Optical interconnects based on optical far-and near-field interactions for high-density data broadcasting” *Optics express* 306, Vol **14**, No. 1 (2006)
- [39] W. Nomura, T. Yatsui, T. Kawazoe, M. Naruse, E. Runge, C.Lienau, M. Ohtsu “Direct observation of optical excitation transfer based on resonant optical near-field interaction” *Appl. Phys. B* **107** 257-262 (2012)
- [40] M. Naruse, T. Miyazaki and F. Kubota, T Kawazoe, K. Kobayashi, S. Sangu, M. Ohtsu “Nanometric summation architecture based on optical-near field interaction between quantum dots” *Optics Letters Vol. 30, No. 2* (2005)

- [41] T. Kwazoe, K. Kobatashi, S. Takubo, and M. Ohtsu “Nonadiabatic photodissociation process using an optical near field” *The Journal of Chemical Physics* **122**, 024715 (2005)
- [42] N.Tate, M. Naruse, W. Nomura, T. Kawazoe, T.Yatsui, M. Hoga, Y. Ohyagi, Y.Sekine, H. Fujita, and M. Ohtsu “Demonstration of modulateble optical near-field interactions between dispersed resonant quantum dots”*Optics Express Vol. 19, No.19* (2011)
- [43] M. Naruse, F. Peper, K Akahane, N. Yamamoto, T. Kawazoe, N. Tate, and M. Ohtsu “Skew Dependence of Nanophotonic Devices Based an Optical Near-Field interactions” *ACM Journal of Emerging Technologies in Computing Systems, Vol.8, No.1* (2012)
- [44] S. Sangu, K. Kobayashi and M. Ohtsu “Optical near fields as photon-matter interacting systems” *Journal of Microscopy, Vol. 202*, Pt 2, May 2001, pp. 279-285.
- [45] Sander F. Wuister, Celso de Mello Donegá, and Andries Meijerink “Local-field effects on the spontaneous emission rate of CdTe and CdSe quantum dots in dielectric media” *J. Chem. Phys.* **121**, 4310 (2004)
- [46] W. Nomura, T. Yatsui, T. Kawazoe M. Naruse, M. Ohtsu “Structural dependency of optical excitation transfer via opticalnear-field interactions between semiconductor quantum dots” *Appl. Phys. B* **100** 181–187 (2010)
- [47] M. Naruse, H. Hori, K. Kobayashi, T. Kawazoe, M. Ohtsu “ Optical pulsation mechanism based on optical near-field interactions” *Appl. Phys. B* **102** 717-723 (2010)
- [48] T. Kawazoe, M. Ohtsu, S. Aso, Y. Sawado, Y. Hosoda, K. Akahane, N.Yamamoto, M.Naruse “Two dimensional array of room-temperature nanophotonic logic gates using InAs quantum dots in mesa Structures” *App. Phys. B* **103**: 537-546

- [49] T. Kawazoe, K. Kobayashi, S. Sangu and M. Ohtsu “Demonstrating nanophotonic switching using near-field pump–probe photoluminescence spectroscopy of CuCl quantum cubes” *Journal of Microscopy*, Vol. **209**, Pt 3 March 2003, pp. 261–266
- [50] T. Kawazoe, K. Kobayashi, K. Akahane, M. Naruse, N. Yamamoto and M. Ohtsu “Demonstration of nanophotonic NOT gate using near-field optically coupled quantum dots” *Appl. Phys. B* **84**, 243–246 (2006)
- [51] T. Kawazoe, K. Kobayashi, S. Sangu, and M. Ohtsu “Demonstration of a nanophotonic switching operation by optical near-field energy transfer” *Appl. Phys. Lett.* **82**, 2957 (2003)
- [52] M. Naruse, H. Hori, K. Kobayashi, P. Holmström, Lars Thylén, and M. Ohtsu “ Lower bound of energy dissipation in optical excitation transfer via optical near-field interactions” *Optics Express* / Vol. **18**, No. S4 (2010)



# Appendix A

## Projection operator method: Effective operator and effective interaction

If we consider an interacting system as a system of consisting an electromagnetic field and isolated quantum system, the Hamiltonian operator  $\hat{H}$  for the total system can be represented as the sum of the Hamiltonian of isolated system  $\hat{H}_0$  and the interaction potential  $\hat{V}$  as follows

$$\hat{H} = \hat{H}_0 + \hat{V} \quad (A1)$$

Let us denote eigenstates and eigenvalues of the Hamiltonian  $\hat{H}$  as  $|\psi_j\rangle$  and  $E_j$ . Then the following Schrödinger equation holds

$$\hat{H} |\psi_j\rangle = E_j |\psi_j\rangle \quad (A2)$$

Similarly, let us denote eigenstates of the Hamiltonian  $\hat{H}_0$  as  $|\phi_j\rangle$ . Then the projection operator  $P$  can be defined as

$$P = \sum_{j=1}^N |\phi_j\rangle\langle\phi_j| \quad (A3)$$

where  $N$  is an arbitrary integer. Acting  $P$  on an arbitrary state  $|\psi\rangle$ , we obtain

$$P |\psi\rangle = \sum_{j=1}^N |\phi_j\rangle\langle\phi_j|\psi\rangle \quad (A4)$$

This relation shows that the projection operator transforms the arbitrary state  $|\psi\rangle$  into the P space spanned by the eigenstate  $|\phi_j\rangle$ . The projection operator is defined based on steady states of the Schrödinger equation. We can use the projection operator  $P$  to derive an effective operator  $\hat{O}_{eff}$  of an arbitrary operator  $\hat{O}$  corresponding to a physical observable. Due to the orthonormalization of the eigenstate  $|\phi_j\rangle$ , the projection operator  $P$  satisfies the following relation

$$P = P^+, \quad P^2 = P \quad (A5)$$

The complimentary operator  $Q$  is then given by

$$Q = 1 - P \quad (A6)$$

Similarly,  $Q$  satisfies the following relations

$$Q = Q^+, \quad Q^2 = Q \quad (A7)$$

Here, any state in the P space is orthogonal to any state in the Q space

$$PQ = QP = 0 \quad (A8)$$

Since  $|\phi_j\rangle$  is an eigenstate of  $\hat{H}_0$ , the commutation between the projection operator and  $\hat{H}_0$  is zero

$$\begin{aligned} [P, \hat{H}_0] &= P\hat{H}_0 - \hat{H}_0P = 0 \\ [Q, \hat{H}_0] &= Q\hat{H}_0 - \hat{H}_0Q = 0 \end{aligned} \quad (A9)$$

Now, let us divide the eigenstates  $|\psi_j\rangle$  into two groups and define  $|\psi_j^{(1)}\rangle$  in the P space and  $|\psi_j^{(2)}\rangle$  in the Q space as follows

$$\begin{aligned} |\psi_j^{(1)}\rangle &= P|\psi_j\rangle \\ |\psi_j^{(2)}\rangle &= Q|\psi_j\rangle \end{aligned} \quad (A10)$$

Then, from Equation (A6) for  $|\psi_j^{(1)}\rangle$  and  $|\psi_j^{(2)}\rangle$ , we obtain the following equation

$$|\psi_j\rangle = P|\psi_j^{(1)}\rangle + Q|\psi_j^{(2)}\rangle \quad (A11)$$

From Equations (A1) and (A2), we have

$$(E_j - \hat{H}_0)|\psi_j\rangle = \hat{V}|\psi_j\rangle \quad (A12)$$

Inserting (A11) into (A12), we have got the following relation

$$(E_j - \hat{H}_0)P|\psi_j^{(1)}\rangle + (E_j - \hat{H}_0)Q|\psi_j^{(2)}\rangle = \hat{V}P|\psi_j^{(1)}\rangle + \hat{V}Q|\psi_j^{(2)}\rangle \quad (A13)$$

If we operate  $P$  from the left side of Equation (A13), we can obtain

$$(E_j - \hat{H}_0)P^2|\psi_j^{(1)}\rangle + (E_j - \hat{H}_0)PQ|\psi_j^{(2)}\rangle = P\hat{V}P|\psi_j^{(1)}\rangle + P\hat{V}Q|\psi_j^{(2)}\rangle$$

and using Equations (A5) and (A8), we have

$$(E_j - \hat{H}_0)P|\psi_j^{(1)}\rangle = P\hat{V}P|\psi_j^{(1)}\rangle + P\hat{V}Q|\psi_j^{(2)}\rangle \quad (A14)$$

Similarly operating  $Q$  from the left side on Equation (A13), we obtain

$$(E_j - \hat{H}_0)Q|\psi_j^{(2)}\rangle = Q\hat{V}P|\psi_j^{(1)}\rangle + Q\hat{V}Q|\psi_j^{(2)}\rangle \quad (A15)$$

From Equation (A15), we can express  $Q|\psi_j^{(2)}\rangle$  by  $P|\psi_j^{(1)}\rangle$  as follows

$$(E_j - \hat{H}_0 - Q\hat{V})Q|\psi_j^{(2)}\rangle = Q\hat{V}P|\psi_j^{(1)}\rangle \quad (A16)$$

and dividing both sides by  $(E_j - \hat{H}_0 - Q\hat{V})$ , we arrive at

$$\begin{aligned} Q|\psi_j^{(2)}\rangle &= (E_j - \hat{H}_0 - Q\hat{V})^{-1}Q\hat{V}P|\psi_j^{(1)}\rangle \\ &= \left\{ (E_j - \hat{H}_0) \left[ 1 - (E_j - \hat{H}_0)^{-1}Q\hat{V} \right] \right\}^{-1} Q\hat{V}P|\psi_j^{(1)}\rangle \\ &= \hat{J}(E_j - \hat{H}_0)^{-1}Q\hat{V}P|\psi_j^{(1)}\rangle \end{aligned} \quad (A17)$$

where the operator  $\hat{J}$  is defined by

$$\hat{J} = \left[ 1 - (E_j - \hat{H}_0)^{-1}Q\hat{V} \right]^{-1} \quad (A18)$$

If we substitute Equation (A17) into the second term on the right hand side in

Equation (A14), we obtain the equation for  $P|\psi_j^{(1)}\rangle$  as follows

$$\begin{aligned} (E_j - \hat{H}_0)P|\psi_j^{(1)}\rangle &= P\hat{V}P|\psi_j^{(1)}\rangle + P\hat{V}\hat{J}(E_j - \hat{H}_0)^{-1}Q\hat{V}P|\psi_j^{(1)}\rangle \\ &= P\hat{V}\hat{J} \left\{ \hat{J}^{-1} + (E_j - \hat{H}_0)^{-1}Q\hat{V} \right\} P|\psi_j^{(1)}\rangle \\ &= P\hat{V}\hat{J}P|\psi_j^{(1)}\rangle \end{aligned} \quad (A19)$$

Further, inserting Equation (A17) into Equation (A11), the following equation for  $|\psi_j\rangle$  is obtained

$$\begin{aligned} |\psi_j\rangle &= P|\psi_j^{(1)}\rangle + Q|\psi_j^{(2)}\rangle = P|\psi_j^{(1)}\rangle + \hat{J}(E_j - \hat{H}_0)^{-1}Q\hat{V}P|\psi_j^{(1)}\rangle \\ &= \hat{J} \left\{ \hat{J}^{-1} + (E_j - \hat{H}_0)^{-1}Q\hat{V} \right\} P|\psi_j^{(1)}\rangle = \hat{J}P|\psi_j^{(1)}\rangle \end{aligned} \quad (A20)$$

Therefore, we can rewrite Equation (A20) as  $|\psi_j\rangle = C\hat{J}P|\psi_j^{(1)}\rangle$  where  $C$  is the normalization constant. Taking the conjugate, we have  $\langle\psi_j| = C^*P\hat{J}^+\langle\psi_j^{(1)}|$ . From orthogonality we can find  $C$  as follows

$$\begin{aligned} \langle\psi_j|\psi_j\rangle &= C^*C(P\hat{J}^+\hat{J}P)\langle\psi_j^{(1)}|\psi_j^{(1)}\rangle \\ |C|^2 (P\hat{J}^+\hat{J}P) &= 1 \quad \text{and we have } C = (P\hat{J}^+\hat{J}P)^{-1/2} \end{aligned}$$

Finally

$$|\psi_j\rangle = \hat{J}P(P\hat{J}^+\hat{J}P)^{-1/2}|\psi_j^{(1)}\rangle \quad (A21)$$

Since  $|\psi_j\rangle$  has been expressed in terms of  $|\psi_j^{(1)}\rangle$ , we can obtain the effective operator  $\hat{O}_{eff}$  from the following relation

$$\langle\psi_i|\hat{O}|\psi_j\rangle=\langle\psi_i^{(1)}|\hat{O}_{eff}|\psi_j^{(1)}\rangle \quad (A22)$$

Substituting Equation (A21) into the left-hand side of Equation (A22) and comparing it with the right-hand side, we arrive at

$$\hat{O}_{eff}=(P\hat{J}^+\hat{J}P)^{-1/2}(P\hat{J}^+\hat{O}\hat{J}P)(P\hat{J}^+\hat{J}P)^{-1/2} \quad (A23)$$

Taking  $\hat{V}$  as  $\hat{O}$  the effective interaction operator

$$\hat{V}_{eff}=(P\hat{J}^+\hat{J}P)^{-1/2}(P\hat{J}^+\hat{V}\hat{J}P)(P\hat{J}^+\hat{J}P)^{-1/2} \quad (A24)$$

where  $\hat{V}_{eff}$  operates only on any states in the  $P$  space. Having the bare interaction  $\hat{V}$ , we can find  $\hat{V}_{eff}$  by obtaining the unknown operator  $\hat{J}$ .

To obtain the form of  $\hat{J}$ , let us consider operator relation  $[\hat{J},\hat{H}_0]P$  and operate it on the state  $|\psi_j\rangle$

$$[\hat{J},\hat{H}_0]P|\psi_j\rangle=(\hat{J}\hat{H}_0-\hat{H}_0\hat{J})P|\psi_j\rangle=\{(E_j-\hat{H}_0)\hat{J}-\hat{J}(E_j-\hat{H}_0)\}P|\psi_j\rangle \quad (A25)$$

Since  $\hat{H}=\hat{H}_0+\hat{V}$  and  $(E_j-\hat{H}_0)|\psi_j\rangle=\hat{V}|\psi_j\rangle$  replacing the first term  $(E_j-\hat{H}_0)$  in Equation (A25) by  $\hat{V}$  we have got

$$[\hat{J},\hat{H}_0]P|\psi_j\rangle=\hat{V}\hat{J}|\psi_j\rangle-\hat{J}(E_j-\hat{H}_0)P|\psi_j\rangle \quad (A26)$$

Using Equations (A11), (A14) and (A17), the second term of Equation (A26) can be changed to

$$\begin{aligned} \hat{J}(E_j-\hat{H}_0)P|\psi_j\rangle &= \hat{J}(E_j-\hat{H}_0)P|\psi_j^{(1)}\rangle = \hat{J}\{P\hat{V}P|\psi_j^{(1)}\rangle + P\hat{V}Q|\psi_j^{(2)}\rangle\} \\ &= \hat{J}P\hat{V}\{P|\psi_j^{(1)}\rangle + \hat{J}(E_j-\hat{H}_0)^{-1}Q\hat{V}P|\psi_j^{(1)}\rangle\} = \hat{J}P\hat{V}\hat{J}\{\hat{J}^{-1} + (E_j-\hat{H}_0)^{-1}Q\hat{V}\}P|\psi_j^{(1)}\rangle \end{aligned} \quad (A27)$$

Using the relations  $\hat{J}=[1-(E_j-\hat{H}_0)^{-1}Q\hat{V}]^{-1}$  and  $P|\psi_j^{(1)}\rangle=P|\psi_j\rangle$ , we have

$$\hat{J}(E_j-\hat{H}_0)P|\psi_j\rangle=\hat{J}P\hat{V}\hat{J}P|\psi_j^{(1)}\rangle \quad (A28)$$

So, we can rewrite Equation (A26) as

$$\left[ \hat{J}, \hat{H}_0 \right] P |\psi_j\rangle = \hat{V} \hat{J} P |\psi_j\rangle - \hat{J} P \hat{V} \hat{J} P |\psi_j\rangle \quad (A29)$$

Therefore, for operator  $\hat{J}$ , we have

$$\left[ \hat{J}, \hat{H}_0 \right] P = \hat{V} \hat{J} P - \hat{J} P \hat{V} \hat{J} P \quad (A30)$$

To solve Equation (A30) perturbatively, let us assume

$$\hat{J} = \sum_{n=0}^{\infty} g^n \hat{J}^{(n)} \quad (A31)$$

where the  $n$ th term contains  $n$   $\hat{V}$  s and  $\hat{J}^{(0)} = P$ . If we substitute Equation (A31) into equation (A30) and equalize the terms of order  $g^n$  on both sides, we obtain  $\hat{J}^{(1)}, \dots, \hat{J}^{(n)}$ .

For example, by using the identity (A30), we can write the following identity

$$Q \left[ \hat{J}^{(1)}, \hat{H}_0 \right] P = Q \hat{V} \hat{J}^{(0)} P - Q \hat{J}^{(0)} P \hat{V} \hat{J}^{(0)} P = Q \hat{V} P \quad (A32)$$

where, we have used the following identities

$$\hat{J}^{(0)} = P \quad PQ = QP = 0$$

Taking the matrix elements of Equation (A32) with state ket  $|\psi_j\rangle$ , we have

$$\begin{aligned} \langle \psi_i | Q \left[ \hat{J}^{(1)}, \hat{H}_0 \right] P |\psi_j\rangle &= \langle \psi_i | Q (\hat{J}^{(1)} \hat{H}_0 - \hat{H}_0 \hat{J}^{(1)}) P |\psi_j\rangle \\ &= \langle \psi_i | Q \hat{J}^{(1)} (E_P^0 - E_Q^0) P |\psi_j\rangle = \langle \psi_i | Q \hat{V} P |\psi_j\rangle \end{aligned} \quad (A33)$$

where  $E_P^0$  and  $E_Q^0$  are the eigenvalues of the Hamiltonian  $\hat{H}_0$  in the  $P$  and  $Q$  spaces, respectively. From Equation (A33), we have

$$\langle \psi_i | Q \hat{J}^{(1)} (E_P^0 - E_Q^0) P |\psi_j\rangle = \langle \psi_i | Q \hat{V} P |\psi_j\rangle \quad (A34)$$

and for  $\hat{J}^{(1)}$ , we obtain  $\hat{J}^{(1)} (E_P^0 - E_Q^0) = Q \hat{V} P$ . Multiplying both sides from the right by  $(E_P^0 - E_Q^0)^{-1}$ , we obtain the final expression for  $\hat{J}^{(1)}$  as follows.

$$\hat{J}^{(1)} = Q \hat{V} (E_P^0 - E_Q^0)^{-1} P \quad (A35)$$

# Appendix B

## Derivation of the interaction potential

The effective interaction in the  $P$  space is given by

$$\hat{V}_{eff} = (P\hat{J}^+\hat{J}P)^{-1/2}(P\hat{J}^+\hat{V}\hat{J}P)(P\hat{J}^+\hat{J}P)^{-1/2} \quad (B1)$$

The bare interaction between the two subsystems in a dipole approximation is

$$\hat{V} = -\left\{\hat{\mu}_s \cdot \hat{D}^\perp(\vec{r}_s) + \hat{\mu}_p \cdot \hat{D}^\perp(\vec{r}_p)\right\} \quad (B2)$$

we can represent electric displacement operator  $\hat{D}(\vec{r})$  in terms of vector potential  $\vec{A}(\vec{r})$  and conjugate momentum  $\hat{\Pi}(\vec{r})$

$$\hat{\Pi}(\vec{r}) = \frac{1}{4\pi c^2} \frac{\partial \vec{A}}{\partial t} - \frac{1}{c} \hat{P}(\vec{r}) = -\frac{1}{4\pi c} \hat{E}^\perp(\vec{r}) - \frac{1}{c} \hat{P}^\perp(\vec{r}) = -\frac{1}{4\pi c} \left[ \hat{E}^\perp(\vec{r}) + 4\pi \hat{P}^\perp(\vec{r}) \right] \quad (B3)$$

Since  $\hat{D}^\perp(\vec{r}) = \hat{E}^\perp(\vec{r}) + 4\pi \hat{P}^\perp(\vec{r})$ , we have  $\hat{\Pi}(\vec{r}) = -\frac{1}{4\pi c} \hat{D}^\perp(\vec{r})$

where  $\hat{P}^\perp(\vec{r})$  and  $\hat{E}^\perp(\vec{r})$  are the transverse components of the polarization and electric fields. The mode expansion of  $\vec{A}(\vec{r})$  and  $\hat{\Pi}(\vec{r})$  in terms of the electron creation and annihilation is

$$\vec{A}(\vec{r}) = \sum_{\vec{k}} \sum_{\lambda=1}^2 \left( \frac{2\pi\hbar c^2}{V\omega_{\vec{k}}} \right)^{1/2} \vec{e}_\lambda(\vec{k}) \left\{ \hat{a}_\lambda(\vec{k}) e^{i\vec{k}\vec{r}} + \hat{a}_\lambda^+(\vec{k}) e^{-i\vec{k}\vec{r}} \right\} \quad (B4)$$

$$\begin{aligned} \hat{\Pi}(\vec{r}) &= \frac{1}{4\pi c^2} \frac{\partial \vec{A}}{\partial t} = \frac{1}{4\pi c^2} \frac{\partial}{\partial t} \left\{ \left( \frac{2\pi\hbar c^2}{V\omega_{\vec{k}}} \right)^{1/2} \sum_{\vec{k}} \sum_{\lambda=1}^2 \vec{e}_\lambda(\vec{k}) \left( \hat{a}_\lambda(\vec{k}) e^{i\vec{k}\vec{r}} + \hat{a}_\lambda^+(\vec{k}) e^{-i\vec{k}\vec{r}} \right) \right\} = \\ &= \frac{1}{4\pi c} \left( \frac{2\pi\hbar}{V\omega_{\vec{k}}} \right)^{1/2} \sum_{\vec{k}} \sum_{\lambda=1}^2 \vec{e}_\lambda(\vec{k}) \left\{ \hat{a}_\lambda(\vec{k}) e^{i\vec{k}\vec{r}} (i\vec{k}\dot{\vec{r}}) + \hat{a}_\lambda^+(\vec{k}) e^{-i\vec{k}\vec{r}} (-i\vec{k}\dot{\vec{r}}) \right\} \end{aligned} \quad (B5)$$

So, we have

$$\hat{\Pi}(\vec{r}) = \frac{1}{4\pi c^2} \frac{\partial \vec{A}}{\partial t} = -\frac{i}{4\pi c} \sum_{\vec{k}} \sum_{\lambda=1}^2 \left( \frac{2\pi\hbar\omega_{\vec{k}}}{V} \right)^{1/2} \vec{e}_\lambda(\vec{k}) \left\{ \hat{a}_\lambda(\vec{k}) e^{i\vec{k}\vec{r}} - \hat{a}_\lambda^+(\vec{k}) e^{-i\vec{k}\vec{r}} \right\} \quad (B5)$$

Since we have  $\hat{D}^\perp(\vec{r}) = 4\pi c\hat{\Pi}(\vec{r})$ ,

$$\hat{D}^\perp(\vec{r}) = i \sum_{\vec{k}} \sum_{\lambda=1}^2 \left( \frac{2\pi\hbar\omega_{\vec{k}}}{V} \right)^{1/2} \vec{e}_\lambda(\vec{k}) \left\{ \hat{a}_\lambda(\vec{k}) e^{i\vec{k}\vec{r}} - \hat{a}_\lambda^+(\vec{k}) e^{-i\vec{k}\vec{r}} \right\} \quad (B6)$$

where  $\hat{a}_\lambda(\vec{k})$  and  $\hat{a}_\lambda^+(\vec{k})$  are the creation and annihilation operators of photon,  $\vec{k}$  is wavevector,  $\omega_{\vec{k}}$  is angular frequency,  $\vec{e}_\lambda(\vec{k})$  is unit vector in polarization direction and  $V$  is quantization volume.

Rewriting the creation and annihilation operators of photon,  $\hat{a}_\lambda(\vec{k})$  and  $\hat{a}_\lambda^+(\vec{k})$ , in terms of the exciton-polariton creation  $\hat{\xi}^+(\vec{k})$  and annihilation  $\hat{\xi}(\vec{k})$  operators and defining  $\hat{\mu}_s = \vec{\mu}_s(\hat{B}(\vec{r}_s) + \hat{B}^+(\vec{r}_s))$ , we have

$$\begin{aligned} \hat{V} &= -\left(\hat{B}(\vec{r}_s) + \hat{B}^+(\vec{r}_s)\right) \vec{\mu}_s \cdot i \sum_{\vec{k}} \sum_{\lambda=1}^2 \left( \frac{2\pi\hbar\omega_{\vec{k}}}{V} \right)^{1/2} \vec{e}_\lambda(\vec{k}) \left\{ \hat{a}_\lambda(\vec{k}) e^{i\vec{k}\vec{r}_s} - \hat{a}_\lambda^+(\vec{k}) e^{-i\vec{k}\vec{r}_s} \right\} - \\ & - \left(\hat{B}(\vec{r}_p) + \hat{B}^+(\vec{r}_p)\right) \vec{\mu}_p \cdot i \sum_{\vec{k}} \sum_{\lambda=1}^2 \left( \frac{2\pi\hbar\omega_{\vec{k}}}{V} \right)^{1/2} \vec{e}_\lambda(\vec{k}) \left\{ \hat{a}_\lambda(\vec{k}) e^{i\vec{k}\vec{r}_p} - \hat{a}_\lambda^+(\vec{k}) e^{-i\vec{k}\vec{r}_p} \right\} = \\ & = -i \sum_{\vec{k}} \sum_{\lambda=1}^2 \left( \frac{2\pi\hbar\omega_{\vec{k}}}{V} \right)^{1/2} \left( \hat{B}(\vec{r}_s) + \hat{B}^+(\vec{r}_s) \right) \vec{\mu}_s \cdot \vec{e}_\lambda(\vec{k}) \cdot \left[ \hat{a}_\lambda(\vec{k}) e^{i\vec{k}\vec{r}_s} - \hat{a}_\lambda^+(\vec{k}) e^{-i\vec{k}\vec{r}_s} \right] - \\ & - i \sum_{\vec{k}} \sum_{\lambda=1}^2 \left( \frac{2\pi\hbar\omega_{\vec{k}}}{V} \right)^{1/2} \left( \hat{B}(\vec{r}_p) + \hat{B}^+(\vec{r}_p) \right) \vec{\mu}_p \cdot \vec{e}_\lambda(\vec{k}) \cdot \left[ \hat{a}_\lambda(\vec{k}) e^{i\vec{k}\vec{r}_p} - \hat{a}_\lambda^+(\vec{k}) e^{-i\vec{k}\vec{r}_p} \right] \end{aligned} \quad (B7)$$

where  $\hat{B}(\vec{r})$  and  $\hat{B}^+(\vec{r})$  are the creation and annihilation operators leading to electric dipole transitions, and creation and annihilation operators are defined by

$$\hat{a}(\vec{k}) = W^*(k)\xi(k) - y(k)\xi^+(k) \quad -\hat{a}^+(-k) = y^*(k)\xi(k) - W(k)\xi^+(-k) \quad (B8)$$

Taking the first part of Equation (B7), we obtain

$$\begin{aligned} & \left( \vec{\mu}_s \cdot \vec{e}_\lambda(\vec{k}) \right) \left[ \hat{B}(\vec{r}_s) + \hat{B}^+(\vec{r}_s) \right] \left[ \hat{a}_\lambda(\vec{k}) e^{i\vec{k}\vec{r}_s} - \hat{a}_\lambda^+(\vec{k}) e^{-i\vec{k}\vec{r}_s} \right] = \left( \vec{\mu}_s \cdot \vec{e}_\lambda(\vec{k}) \right) \times \\ & \times \left\{ \left[ \hat{B}(\vec{r}_s) + \hat{B}^+(\vec{r}_s) \right] \left[ W^*(k)\xi(k) - y(k)\xi^+(k) \right] e^{i\vec{k}\vec{r}_s} \right\} + \left( \vec{\mu}_s \cdot \vec{e}_\lambda(\vec{k}) \right) \times \\ & \times \left\{ \left[ y^*(-k)\xi(-k) - W(-k)\xi^+(k) \right] e^{-i\vec{k}\vec{r}_s} \right\} = \left( \vec{\mu}_s \cdot \vec{e}_\lambda(\vec{k}) \right) \left[ \hat{B}(\vec{r}_s) + \hat{B}^+(\vec{r}_s) \right] \times \\ & \times \left[ W^*(k) e^{i\vec{k}\vec{r}_s} \xi(k) - y(k) e^{i\vec{k}\vec{r}_s} \xi^+(k) + y^*(-k) e^{-i\vec{k}\vec{r}_s} \xi(-k) - W(-k) e^{-i\vec{k}\vec{r}_s} \xi^+(k) \right] = \\ & = \left( \vec{\mu}_s \cdot \vec{e}_\lambda(\vec{k}) \right) \left[ \hat{B}(\vec{r}_s) + \hat{B}^+(\vec{r}_s) \right] \left( W^*(k) e^{i\vec{k}\vec{r}_s} \xi(k) + y^*(-k) e^{-i\vec{k}\vec{r}_s} \xi(-k) \right) - \\ & - \left( \vec{\mu}_s \cdot \vec{e}_\lambda(\vec{k}) \right) \left[ \hat{B}(\vec{r}_s) + \hat{B}^+(\vec{r}_s) \right] \left( W(-k) e^{-i\vec{k}\vec{r}_s} \xi^+(k) + y(k) e^{i\vec{k}\vec{r}_s} \xi^+(-k) \right) = \end{aligned} \quad (B9)$$

by changing  $k \rightarrow -k$ , we have

$$\begin{aligned}
&= \left( \vec{\mu}_s \cdot \vec{e}_\lambda(\vec{k}) \right) \left[ \hat{B}(\vec{r}_s) + \hat{B}^+(\vec{r}_s) \right] \left[ \left( W^*(k) + y^*(k) \right) e^{i\vec{k}\vec{r}_s} \cdot \hat{\xi}(k) \right] + \\
&+ \left( \vec{\mu}_s \cdot \vec{e}_\lambda(\vec{k}) \right) \left[ \hat{B}(\vec{r}_s) + \hat{B}^+(\vec{r}_s) \right] \left[ \left( W(-k) + y(-k) \right) e^{-i\vec{k}\vec{r}_s} \cdot \hat{\xi}^+(k) \right]
\end{aligned} \tag{B10}$$

where we have the following relations

$$y(k) = -\frac{E(k) - \hbar\omega_k}{E(k) + \hbar\omega_k} W(k) = -\frac{\Omega(k) - \omega_k}{\Omega(k) + \omega_k} W(k) \tag{B11}$$

$$W(k) = \frac{E(k) + \hbar\omega_k}{2\sqrt{E(k)\hbar\omega_k}} \sqrt{\frac{E^2(k) - E_m^2}{2E^2(k) - E_m^2 - \hbar^2\omega_k^2}} = \frac{\Omega(k) + \omega_k}{2\sqrt{\Omega_k\omega_k}} \sqrt{\frac{\Omega^2(k) - \Omega^2}{2\Omega^2(k) - \Omega^2 - \omega_k^2}} \tag{B12}$$

where  $E(k) = \hbar\Omega(k)$  and  $E_m = \hbar\Omega$  are the eigenenergy of exciton-polariton and excitation energy of macroscopic subsystem. So, we have got

$$W(k) + y(k) = W(k) \left[ 1 - \frac{\Omega(k) - \omega_k}{\Omega(k) + \omega_k} \right] = \sqrt{\frac{\omega_k}{\Omega(k)}} \sqrt{\frac{\Omega^2(k) - \Omega^2}{2\Omega^2(k) - \Omega^2 - \omega_k^2}} \tag{B13}$$

Here  $\omega_k \equiv \omega(k) = ck$  and we define  $f(k)$  function as follows

$$f(k) = \frac{ck}{\sqrt{\Omega(k)}} \sqrt{\frac{\Omega^2(k) - \Omega^2}{2\Omega^2(k) - \Omega^2 - (ck)^2}} \tag{B14}$$

where  $f(k) = f(-k) = f^*(k)$ . So, the last expression changes to

$$W(-k) + y(-k) = \frac{1}{\sqrt{\omega(-k)}} \frac{\omega(-k)}{\Omega(k)} \sqrt{\frac{\Omega^2(-k) - \Omega^2}{2\Omega^2(-k) - \Omega^2 - (ck)^2}} = \frac{f(-k)}{\sqrt{\omega(-k)}} \tag{B15}$$

So, Equation (B10) changes to

$$\begin{aligned}
&\left[ \hat{B}(\vec{r}_s) + \hat{B}^+(\vec{r}_s) \right] \left( \vec{\mu}_s \cdot \vec{e}_\lambda(\vec{k}) \right) \left[ \left( W^*(k) + y^*(k) \right) e^{i\vec{k}\vec{r}_s} \cdot \hat{\xi}(k) \right] + \\
&+ \left[ \hat{B}(\vec{r}_s) + \hat{B}^+(\vec{r}_s) \right] \left( \vec{\mu}_s \cdot \vec{e}_\lambda(\vec{k}) \right) \left[ \left( W(-k) + y(-k) \right) e^{-i\vec{k}\vec{r}_s} \cdot \hat{\xi}^+(k) \right] = \\
&= \frac{\left[ \hat{B}(\vec{r}_s) + \hat{B}^+(\vec{r}_s) \right]}{\sqrt{\omega(k)}} \left( \vec{\mu}_s \cdot \vec{e}_\lambda(\vec{k}) \right) \left\{ f(k) e^{i\vec{k}\vec{r}_s} \hat{\xi}(k) - f^*(k) e^{-i\vec{k}\vec{r}_s} \hat{\xi}^+(k) \right\}
\end{aligned} \tag{B16}$$



Inserting the summation over  $\lambda$ , we obtain

$$\begin{aligned}
& -i \sum_{\vec{k}} \left( \frac{2\pi\hbar\omega_{\vec{k}}}{V} \right)^{1/2} \left[ \hat{B}(\vec{r}_s) + \hat{B}^+(\vec{r}_s) \right] \frac{1}{\sqrt{\omega(k)}} \left\{ \sum_{\lambda=1}^2 (\vec{\mu}_s \cdot \vec{e}_\lambda(\vec{k})) f(k) e^{i\vec{k}\vec{r}_s} \cdot \hat{\xi}(k) \right\} - \\
& -i \sum_{\vec{k}} \left( \frac{2\pi\hbar\omega_{\vec{k}}}{V} \right)^{1/2} \left[ \hat{B}(\vec{r}_s) + \hat{B}^+(\vec{r}_s) \right] \frac{1}{\sqrt{\omega(k)}} \left\{ \sum_{\lambda=1}^2 (\vec{\mu}_s \cdot \vec{e}_\lambda(\vec{k})) f^*(k) e^{-i\vec{k}\vec{r}_s} \cdot \hat{\xi}^+(k) \right\} = \\
& = i \sum_{\vec{k}} \left( \frac{2\pi\hbar\omega_{\vec{k}}}{V} \right)^{1/2} \left[ \hat{B}(\vec{r}_s) + \hat{B}^+(\vec{r}_s) \right] \frac{1}{\sqrt{\omega(k)}} \left\{ K_s(\vec{k}) \cdot \hat{\xi}(k) - K_s^*(\vec{k}) \hat{\xi}^+(k) \right\}
\end{aligned} \tag{B17}$$

where  $K_\alpha$  and  $K_\alpha^*$  are the coupling coefficients between the probe (sample) and the exciton-polariton and defined as  $K_\alpha = \sum_{\lambda=1}^2 (\vec{\mu}_\alpha \cdot \vec{e}_\lambda(\vec{k})) f^*(k) e^{-i\vec{k}\vec{r}_\alpha}$ .

Finally, after simplifications, we have

$$\begin{aligned}
\hat{V} = & -i \sum_{\vec{k}} \left( \frac{2\pi\hbar}{V} \right)^{1/2} \left( \hat{B}(\vec{r}_s) + \hat{B}^+(\vec{r}_s) \right) (K_s(\vec{k}) \cdot \hat{\xi}(k) - K_s^*(\vec{k}) \hat{\xi}^+(k)) - \\
& -i \sum_{\vec{k}} \left( \frac{2\pi\hbar}{V} \right)^{1/2} \left( \hat{B}(\vec{r}_p) + \hat{B}^+(\vec{r}_p) \right) (K_p(\vec{k}) \cdot \hat{\xi}(k) - K_p^*(\vec{k}) \hat{\xi}^+(k))
\end{aligned} \tag{B18}$$

Taking the summation for S and P, we have

$$\hat{V} = -i \sum_{\alpha=s}^p \sum_{\vec{k}} \left( \frac{2\pi\hbar}{V} \right)^{1/2} \left( \hat{B}(\vec{r}_\alpha) + \hat{B}^+(\vec{r}_\alpha) \right) (K_\alpha(\vec{k}) \cdot \hat{\xi}(k) - K_\alpha^*(\vec{k}) \hat{\xi}^+(k)) \tag{B19}$$

The effective sample probe tip interaction in the  $P$  space is defined as

$$V_{eff}(2,1) = \langle \phi_2 | V_{eff} | \phi_1 \rangle \tag{B20}$$

Inserting the expression (B1) in Equation (B20), we have

$$V_{eff}(2,1) = \langle \phi_2 | (P\hat{J}^+ \hat{J}P)^{-1/2} (P\hat{J}^+ \hat{V} \hat{J}P) (P\hat{J}^+ \hat{J}P)^{-1/2} | \phi_1 \rangle \tag{B21}$$

Since  $C = (P\hat{J}^+ \hat{J}P)^{-1/2}$  is a normalization constant and the first order approximation of  $\hat{J}$  gives  $\hat{J}^{(1)} = P + Q\hat{V}(E_p^{(0)} - E_Q^{(0)})^{-1}P$ , we get

$$\begin{aligned}
(P\hat{J}^+ \hat{V} \hat{J}P) &= \left[ P(P + Q\hat{V}(E_p^0 - E_Q^0)^{-1}P)^+ \hat{V}(P + Q\hat{V}(E_p^0 - E_Q^0)^{-1}P)P \right] = \\
&= \left[ (P + P(E_p^0 - E_Q^0)^{-1}\hat{V}Q)\hat{V}(P + Q\hat{V}(E_p^0 - E_Q^0)^{-1}P) \right] = \\
&= P\hat{V}Q\hat{V}(E_p^0 - E_Q^0)^{-1}P + P(E_p^0 - E_Q^0)^{-1}\hat{V}Q\hat{V}P
\end{aligned} \tag{B22}$$

Therefore,

$$\begin{aligned}
V_{eff}(2,1) &= \langle \phi_2 | P\hat{V}Q\hat{V}(E_p^0 - E_Q^0)^{-1}P | \phi_1 \rangle + \langle \phi_2 | P(E_p^0 - E_Q^0)^{-1}\hat{V}Q\hat{V}P | \phi_1 \rangle = \\
&= \sum_m \langle \phi_2 | P\hat{V}Q | m \rangle \langle m | Q\hat{V}(E_p^0 - E_Q^0)^{-1}P | \phi_1 \rangle + \sum_m \langle \phi_2 | P(E_p^0 - E_Q^0)^{-1}\hat{V}Q | m \rangle \times \\
&\times \langle m | Q\hat{V}P | \phi_1 \rangle = \sum_m \langle \phi_2 | P\hat{V}Q | m \rangle \langle m | Q\hat{V}P | \phi_1 \rangle \left( \frac{1}{(E_{p1}^0 - E_{Qm}^0)} - \frac{1}{(E_{p2}^0 - E_{Qm}^0)} \right)
\end{aligned} \tag{B23}$$

and finally the effective interaction in the  $P$  space is

$$V_{eff}(2,1) = \sum_m \langle \phi_2 | P\hat{V}Q | m \rangle \langle m | Q\hat{V}P | \phi_1 \rangle \left( \frac{1}{(E_{p1}^0 - E_{Qm}^0)} - \frac{1}{(E_{p2}^0 - E_{Qm}^0)} \right) \tag{B24}$$

where  $E_{p1}^0$  and  $E_{p2}^0$  are the eigenenergies of  $|\phi_1\rangle$  and  $|\phi_2\rangle$  in the  $P$  space and  $E_{Qm}^0$  is the eigenenergy of  $|m\rangle$  in the  $Q$  space. The matrix element  $\langle m | Q\hat{V}P | \phi_1 \rangle$  in Equation (B24) represents the virtual transition from the initial state  $|\phi_1\rangle$  in the  $P$  space to the intermediate state  $|m\rangle$  in the  $Q$  space, while the matrix element  $\langle \phi_2 | P\hat{V}Q | m \rangle$  represents the subsequent virtual transition from the intermediate state  $|m\rangle$  in the  $Q$  space to the final state  $|\phi_2\rangle$  in the  $P$  space. To find the bare interaction in the  $P$  space, we have to calculate transition matrix elements shown above. First, note that among arbitrary intermediate states only two intermediate states can contribute to nonzero matrix elements. We define  $|\phi_1\rangle$  and  $|\phi_2\rangle$  states in the  $P$  space as  $|\phi_1\rangle = |s^*\rangle |p\rangle \otimes |O_{(M)}\rangle$  and  $|\phi_2\rangle = |s\rangle |p^*\rangle \otimes |O_{(M)}\rangle$  and intermediate  $|m\rangle$  states in the  $Q$  space as  $|m\rangle = |s\rangle |p\rangle \otimes |\vec{k}\rangle$  and  $|m\rangle = |s^*\rangle |p^*\rangle \otimes |\vec{k}\rangle$ .

Inserting Equation (B18) and  $|\phi_1\rangle$ ,  $|\phi_2\rangle$  and  $|m\rangle$  states in to (B24), we obtain

$$\begin{aligned}
V_{eff}(2,1) &= - \left( \frac{2\pi\hbar}{V} \right) \sum_m \sum_k \langle \phi_2 | \sum_{\alpha=s}^p \left\{ \left( \hat{B}(\vec{r}_\alpha) + \hat{B}^+(\vec{r}_\alpha) \right) (K_\alpha(\vec{k})\hat{\xi}(k) - K_\alpha^*(\vec{k})\hat{\xi}^+(k)) \right\} | m \rangle \\
&\langle m | \sum_{\alpha=s}^p \left\{ \left( \hat{B}(\vec{r}_\alpha) + \hat{B}^+(\vec{r}_\alpha) \right) (K_\alpha(\vec{k})\hat{\xi}(k) - K_\alpha^*(\vec{k})\hat{\xi}^+(k)) \right\} | \phi_1 \rangle \left( \frac{1}{E_{p1}^0 - E_{Qm}^0} - \frac{1}{E_{p2}^0 - E_{Qm}^0} \right)
\end{aligned} \tag{B25}$$

Since  $\hat{B}(\vec{r}_\alpha)(|s\rangle, |p\rangle) = 0$ ,  $\hat{B}^+(\vec{r}_\alpha)(|s^*\rangle, |p^*\rangle) = 0$ ,  $\hat{\xi}^+(k)|\vec{k}\rangle = 0$ ,  
and  $\hat{\xi}(k)|O_{(M)}\rangle = 0$  the only terms survived in (B25) are

$$\begin{aligned}
V_{\text{eff}}(2,1) = & -\left(\frac{2\pi\hbar}{V}\right) \sum_{\vec{k}} \langle O_{(M)} | \otimes \langle p^* | \langle s | \left( \hat{B}^+(\vec{r}_p) K_p(\vec{k}) \hat{\xi}(k) \right) | s \rangle | p \rangle \otimes |\vec{k}\rangle \times \\
& \langle \vec{k} | \otimes \langle p | \langle s | \left( -\hat{B}(\vec{r}_s) K_s^*(\vec{k}) \hat{\xi}^+(k) \right) | s^* \rangle | p \rangle \otimes | O_{(M)} \rangle \left( \frac{1}{E_{P1}^0 - E_{Qm}^0} - \frac{1}{E_{P2}^0 - E_{Qm}^0} \right) + \\
& + \left( -\frac{2\pi\hbar}{V} \right) \sum_{\vec{k}} \langle O_{(M)} | \otimes \langle p^* | \langle s | \left( \hat{B}(\vec{r}_s) K_s(\vec{k}) \hat{\xi}(k) \right) | s^* \rangle | p^* \rangle \otimes |\vec{k}\rangle \times \\
& \langle \vec{k} | \otimes \langle p^* | \langle s^* | \left( -\hat{B}^+(\vec{r}_p) K_p^*(\vec{k}) \hat{\xi}^+(k) \right) | s^* \rangle | p \rangle \otimes | O_{(M)} \rangle \left( \frac{1}{E_{P1}^0 - E_{Qm}^0} - \frac{1}{E_{P2}^0 - E_{Qm}^0} \right)
\end{aligned} \tag{B26}$$

$$\begin{aligned}
V_{\text{eff}}(2,1) = & 2 \left( \frac{2\pi\hbar}{V} \right) \sum_{\vec{k}} K_p(\vec{k}) K_s^*(\vec{k}) \left( \frac{1}{E(s^*) + E(p) - (E(s) + E(p) + \hbar\Omega(k))} \right) + \\
& + 2 \left( \frac{2\pi\hbar}{V} \right) \sum_{\vec{k}} K_s(\vec{k}) K_p^*(\vec{k}) \left( \frac{1}{E(s^*) + E(p) - (E(s^*) + E(p^*) + \hbar\Omega(k))} \right) = \\
= & 2 \left( \frac{2\pi\hbar}{V} \right) \sum_{\vec{k}} K_p(\vec{k}) K_s^*(\vec{k}) \left( \frac{1}{E(s^*) - E(s) - \hbar\Omega(k)} \right) + \\
& + 2 \left( \frac{2\pi\hbar}{V} \right) \sum_{\vec{k}} K_s(\vec{k}) K_p^*(\vec{k}) \left( \frac{1}{E(p) - E(p^*) - \hbar\Omega(k)} \right)
\end{aligned} \tag{B27}$$

where  $E(s)$ ,  $E(s^*)$  and  $E(p)$ ,  $E(p^*)$  are the ground and excited energies of  $|s\rangle$  and  $|p\rangle$  states, respectively.  $E(s^*) - E(s) = \hbar\Omega_0(s)$  and  $E(p^*) - E(p) = \hbar\Omega_0(p)$  are the differences between the excited and ground state energies and  $E(k) = \hbar\Omega(k)$  is the excitation energy. Replacing summation over  $\vec{k}$  by

integration  $\frac{V}{(2\pi)^3} \int d^3k$ , we have

$$V_{\text{eff}}(2,1) = -\frac{1}{(2\pi)^2} \int d^3k \left( \frac{K_p(\vec{k}) K_s^*(\vec{k})}{\Omega(k) - \Omega_0(s)} + \frac{K_s(\vec{k}) K_p^*(\vec{k})}{\Omega(k) + \Omega_0(p)} \right) \tag{B28}$$

Similarly, we can calculate  $V_{eff}(1,2) = \langle \phi_1 | V_{eff} | \phi_2 \rangle$  as

$$V_{eff}(1,2) = -\frac{1}{(2\pi)^2} \int d^3k \left( \frac{K_s(\vec{k})K_p^*(\vec{k})}{\Omega(k) - \Omega_0(p)} + \frac{K_p(\vec{k})K_s^*(\vec{k})}{\Omega(k) + \Omega_0(s)} \right) \quad (B29)$$

The total amplitude of effective interaction potential is defined as a sum of  $V_{eff}(1,2)$  and  $V_{eff}(2,1)$  as follows

$$V_{eff}(\vec{r}) = -\frac{1}{4\pi^2} \sum_{\lambda=1}^2 \sum_{\alpha=p,s} \int d^3k \left[ (\vec{\mu}_s \cdot \vec{e}_\lambda(\vec{k})) (\vec{\mu}_p \cdot \vec{e}_\lambda(\vec{k})) \hbar f^2(k) \right] \left( \frac{e^{i\vec{k}\vec{r}}}{E(k) + E(\alpha)} + \frac{e^{-i\vec{k}\vec{r}}}{E(k) - E(\alpha)} \right) \quad (B30)$$

The summation over  $\lambda$  is  $\sum_{\lambda=1}^2 \vec{e}_{\lambda i}(\vec{k}) \vec{e}_{\lambda j}(\vec{k}) = \delta_{ij} - \hat{k}_i \hat{k}_j$ . Therefore, we obtain

$$\sum_{\lambda=1}^2 (\vec{\mu}_s \cdot \vec{e}_\lambda(\vec{k})) (\vec{\mu}_p \cdot \vec{e}_\lambda(\vec{k})) = \sum_{\lambda=1}^2 \sum_{i,j} (\vec{\mu}_{s i} \cdot \vec{e}_{\lambda i}(\vec{k})) (\vec{\mu}_{p j} \cdot \vec{e}_{\lambda j}(\vec{k})) = \sum_{i,j} \vec{\mu}_{s i} \vec{\mu}_{p j} (\delta_{ij} - \hat{k}_i \hat{k}_j) \quad (B31)$$

Here  $\hat{k}$  is the unit vector and defined as  $\hat{k} \equiv \vec{k}/k$ . Since we have  $d^3k = k^2 dk d\Omega = k^2 dk \sin\theta d\theta d\varphi$  then

$$\delta_{ij} \int e^{\pm i\vec{k}\vec{r}} d\Omega = \delta_{ij} \int_0^{2\pi} \int_{-1}^1 e^{\pm ikr \cos\theta} d(\cos\theta) d\varphi = \delta_{ij} \frac{2\pi}{ikr} (e^{ikr} - e^{-ikr}) \quad (B32)$$

and

$$-\int \hat{k}_i \hat{k}_j e^{\pm i\vec{k}\vec{r}} d\Omega = -\left( \frac{-i\vec{\nabla}_i}{k} \right) \left( \frac{-i\vec{\nabla}_j}{k} \right) \int e^{\pm i\vec{k}\vec{r}} d\Omega = \frac{2\pi}{ik^3} \vec{\nabla}_i \vec{\nabla}_j \left( \frac{e^{ikr} - e^{-ikr}}{r} \right) \quad (B33)$$

Here from  $\vec{p} = \hbar\vec{k}$  and  $\vec{p} = -i\hbar\vec{\nabla}$  we have  $\vec{k} = -i\vec{\nabla}$

So, we arrive at

$$\int (\delta_{ij} - \hat{k}_i \hat{k}_j) e^{\pm i\vec{k}\vec{r}} d\Omega = \delta_{ij} \frac{2\pi}{ikr} (e^{ikr} - e^{-ikr}) + \frac{2\pi}{ik^3} \nabla_i \nabla_j \left( \frac{e^{ikr} - e^{-ikr}}{r} \right) \quad (B34)$$

Taking into account that  $(\vec{\nabla}_i \cdot r) = \hat{r}_i$  and  $(\vec{\nabla}_i \cdot \hat{r}_j) = \delta_{ij}$ , we get

$$\begin{aligned} \int (\delta_{ij} - \hat{k}_i \hat{k}_j) e^{\pm i\vec{k}\vec{r}} d\Omega &= \delta_{ij} \frac{2\pi}{ikr} (e^{ikr} - e^{-ikr}) + \frac{2\pi}{ik^3} \nabla_i \nabla_j \left( \frac{e^{ikr} - e^{-ikr}}{r} \right) = \\ &= 2\pi \left[ \delta_{ij} \frac{(e^{ikr} - e^{-ikr})}{ikr} - \hat{r}_i \hat{r}_j \left( \frac{e^{ikr} - e^{-ikr}}{ikr} \right) + (\delta_{ij} - 3\hat{r}_i \hat{r}_j) \left\{ \frac{(e^{ikr} + e^{-ikr})}{k^2 r^2} - \frac{(e^{ikr} - e^{-ikr})}{ik^3 r^3} \right\} \right] \quad (B35) \end{aligned}$$

Putting Equation (B35) into (B30), we have

$$V_{eff}(\vec{r}) = -\frac{1}{2\pi} \int_{-\infty}^{+\infty} k^2 dk \hbar f^2(k) \sum_{\alpha=s,p} \left( \frac{1}{E(k)+E(\alpha)} + \frac{1}{E(k)-E(\alpha)} \right) \times \left\{ (\vec{\mu}_s \cdot \vec{\mu}_p) e^{i\vec{k}\vec{r}} \left( \frac{1}{ikr} + \frac{1}{k^2 r^2} - \frac{1}{ik^3 r^3} \right) - (\vec{\mu}_s \cdot \hat{r})(\vec{\mu}_p \cdot \hat{r}) e^{i\vec{k}\vec{r}} \left( \frac{1}{ikr} + \frac{3}{k^2 r^2} - \frac{3}{ik^3 r^3} \right) \right\} \quad (B36)$$

where  $E_m = \hbar\Omega$  and  $E_{pol} = m_{pol}c^2$  are the excitation energy of macroscopic subsystem and exciton-polariton energy and

$$E(k) = \hbar\Omega + \frac{(\hbar k)^2}{2m_{pol}} = E_m + \frac{(\hbar ck)^2}{2E_{pol}} \quad (B37)$$

To calculate the integration we can simplify the energy terms as

$$\begin{aligned} \left( \frac{1}{E(k)+E(\alpha)} \right) &= \frac{1}{E_m + \frac{(\hbar ck)^2}{2E_{pol}} + E(\alpha)} = \frac{1}{\frac{(\hbar c)^2}{2E_{pol}} \left( k^2 + \frac{2E_{pol}}{(\hbar c)^2} (E_m + E(\alpha)) \right)} \\ &= \frac{2E_{pol}}{(\hbar c)^2} \frac{1}{\left( k^2 + \frac{2E_{pol}}{(\hbar c)^2} (E_m + E(\alpha)) \right)} = \frac{2E_{pol}}{(\hbar c)^2} \frac{1}{\left( k^2 + \Delta_{\alpha+}^2 \right)} = \frac{2E_{pol}}{(\hbar c)^2} \frac{1}{(k+i\Delta_{\alpha+})(k-i\Delta_{\alpha+})} \end{aligned} \quad (B38)$$

Therefore, Equation (B36) then changes to

$$\begin{aligned} V_{eff}(\vec{r}) &= -\frac{1}{2\pi} \int_{-\infty}^{+\infty} k^2 dk \hbar f^2(k) \sum_{\alpha=s,p} \frac{2E_{pl}}{(\hbar c)^2} \left( \frac{1}{(k+i\Delta_{\alpha+})(k-i\Delta_{\alpha+})} + \frac{1}{(k+i\Delta_{\alpha-})(k-i\Delta_{\alpha-})} \right) \times \\ &\times \left\{ (\vec{\mu}_s \cdot \vec{\mu}_p) e^{i\vec{k}\vec{r}} \left( \frac{1}{ikr} + \frac{1}{k^2 r^2} - \frac{1}{ik^3 r^3} \right) - (\vec{\mu}_s \cdot \hat{r})(\vec{\mu}_p \cdot \hat{r}) e^{i\vec{k}\vec{r}} \left( \frac{1}{ikr} + \frac{3}{k^2 r^2} - \frac{3}{ik^3 r^3} \right) \right\} \equiv \\ &\equiv \sum_{\alpha=s,p} [V_{eff,\alpha+}(\vec{r}) + V_{eff,\alpha-}(\vec{r})] \end{aligned} \quad (B39)$$

where

$$\Delta_{\alpha\pm} \equiv \frac{1}{\hbar c} \sqrt{2E_{pol}(E_m \pm E_{\alpha})} \quad (E_m \succ E_{\alpha})$$

Finally, the the integration of Equation (B39) gives us

$$\begin{aligned} V_{eff,\alpha\pm}(\vec{r}) &= \mp \frac{1}{2} \left[ (\vec{\mu}_s \cdot \vec{\mu}_p) \left\{ \frac{(\Delta_{\alpha+})^2}{r} + \frac{\Delta_{\alpha+}}{r^2} + \frac{1}{r^3} \right\} W_{\alpha\pm} e^{-\Delta_{\alpha\pm} r} \right] \mp \\ &\mp \frac{1}{2} \left[ -(\vec{\mu}_s \cdot \hat{r})(\vec{\mu}_p \cdot \hat{r}) \left\{ \frac{(\Delta_{\alpha+})^2}{r} + \frac{3\Delta_{\alpha+}}{r^2} + \frac{3}{r^3} \right\} W_{\alpha\pm} e^{-\Delta_{\alpha\pm} r} \right] \end{aligned} \quad (B40)$$

where

$$W_{\alpha\pm} = \frac{E_{pol}}{E_\alpha} \frac{E_m^2 - E_\alpha^2}{(E_m \pm E_\alpha)(E_m - E_{pol} \mp E_\alpha) - E_m^2/2} \quad (B41)$$

Taking the angular average of  $(\vec{\mu}_s \cdot \hat{r})(\vec{\mu}_p \cdot \hat{r}) = (\vec{\mu}_s \vec{\mu}_p)/3$ , we find

$$V_{eff}(\vec{r}) = -\frac{(\vec{\mu}_A \cdot \vec{\mu}_B)}{3} \sum_{\alpha=s,p} \left\{ W_{\alpha+}(\Delta_{\alpha+})^2 \frac{e^{-\Delta_{\alpha+}r}}{r} - W_{\alpha-}(\Delta_{\alpha-})^2 \frac{e^{-\Delta_{\alpha-}r}}{r} \right\} \quad (B42)$$

for the effective or optical near-field potential. It consist of the sum of the Yukawa functions  $\Upsilon(\Delta_{\alpha\pm}r) \equiv e^{\Delta_{\alpha\pm}r}/r$  with a shorter interaction range  $\Delta_{\alpha+}$  (heavier effective mass) and a longer interaction range  $\Delta_{\alpha-}$  (lighter effective mass).

# Appendix C

## Optical Near Field Interaction between Quantum Dots for Strong Confinement

The interaction Hamiltonian between an electron and electric field can be written as

$$\hat{H}_{\text{int}} = -\int \psi^\dagger(\vec{r}) \vec{\mu}(\vec{r}) \psi(\vec{r}) \cdot \hat{D}(\vec{r}) d\vec{r} \quad (\text{C1})$$

Here,  $\psi^\dagger(\vec{r})$  is the field operator for electron creation and  $\psi(\vec{r})$  represents the field operator for electron annihilation,  $\vec{\mu}(\vec{r})$  is the dipole moment and  $\hat{D}(\vec{r})$  is the electric displacement vector operator at the position  $\vec{r}$ . We can expand field operators in terms of basis functions as follows

$$\psi(\vec{r}) = \sum_{\nu=c,v} \sum_n \hat{a}_{\nu n} \phi_{\nu n}(\vec{r}) \quad \psi^\dagger(\vec{r}) = \sum_{\nu=c,v} \sum_n \hat{a}_{\nu n}^+ \phi_{\nu n}^*(\vec{r}) \quad (\text{C2})$$

where in quantum dot,  $\phi_{\nu n}(\vec{r})$  and  $\phi_{\nu n}^*(\vec{r})$  are the basis functions that satisfy the boundary conditions for the electron. Here,  $\hat{a}_{\nu n}^+$  is the creation operator for the electron in the conduction band and  $\hat{a}_{\nu n}$  is the annihilation operator for the electron in the valence band. They are specified by the quantum numbers  $(\nu, n)$  where  $\nu = (c, v)$  and indices  $c$  and  $v$  correspond to the conduction and valence bands, respectively. The quantum number  $n$  denotes discrete energy levels in semiconductor quantum dot where  $(n = 1, 2, 3, \dots)$ . The completeness condition or orthonormalization for the basis functions can be written as

$$\sum_{\nu=c,v} \sum_n \phi_{\nu n}^*(\vec{r}) \phi_{\nu n}(\vec{r}') = \delta(\vec{r} - \vec{r}') \quad (\text{C3})$$

The electric displacement operator  $\hat{D}(\vec{r})$  in exciton-polariton base can be written as follows (please refer to Appendix B for derivations)

$$\hat{D} = i \sqrt{\frac{2\pi}{V}} \sum_{\vec{k}} \sum_{\lambda=1}^2 \vec{e}_\lambda(\vec{k}) f(k) \left( \hat{\zeta}_{\vec{k}} e^{i\vec{k}\vec{r}} - \hat{\zeta}_{\vec{k}}^+ e^{-i\vec{k}\vec{r}} \right) \quad (\text{C4})$$

where

$$f(k) = \frac{\hbar ck}{\sqrt{E(k)}} \sqrt{\frac{E^2(k) - E_m^2}{2E^2(k) - E_m^2 - (\hbar ck)^2}} \quad (C5)$$

Here,  $\hat{\zeta}_k^+$  and  $\hat{\zeta}_k$  are the creation and annihilation operators of the exciton-polariton and  $\vec{e}_\lambda(\vec{k})$ ,  $V$  and  $\vec{k}$  are the unit vector related to the polarization direction, quantization volume and the exciton-polariton wavevector, respectively. Here  $E_m$  is the excitation energy of the macroscopic material and  $E(k)$  is the energy related to the exciton-polariton with the wavevector  $\vec{k}$ . Substituting Equations (C2) and (C4) into (C1) gives us the interaction Hamiltonian.

$$\begin{aligned} \hat{H}_{\text{int}} &= -\int \sum_{v=c,v} \sum_n \hat{a}_{vn}^+ \phi_{vn}^*(\vec{r}) \vec{\mu}(\vec{r}) \sum_{v'=c',v'} \sum_{n'} \hat{a}_{v'n'} \phi_{v'n'}(\vec{r}) \cdot \hat{D}(\vec{r}) d\vec{r} = \\ &= -\sum_{v,n,v',n'} \hat{a}_{vn}^+ \hat{a}_{v'n'} \int \phi_{vn}^*(\vec{r}) \vec{\mu}(\vec{r}) \phi_{v'n'}(\vec{r}) \hat{D}(\vec{r}) d\vec{r} = -\sum_{v,n,v',n'} \hat{a}_{vn}^+ \hat{a}_{v'n'} \times \\ &\int \phi_{vn}^*(\vec{r}) \vec{\mu}(\vec{r}) \phi_{v'n'}(\vec{r}) \times \left( i \sqrt{\frac{2\pi}{V}} \sum_{\vec{k}} \sum_{\lambda=1}^2 \vec{e}_\lambda(\vec{k}) f(k) \left( \hat{\zeta}_k^+ e^{i\vec{k}\vec{r}} - \hat{\zeta}_k e^{-i\vec{k}\vec{r}} \right) \right) d\vec{r} = \\ &= \sum_{v,n,v',n',k,\lambda} \left( \hat{a}_{vn}^+ \hat{a}_{v'n'} g_{vmv'n'k\lambda} \cdot \hat{\zeta}_k - \hat{a}_{vn}^+ \hat{a}_{v'n'} g_{vmv'n'-k\lambda} \cdot \hat{\zeta}_k^+ \right) \end{aligned}$$

So, the second quantized form of the interaction Hamiltonian in exciton-polariton base is

$$\hat{H}_{\text{int}} = \sum_{v,n,v',n',k,\lambda} \left( \hat{a}_{vn}^+ \hat{a}_{v'n'} g_{vmv'n'k\lambda} \cdot \hat{\zeta}_k - \hat{a}_{vn}^+ \hat{a}_{v'n'} g_{vmv'n'-k\lambda} \cdot \hat{\zeta}_k^+ \right) \quad (C6)$$

where

$$g_{vmv'n'\pm k\lambda} = -i \sqrt{\frac{2\pi}{V}} f(k) \int \phi_{vn}^*(\vec{r}) \left[ \vec{\mu}(\vec{r}) \cdot \vec{e}_\lambda(\vec{k}) \right] \phi_{v'n'}(\vec{r}) e^{\pm i\vec{k}\vec{r}} d\vec{r} \quad (C7)$$

We can use Wannier function basis to describe the creation and annihilation of electron-hole pairs in a quantum dot because, it represent, the localization of electrons in an atomic site  $\vec{R}$ . Therefore, we can expand the electron field operators in terms of Wannier functions as

$$\psi^+(\vec{r}) = \sum_{v=c,v} \sum_{\vec{R}} \hat{a}_{v\vec{R}}^+ w_{v\vec{R}}^*(\vec{r}) \quad \psi(\vec{r}) = \sum_{v=c,v} \sum_{\vec{R}} \hat{a}_{v\vec{R}} w_{v\vec{R}}(\vec{r}) \quad (C8)$$



Here,  $\hat{a}_{\nu\bar{R}}^+$  is the creation operator of an electron at the position  $\bar{R}$  in the conduction band and  $\hat{a}_{\nu\bar{R}}$  is the annihilation operator of an electron at the site  $\bar{R}$  in the valence band energy band  $\nu$ . We can rewrite these operators in the Wannier representation in terms of  $\hat{a}_{\nu n}$  and  $\hat{a}_{\nu n}^+$ . Integrating both sides of Equation (C8), we have

$$\begin{aligned}\int \psi(\vec{r}) w_{\nu\bar{R}}^*(\vec{r}') d\vec{r}' &= \int \sum_{\nu=c,v} \sum_{\bar{R}} \hat{a}_{\nu\bar{R}} w_{\nu\bar{R}}(\vec{r}) w_{\nu\bar{R}}^*(\vec{r}') d\vec{r}' \\ \int \psi(\vec{r}) w_{\nu\bar{R}}^*(\vec{r}') d\vec{r}' &= \int \hat{a}_{\nu\bar{R}} \cdot \delta(\vec{r} - \vec{r}') d\vec{r}' \\ \hat{a}_{\nu\bar{R}} &= \int \psi(\vec{r}) w_{\nu\bar{R}}^*(\vec{r}) d\vec{r}\end{aligned}\quad (C9)$$

So, we can write creation and annihilation operators in the Wannier representation as

$$\hat{a}_{\nu\bar{R}}^+ = \sum_{\nu'=c,v} \sum_n \hat{a}_{\nu'n}^+ \int w_{\nu\bar{R}}(\vec{r}) \phi_{\nu'n}^*(\vec{r}) d\vec{r} \quad \hat{a}_{\nu\bar{R}} = \sum_{\nu'=c,v} \sum_n \hat{a}_{\nu'n} \int w_{\nu\bar{R}}^*(\vec{r}) \phi_{\nu'n}(\vec{r}) d\vec{r} \quad (C10)$$

In strong-confinement regime, the Bohr radius of an exciton is greater than the size of a quantum dot, the Coulomb interaction is very weak and both electron and hole can move independently. Therefore, the electron-hole states in a spherical quantum dot specified by the quantum numbers  $(\nu = \mu, \mu')$  (where  $\mu = (n, l, m)$  and  $\mu' = (n', l', m')$ ) can be represented by superposition of electrons and holes in Wannier representation as

$$\begin{aligned}|\Phi_\nu\rangle &= \sum_{\bar{R}, \bar{R}'} F_\mu(\vec{r}_e) F_{\mu'}(\vec{r}_h) \hat{a}_{c\bar{R}}^+ \hat{a}_{v\bar{R}'} |\Phi_g\rangle = \sum_{\bar{R}, \bar{R}'} F_\mu(\vec{r}_e) F_{\mu'}(\vec{r}_h) \times \\ &\times \sum_{c,v} \sum_{n,n'} \iint w_{c\bar{R}}(\vec{r}_1) \phi_{cn}^*(\vec{r}_1) \cdot w_{v\bar{R}'}^*(\vec{r}_2) \phi_{vn'}(\vec{r}_2) d\vec{r}_1 d\vec{r}_2 \cdot \hat{a}_{cn}^+ \hat{a}_{vn'} |\Phi_g\rangle = \\ &= \sum_{\bar{R}, \bar{R}'} F_\mu(\vec{r}_e) F_{\mu'}(\vec{r}_h) \sum_{n,n'} h_{\bar{R}n\bar{R}'n'} \hat{a}_{cn}^+ \hat{a}_{vn'} |\Phi_g\rangle\end{aligned}\quad (C11)$$

$$\text{So, we have} \quad |\Phi_\nu\rangle = \sum_{\bar{R}, \bar{R}'} F_\mu(\vec{r}_e) F_{\mu'}(\vec{r}_h) \sum_{n,n'} h_{\bar{R}n\bar{R}'n'} \hat{a}_{cn}^+ \hat{a}_{vn'} |\Phi_g\rangle \quad (C12)$$

where  $F_m^A(\vec{r}_e)$  and  $F_m^A(\vec{r}_h)$  denote the envelope functions for electron and hole in the quantum dot  $A$ , and the overlap integrals are defined as

$$h_{\bar{R}n\bar{R}'n'} = \iint w_{v\bar{R}'}^*(\vec{r}_2) w_{c\bar{R}}(\vec{r}_1) \phi_{cn}^*(\vec{r}_1) \phi_{vn'}(\vec{r}_2) d\vec{r}_1 d\vec{r}_2 \quad (C13)$$

Using Equations (C6) and (C12), we can obtain transition matrix elements from the exciton state  $|\Phi_v\rangle$  to the crystal ground state  $|\Phi_g\rangle$  as follows

$$\begin{aligned}
\langle \Phi_g | \hat{H}_{\text{int}} | \Phi_{m\mu} \rangle &= \langle \Phi_g | \sum_{v,n,v',n',k,\lambda} \left( \hat{a}_{vn}^+ \hat{a}_{v'n'} \mathbf{g}_{vnn'k\lambda} \cdot \hat{\zeta}_{\vec{k}} - \hat{a}_{vn}^+ \hat{a}_{v'n'} \mathbf{g}_{vnn'k\lambda} \cdot \hat{\zeta}_{\vec{k}}^+ \right) \times \\
&\times \sum_{\vec{R}, \vec{R}'} F_{\mu}^A(\vec{r}_e) F_{\mu'}^A(\vec{r}_h) \sum_{n_1, n_1'} h_{\vec{R}n_1 \vec{R}'n_1'} \hat{a}_{cn_1}^+ \hat{a}_{vn_1'} | \Phi_g \rangle = \langle \Phi_g | \sum_{v_1, cn_2} \sum_{k\lambda} (\hat{a}_{v_1}^+ \hat{a}_{cn_2} \mathbf{g}_{v_1cn_2k\lambda} \cdot \hat{\zeta}_{\vec{k}} - \\
&- \hat{a}_{v_1}^+ \hat{a}_{cn_2} \mathbf{g}_{v_1cn_2-k\lambda} \cdot \hat{\zeta}_{\vec{k}}^+) \sum_{\vec{R}, \vec{R}'} F_{\mu}^A(\vec{r}_e) F_{\mu'}^A(\vec{r}_h) \times \sum_{n_3, n_4} h_{\vec{R}n_3 \vec{R}'n_4} \hat{a}_{cn_3}^+ \hat{a}_{vn_4} | \Phi_g \rangle = \\
&= \sum_{v_1, cn_2} \sum_{k\lambda} (\hat{\zeta}_{\vec{k}} \mathbf{g}_{v_1cn_2k\lambda} - \hat{\zeta}_{\vec{k}}^+ \mathbf{g}_{v_1cn_2-k\lambda}) \cdot \sum_{\vec{R}, \vec{R}'} F_{\mu}^A(\vec{r}_e) F_{\mu'}^A(\vec{r}_h) \sum_{n_3, n_4} h_{\vec{R}n_3 \vec{R}'n_4} \cdot \delta_{n_1n_4} \delta_{n_2n_3}
\end{aligned} \tag{C14}$$

where, the expectation value leads the delta function

$$\langle \Phi_g | \hat{a}_{v_1}^+ \hat{a}_{cn_2} \hat{a}_{cn_3}^+ \hat{a}_{vn_4} | \Phi_g \rangle = \delta_{n_1n_4} \delta_{n_2n_3}$$

$$\begin{aligned}
\langle \Phi_g | \hat{H}_{\text{int}} | \Phi_{m\mu} \rangle &= \sum_{n_1, n_2} \sum_{\vec{R}, \vec{R}'} F_{\mu}^A(\vec{r}_e) F_{\mu'}^A(\vec{r}_h) \sum_{\vec{k}} \sum_{\lambda=1}^2 (\hat{\zeta}_{\vec{k}} \mathbf{g}_{v_1cn_2k\lambda} - \hat{\zeta}_{\vec{k}}^+ \mathbf{g}_{v_1cn_2-k\lambda}) \sum_{n_3, n_4} h_{\vec{R}n_3 \vec{R}'n_4} \times \\
&\times \langle \Phi_g | \hat{a}_{v_1}^+ \hat{a}_{cn_2} \hat{a}_{cn_3}^+ \hat{a}_{vn_4} | \Phi_g \rangle = \sum_{n_1, n_2} \sum_{\vec{R}, \vec{R}'} F_{\mu}^A(\vec{r}_e) F_{\mu'}^A(\vec{r}_h) \sum_{\vec{k}} \sum_{\lambda=1}^2 (\hat{\zeta}_{\vec{k}} \mathbf{g}_{v_1cn_2k\lambda} - \hat{\zeta}_{\vec{k}}^+ \mathbf{g}_{v_1cn_2-k\lambda}) \times \\
&\times \sum_{n_3, n_4} h_{\vec{R}n_3 \vec{R}'n_4} \delta_{n_1n_4} \delta_{n_2n_3}
\end{aligned}$$

So, we find the expression for transition matrix elements as

$$\langle \Phi_g | \hat{H}_{\text{int}} | \Phi_{m\mu} \rangle = \sum_{n_1, n_2} \sum_{\vec{R}, \vec{R}'} F_{\mu}^A(\vec{r}_e) F_{\mu'}^A(\vec{r}_h) \sum_{\vec{k}} \sum_{\lambda=1}^2 (\hat{\zeta}_{\vec{k}} \mathbf{g}_{v_1cn_2k\lambda} - \hat{\zeta}_{\vec{k}}^+ \mathbf{g}_{v_1cn_2-k\lambda}) h_{\vec{R}n_2 \vec{R}'n_1} \tag{C15}$$

Using the orthonormalization property of the functions  $\phi_{v_n}(\vec{r})$  and  $\phi_{v_n}^*(\vec{r})$ , the product of  $g$  and  $h$  can be simplified to

$$\begin{aligned}
\sum_{n_1, n_2} \mathbf{g}_{v_1cn_2k\lambda} h_{\vec{R}n_2 \vec{R}'n_1} &= \sum_{n_1, n_2} -i \sqrt{\frac{2\pi}{V}} f(k) \int \phi_{v_1}^*(\vec{r}) [\vec{\mu}(\vec{r}) \cdot \vec{e}_{\lambda}(\vec{k})] e^{i\vec{k}\vec{r}} \phi_{cn_2}(\vec{r}) d\vec{r} \times \\
\iint w_{v\vec{R}}^*(\vec{r}_2) w_{c\vec{R}'}(\vec{r}_1) \phi_{cn_1}^*(\vec{r}_1) \phi_{v_2}(\vec{r}_2) d\vec{r}_1 d\vec{r}_2 &= -i \sqrt{\frac{2\pi}{V}} f(k) \int \sum_{n_1, n_2} \sum_{cv} \phi_{v_1}^*(\vec{r}) \phi_{cn_2}(\vec{r}') d\vec{r}' \times \\
&\times \int w_{v\vec{R}}^*(\vec{r}_2) \vec{\mu}(\vec{r}) w_{c\vec{R}'}(\vec{r}_1) \vec{e}_{\lambda}(\vec{k}) e^{i\vec{k}\vec{r}} d\vec{r}_1 \int \sum_{n_1, n_2} \sum_{cv} \phi_{cn_1}^*(\vec{r}_1) \phi_{v_2}(\vec{r}_2) d\vec{r}_2 = -i \sqrt{\frac{2\pi}{V}} f(k) \times \\
&\times \int w_{v\vec{R}}^*(\vec{r}) \vec{\mu}(\vec{r}) w_{c\vec{R}'}(\vec{r}) \vec{e}_{\lambda}(\vec{k}) e^{i\vec{k}\vec{r}} d\vec{r} \approx -i \sqrt{\frac{2\pi}{V}} f(k) [\vec{\mu}(\vec{r}) \cdot \vec{e}_{\lambda}(\vec{k})] e^{i\vec{k}\vec{r}} \delta_{\vec{R}\vec{R}'}
\end{aligned} \tag{C16}$$

where the spatial locality of the Wannier functions provides  $\delta_{\vec{R}\vec{R}'}$ . So, we have

$$\sum_{n_1, n_2} g_{\nu n_1 c n_2 k \lambda} h_{\vec{R} n_2 \vec{R}' n_1} \approx -i \sqrt{\frac{2\pi}{V}} f(k) [\vec{\mu}(\vec{r}) \cdot \vec{e}_\lambda(\vec{k})] e^{i\vec{k}\vec{R}} \delta_{\vec{R}\vec{R}'} \quad (C17)$$

where the transition dipole moment is defined as

$$\vec{\mu} = \int w_{\vec{R}}^*(\vec{r}) \vec{\mu}(\vec{r}) w_{\vec{R}}(\vec{r}) d\vec{r} \quad (C18)$$

Therefore, Equation (C14) can be reduced to

$$\langle \Phi_g | \hat{H}_{\text{int}} | \Phi_{m\mu} \rangle = \sum_{\vec{R}, \vec{R}'} F_\mu^A(\vec{r}_e) F_{\mu'}^A(\vec{r}_h) \sum_{\vec{k}} \sum_{\lambda=1}^2 \left( \sum_{n_1, n_2} \hat{\zeta}_{\vec{k}}^- g_{\nu n_1 c n_2 k \lambda} \cdot h_{\vec{R} n_2 \vec{R}' n_1} - \sum_{n_1, n_2} \hat{\zeta}_{\vec{k}}^+ g_{\nu n_1 c n_2 -k \lambda} \cdot h_{\vec{R} n_2 \vec{R}' n_1} \right)$$

and

$$\begin{aligned} \langle \Phi_g | \hat{H}_{\text{int}} | \Phi_{\mu\mu'} \rangle &= \sum_{n_1, n_2} \sum_{\vec{R}, \vec{R}'} F_\mu(\vec{r}_e) F_{\mu'}(\vec{r}_h) \sum_{\vec{k}} \sum_{\lambda=1}^2 (\hat{\zeta}_{\vec{k}}^- g_{\nu n_1 c n_2 k \lambda} - \hat{\zeta}_{\vec{k}}^+ g_{\nu n_1 c n_2 -k \lambda}) h_{\vec{R} n_2 \vec{R}' n_1} = \\ &= \sum_{\vec{R}, \vec{R}'} F_\mu(\vec{r}_e) F_{\mu'}(\vec{r}_h) \sum_{\vec{k}} \sum_{\lambda=1}^2 \left( -i \sqrt{\frac{2\pi}{V}} f(k) [\vec{\mu}(\vec{r}) \cdot \vec{e}_\lambda(\vec{k})] e^{i\vec{k}\vec{R}} \delta_{\vec{R}\vec{R}'} \cdot \hat{\zeta}_{\vec{k}}^- \right) - \\ &- \sum_{\vec{R}, \vec{R}'} F_\mu(\vec{r}_e) F_{\mu'}(\vec{r}_h) \sum_{\vec{k}} \sum_{\lambda=1}^2 \left( -i \sqrt{\frac{2\pi}{V}} f(k) [\vec{\mu}(\vec{r}) \cdot \vec{e}_\lambda(\vec{k})] e^{-i\vec{k}\vec{R}} \delta_{\vec{R}\vec{R}'} \cdot \hat{\zeta}_{\vec{k}}^+ \right) = \quad (C19) \\ &= \sum_{\vec{R}, \vec{R}'} -i \sqrt{\frac{2\pi}{V}} f(k) \sum_{\lambda=1}^2 [\vec{\mu}(\vec{r}) \cdot \vec{e}_\lambda(\vec{k})] F_\mu(\vec{r}_e) F_{\mu'}(\vec{r}_h) (\hat{\zeta}_{\vec{k}}^- \cdot e^{i\vec{k}\vec{R}} - \hat{\zeta}_{\vec{k}}^+ \cdot e^{-i\vec{k}\vec{R}}) \delta_{\vec{R}\vec{R}'} = \\ &= -i \sqrt{\frac{2\pi}{V}} \sum_{\vec{R}} \sum_{\vec{k}} \sum_{\lambda=1}^2 f(k) [\vec{\mu}(\vec{r}) \cdot \vec{e}_\lambda(\vec{k})] F_\mu(\vec{r}_e) F_{\mu'}(\vec{r}_h) (\hat{\zeta}_{\vec{k}}^- \cdot e^{i\vec{k}\vec{R}} - \hat{\zeta}_{\vec{k}}^+ \cdot e^{-i\vec{k}\vec{R}}) \end{aligned}$$

So, finally we have

$$\langle \Phi_g | \hat{H}_{\text{int}} | \Phi_{\mu\mu'} \rangle = -i \sqrt{\frac{2\pi\hbar}{V}} \sum_{\vec{R}} \sum_{\vec{k}} \sum_{\lambda=1}^2 f(k) [\vec{\mu}(\vec{r}) \cdot \vec{e}_\lambda(\vec{k})] F_\mu(\vec{r}_e) F_{\mu'}(\vec{r}_h) (\hat{\zeta}_{\vec{k}}^- \cdot e^{i\vec{k}\vec{R}} - \hat{\zeta}_{\vec{k}}^+ \cdot e^{-i\vec{k}\vec{R}})$$

Here the long wave approximation  $e^{\pm i\vec{k}\vec{R}} \approx 1$  is not applied, which is usually used for far-field light. The optical near-field interaction in the lowest order can be written as follows

$$V_{\text{eff}} = \hbar U = \sum_m \langle \psi_f^P | P \hat{V} Q | m^Q \rangle \langle m^Q | Q \hat{V} P | \psi_i^P \rangle \left( \frac{1}{E_{0i}^P - E_{0m}^Q} + \frac{1}{E_{0f}^P - E_{0m}^Q} \right) \quad (C20)$$

$E_{0i}^P$  and  $E_{0f}^P$  are the eigenenergies of initial  $|\psi_i^P\rangle$  and final  $|\psi_f^P\rangle$  states of the unperturbed Hamiltonian in the  $P$  space and  $E_{0m}^Q$  is the eigenenergy of the intermediate state  $|m^Q\rangle$  in the  $Q$  space. Here we set the initial and final states in the  $P$  space as

$$|\psi_i^P\rangle = |\Phi_{\mu_A\mu'_A}^A\rangle |\Phi_g^B\rangle |0\rangle \quad |\psi_f^P\rangle = |\Phi_g^A\rangle |\Phi_{\mu_B\mu'_B}^B\rangle |0\rangle \quad (C21)$$

The intermediate states in the  $Q$  space include the exciton-polaritons with the wavevector  $\vec{k}$

$$|m^Q\rangle = |\Phi_g^A\rangle |\Phi_g^B\rangle |\vec{k}\rangle \quad |m^Q\rangle = |\Phi_{\mu_A\mu'_A}^A\rangle |\Phi_{\mu_B\mu'_B}^B\rangle |\vec{k}\rangle \quad (C22)$$

Using these states in Equation (C20), we have

$$\begin{aligned} \hbar U &= \langle 0 | \langle \Phi_g^A | \langle \Phi_{\mu_B\mu'_B}^B | \hat{V} | \Phi_g^B \rangle | \Phi_g^A \rangle | \vec{k} \rangle \langle \vec{k} | \langle \Phi_g^B | \langle \Phi_g^A | \hat{V} | \Phi_{\mu_A\mu'_A}^A \rangle | \Phi_g^B \rangle | 0 \rangle \times \\ &\times \left( \frac{1}{E_{0i}^P - E_{0m}^Q} + \frac{1}{E_{0f}^P - E_{0m}^Q} \right) + \langle 0 | \langle \Phi_{\mu_B\mu'_B}^B | \langle \Phi_g^A | \hat{V} | \Phi_{\mu_A\mu'_A}^A \rangle | \Phi_{\mu_B\mu'_B}^B \rangle | \vec{k} \rangle \times \\ &\times \langle \vec{k} | \langle \Phi_{\mu_A\mu'_A}^A | \langle \Phi_{\mu_B\mu'_B}^B | \hat{V} | \Phi_g^B \rangle | \Phi_{\mu_A\mu'_A}^A \rangle | 0 \rangle \left( \frac{1}{E_{0i}^P - E_{0m}^Q} + \frac{1}{E_{0f}^P - E_{0m}^Q} \right) \end{aligned} \quad (C23)$$

Inserting the expression of matrix elements (C19) into Equation (C23), and operating the exciton-polariton creation  $\zeta_{\vec{k}}^+$  and annihilation  $\zeta_{\vec{k}}^-$  operators from the left hand side to the  $\vec{k}$  state, we obtain

$$\begin{aligned} \hbar U &= \left( \frac{2\pi\hbar}{V} \right) \sum_{\vec{R}} \sum_{\vec{k}} \sum_{\lambda=1}^2 \left[ \vec{\mu}_A \cdot \vec{e}_\lambda(\vec{k}) \right] \left[ \vec{\mu}_B \cdot \vec{e}_\lambda(\vec{k}) \right] f^2(k) F_{\mu_A}^A(\vec{r}_e) F_{\mu'_A}^A(\vec{r}_h) \times \\ &\times F_{\mu_B}^{B*}(\vec{r}_e) F_{\mu'_B}^{B*}(\vec{r}_h) e^{i\vec{k}(\vec{r}_B - \vec{r}_A)} \left( \frac{1}{(E(A^*) - E(A)) - \hbar\Omega(k)} + \frac{1}{(E(B^*) - E(B)) - \hbar\Omega(k)} \right) + \\ &+ \left( \frac{2\pi\hbar}{V} \right) \sum_{\vec{R}} \sum_{\vec{k}} \sum_{\lambda=1}^2 \left[ \vec{\mu}_A \cdot \vec{e}_\lambda(\vec{k}) \right] \left[ \vec{\mu}_B \cdot \vec{e}_\lambda(\vec{k}) \right] f^2(k) F_{\mu_A}^A(\vec{r}_e) F_{\mu'_A}^A(\vec{r}_h) \times \\ &\times F_{\mu_B}^{B*}(\vec{r}_e) F_{\mu'_B}^{B*}(\vec{r}_h) e^{i\vec{k}(\vec{r}_A - \vec{r}_B)} \left( \frac{1}{(E(B) - E(B^*)) - \hbar\Omega(k)} + \frac{1}{(E(A) - E(A^*)) - \hbar\Omega(k)} \right) \end{aligned} \quad (C24)$$

since  $\sum_{\vec{k}} \rightarrow \frac{V}{(2\pi)^3} \int d^3k$  and  $E(A^*) - E(A) = \hbar\Omega_0(A)$   $E(B^*) - E(B) = \hbar\Omega_0(B)$ ,

we have

$$\begin{aligned}
\hbar U &= \left( \frac{2\pi\hbar}{V} \right) \frac{V}{(2\pi)^3} \sum_{\vec{R}} \sum_{\lambda=1}^2 \int d^3k \left[ \vec{\mu}_A \cdot \vec{e}_\lambda(\vec{k}) \right] \left[ \vec{\mu}_B \cdot \vec{e}_\lambda(\vec{k}) \right] \hbar f^2(k) \times \\
&\times F_{\mu_A}^A(\vec{r}_e) F_{\mu_A}^A(\vec{r}_h) F_{\mu_B}^{B*}(\vec{r}_e) F_{\mu_B}^{B*}(\vec{r}_h) \left( \frac{e^{-i\vec{k}(\vec{r}_A - \vec{r}_B)}}{\hbar\Omega_0(A) - \hbar\Omega(k)} + \frac{e^{-i\vec{k}(\vec{r}_A - \vec{r}_B)}}{\hbar\Omega_0(B) - \hbar\Omega(k)} \right) + \\
&+ \left( \frac{2\pi\hbar}{V} \right) \frac{V}{(2\pi)^3} \sum_{\vec{R}} \sum_{\lambda=1}^2 \int d^3k \left[ \vec{\mu}_A \cdot \vec{e}_\lambda(\vec{k}) \right] \left[ \vec{\mu}_B \cdot \vec{e}_\lambda(\vec{k}) \right] \hbar f^2(k) \times \\
&\times F_{\mu_A}^A(\vec{r}_e) F_{\mu_A}^A(\vec{r}_h) F_{\mu_B}^{B*}(\vec{r}_e) F_{\mu_B}^{B*}(\vec{r}_h) \left( -\frac{e^{i\vec{k}(\vec{r}_A - \vec{r}_B)}}{\hbar\Omega_0(k) + \hbar\Omega_0(B)} - \frac{e^{i\vec{k}(\vec{r}_A - \vec{r}_B)}}{\hbar\Omega_0(k) + \hbar\Omega_0(A)} \right)
\end{aligned} \tag{C25}$$

and

$$\begin{aligned}
\hbar U &= -\frac{1}{(2\pi)^2} \iint F_{\mu_A}^A(\vec{r}_e) F_{\mu_A}^A(\vec{r}_h) F_{\mu_B}^{B*}(\vec{r}_e) F_{\mu_B}^{B*}(\vec{r}_h) \sum_{\lambda=1}^2 \int d^3k \left[ \vec{\mu}_A \cdot \vec{e}_\lambda(\vec{k}) \right] \times \\
&\times \left[ \vec{\mu}_B \cdot \vec{e}_\lambda(\vec{k}) \right] \hbar f^2(k) \left( \frac{e^{i\vec{k}\vec{r}_{AB}}}{E(k) + E(A)} + \frac{e^{-i\vec{k}\vec{r}_{AB}}}{E(k) - E(A)} \right) d^3r_A d^3r_B - \\
&- \frac{1}{(2\pi)^2} \iint F_{\mu_A}^A(\vec{r}_e) F_{\mu_A}^A(\vec{r}_h) F_{\mu_B}^{B*}(\vec{r}_e) F_{\mu_B}^{B*}(\vec{r}_h) \sum_{\lambda=1}^2 \int d^3k \left[ \vec{\mu}_A \cdot \vec{e}_\lambda(\vec{k}) \right] \times \\
&\times \left[ \vec{\mu}_B \cdot \vec{e}_\lambda(\vec{k}) \right] \hbar f^2(k) \left( \frac{e^{i\vec{k}\vec{r}_{AB}}}{E(k) + E(B)} + \frac{e^{-i\vec{k}\vec{r}_{AB}}}{E(k) - E(B)} \right) d^3r_A d^3r_B
\end{aligned} \tag{C26}$$

Finally, we arrive at

$$\hbar U = \iint F_{\mu_A}^A(\vec{r}_e) F_{\mu_A}^A(\vec{r}_h) F_{\mu_B}^{B*}(\vec{r}_e) F_{\mu_B}^{B*}(\vec{r}_h) \{ \Upsilon_A(\vec{r}_{AB}) + \Upsilon_B(\vec{r}_{AB}) \} d^3r_A d^3r_B \tag{C27}$$

where we have

$$\begin{aligned}
\Upsilon_\alpha(\vec{r}_{AB}) &= -\frac{1}{4\pi^2} \sum_{\lambda=1}^2 \int d^3k \left[ \vec{\mu}_A \cdot \vec{e}_\lambda(\vec{k}) \right] \left[ \vec{\mu}_B \cdot \vec{e}_\lambda(\vec{k}) \right] \hbar f^2(k) \times \\
&\times \left( \frac{e^{i\vec{k}\vec{r}_{AB}}}{E(k) + E(\alpha)} + \frac{e^{-i\vec{k}\vec{r}_{AB}}}{E(k) - E(\alpha)} \right) d^3k
\end{aligned} \tag{C28}$$

Here,  $(\alpha = A, B)$ ,  $r_{AB} = |\vec{r}_{AB}| = |\vec{r}_A - \vec{r}_B|$ ,  $\mu_\alpha$  is transition dipole moment and  $E_\alpha$  is the exciton energy in QD $\alpha$ , and  $E(k)$  denotes the eigenenergy of exciton-polariton with

$$E(k) = \hbar\Omega + \frac{(\hbar k)^2}{2m_{pol}} = E_m + \frac{(\hbar ck)^2}{2E_{pol}} \tag{C29}$$

$E_m$  is the electronic excitation energy of the macroscopic subsystem,  $m_{pol}$  and  $E_{pol} = m_{pol}c^2$  are the effective mass and the energy of exciton-polariton.

After taking the integration over  $k$  and approximations, Equation (C28) can be simplified to (refer to Appendix B and Appendix D)

$$\Upsilon = -\frac{(\vec{\mu}_A \cdot \vec{\mu}_B)}{3} \sum_{\alpha=A,B} \left\{ W_{\alpha+} (\Delta_{\alpha+})^2 \frac{e^{-\Delta_{\alpha+}r}}{r} - W_{\alpha-} (\Delta_{\alpha-})^2 \frac{e^{-\Delta_{\alpha-}r}}{r} \right\} \quad (C29)$$

where  $W_{\alpha\pm}$  and  $\Delta_{\alpha\pm}$  are the constants and defined as

$$W_{\alpha\pm} = \frac{E_{pol}}{E_\alpha} \frac{E_m^2 - E_\alpha^2}{(E_m \pm E_\alpha)(E_m - E_{pol} \mp E_\alpha) - E_m^2/2} \quad (C30)$$

$$\text{and } \Delta_{\alpha\pm} \equiv \frac{1}{\hbar c} \sqrt{2E_{pol}(E_m \pm E_\alpha)}, \quad (E_m \succ E_\alpha) \quad (C31)$$

# Appendix D

## Derivation of the probe sample interaction potential

The prope sample interaction potential  $V_{eff}(p, s)$  defined as

$$V_{eff}^{p,s} = -\frac{1}{(2\pi)^2} \int d^3k \sum_{\lambda=1}^2 (\vec{\mu}_s \cdot \vec{e}_\lambda(\vec{k})) (\vec{\mu}_p \cdot \vec{e}_\lambda(\vec{k})) f^2 \left( \frac{e^{i\vec{k}(\vec{r}_p - \vec{r}_s)}}{\frac{\hbar}{2m_p}(k^2 - \Delta_{\alpha-}^2)} + \frac{e^{i\vec{k}(\vec{r}_s - \vec{r}_p)}}{\frac{\hbar}{2m_p}(k^2 + \Delta_{\alpha-}^2)} \right) \quad (D1)$$

where we approximate some of the terms as a constant, define  $f(k)$  as  $f$  and heavy and light effective masses  $\Delta_{\alpha+}$  and  $\Delta_{\alpha-}$  as

$$\Delta_{\alpha+} = \left( \frac{3\pi^2 m_p}{m_{eS} a_S^2} + \frac{2m_p \Omega}{\hbar} \right)^{1/2} \quad \Delta_{\alpha-} = \left( \frac{3\pi^2 m_p}{m_{eS} a_S^2} - \frac{2m_p \Omega}{\hbar} \right)^{1/2} \quad (D2)$$

Now let us change the coordinate system from cartesian coordinates to spherical coordinates and take into account that  $d^3k = k^2 dk \sin\theta d\theta d\phi$  in spherical coordinates.

$$\begin{aligned} \frac{1}{(2\pi)^2} \int \frac{e^{i\vec{k}\vec{r}}}{k^2 + \Delta_+^2} d^3k &= \frac{1}{(2\pi)^3} \int_0^\infty k^2 \frac{e^{ikr \cos\theta}}{k^2 + \Delta_+^2} dk \int_0^{2\pi} d\phi \int_0^\pi \sin\theta d\theta = \\ &= \frac{1}{2\pi} \int_0^\infty \frac{k^2}{k^2 + \Delta_+^2} dk \int_0^\pi \sin\theta e^{ikr \cos\theta} d\theta \end{aligned} \quad (D3)$$

the first part of the integral is evaluated as

$$\int_0^\pi \sin\theta e^{ikr \cos\theta} d\theta = \int_0^\pi e^{ikr \cos\theta} d(\cos\theta) = \left[ \frac{e^{ikr} - e^{-ikr}}{ikr} \right] \quad (D4)$$

so we have

$$\begin{aligned} \frac{1}{2\pi} \int_0^\infty dk \frac{k^2}{k^2 + \Delta_+^2} \left[ \frac{e^{ikr} - e^{-ikr}}{ikr} \right] &= \frac{1}{2\pi i r} \left[ \int_0^\infty dk \frac{ke^{ikr}}{k^2 + \Delta_+^2} + \int_{-\infty}^0 dk \frac{ke^{ikr}}{k^2 + \Delta_+^2} \right] = \\ &= \frac{1}{2\pi i r} \int_{-\infty}^\infty dk \frac{ke^{ikr}}{k^2 + \Delta_+^2} \end{aligned} \quad (D5)$$

To obtain the last integral we use the complex integration,. The residue at  $k = im$  gives

$$\int_{-\infty}^{\infty} dk \frac{ke^{ikr}}{k^2 + \Delta_+^2} = \int_{-\infty}^{\infty} dk \frac{ke^{ikr}}{(k + i\Delta_+)(k - i\Delta_+)} = 2\pi i \left( \frac{e^{-\Delta_+ r}}{2} \right) = \pi i e^{-\Delta_+ r} \quad (D6)$$

Finally we have

$$\frac{1}{2\pi} \int \frac{e^{i\vec{k}\vec{r}}}{k^2 + \Delta_+^2} d^3k = \frac{e^{-\Delta_+ r}}{2r} \quad (D7)$$

In a similar way the following integral can be derived for light effective mass

$$\frac{1}{(2\pi)^3} \int \frac{e^{i\vec{k}\vec{r}}}{k^2 - \Delta_-^2} d^3k = \frac{e^{i\Delta_- r}}{2r} \quad (D8)$$

Since we have  $\sum_{\lambda=1}^2 \vec{e}_{\lambda i}(\vec{k}) \vec{e}_{\lambda j}(\vec{k}) = \delta_{ij} - \hat{k}_i \hat{k}_j$  and therefore

$$\sum_{\lambda=1}^2 (\vec{\mu}_s \cdot \vec{e}_{\lambda}(\vec{k})) (\vec{\mu}_p \cdot \vec{e}_{\lambda}(\vec{k})) = \sum_{i,j} \vec{\mu}_{si} \vec{\mu}_{pj} (\delta_{ij} - \hat{k}_i \hat{k}_j) \quad (D9)$$

Finally effective probe-sample interaction is derived as

$$V_{eff}(p, s) = -\frac{1}{2} \sum_{i,j=1}^3 (\vec{\mu}_{si} \cdot \vec{\mu}_{pj}) \delta_{ij} \left[ \frac{\exp(-\Delta_+ r)}{r} + \frac{\exp(i\Delta_- r)}{r} \right] \quad (D10)$$

Since the eigenenergies of sample ( $\hbar\Omega_0(s)$ ) and probe ( $\hbar\Omega_0(p)$ ) is larger than the energy of macroscopic matter excitation  $\hbar\Omega$ ,  $\Delta_+$  and  $\Delta_-$  can be approximated as

$$\Delta_+ \approx \sqrt{\frac{3\pi^2 m_P}{m_{eS} a_P^2}} \quad \text{and} \quad \Delta_- \approx \sqrt{\frac{3\pi^2 m_P}{m_{eS} a_S^2}} \quad (D11)$$

Finally, it follows that

$$V_{eff}(p, s) \propto \frac{\exp(-\pi\mu_P r/a_P)}{r} + \frac{\exp(i\pi\mu_S r/a_S)}{r} \quad (D12)$$

where we have

$$\mu_P = \frac{\sqrt{3}m_P}{m_{eP}} \quad \mu_S = \frac{\sqrt{3}m_S}{m_{eS}} \quad (D13)$$